Fall 2007

The leaching behavior of arsenic, selenium and other trace elements in coal fly ash

Tian Wang

Department: Civil, Architectural and Environmental Engineering

THE LEACHING BEHAVIOR OF ARSENIC, SELENIUM AND OTHER TRACE ELEMENTS IN COAL FLY ASH

by

TIAN WANG

A DISSERTATION

Presented to the Faculty of the Graduate School of the

UNIVERSITY OF MISSOURI-ROLLA

In Partial Fulfillment of the Requirements for the Degree

DOCTOR OF PHILOSOPHY

in

CIVIL ENGINEERING

2007

Jianmin Wang, Advisor	Craig D. Adams
Joel G. Burken	Glenn C. Morrison
Charles Chusuei	Ken Ladwig

PUBLICATION DISSERTATION OPTION

This dissertation has been prepared in the form of seven journal articles for peer-review. These articles are presented in Paper I through Paper V. Paper I has been prepared according to the style used by Waste Management and pages 13 to 43 have been submitted to this publication. Paper II has been prepared in the style used by the Journal of Environmental Quality and pages 44 to 73 have been submitted to this publication. Paper III has been prepared in the style used by Chemosphere and pages 74 to 99 have been submitted to this publication. Paper IV has been prepared in the style used by Environmental Science and Technology and pages 100 to 124 have been submitted to this publication. Paper V has been prepared in the style used by Environmental Science and Technology and pages 125 to 149 have been submitted to this publication.

NOTE: The sections of Introduction, Purposes and Objectives, Materials and Experimental, Conclusions, Significance and Impacts, Future Works, and Appendices contain supplemental information for the journal articles. They present some information required to complete this dissertation but not necessary for submission to any of the aforementioned journals.

ABSTRACT

Trace elements in coal fly ash have long been an environmental concern in terms of their toxicity and mobility. Among them, arsenic and selenium are two oxyanionic elements of greatest concern, the regulation for arsenic in drinking water is even stricter with MCL of 10 ug/L since January 2006. Therefore, understanding the leaching process of these trace elements in fly ash during ash disposal and reuse is important in developing novel methods to control their leaching and protecting water quality.

The goals of this study are four fold, they are: (1) to investigate the leaching behavior of arsenic and selenium from fly ash as well as their affecting factors; (2) to analyze the speciation of arsenic and selenium in fly ash leachate; (3) to develop a modeling approach to quantify the availability and stability of trace cationic elements in fly ash; (4) to apply this model to describe the leaching/adsorption behavior of arsenic and selenium on fly ash, as well as the calcium effect on arsenic (V) adsorption process.

This research shows that pH is one of the most important factors affecting arsenic and selenium leaching from fly ash, which is also dependent upon the types of fly ash, solid-to-liquid ratio and leaching time. The leaching of arsenic and selenium from fly ash is governed by adsorption/desorption process in samples with low calcium concentration, but likely controlled by the calcium phase in samples with high calcium concentration. The total leachable mass and adsorption constant of trace cationic elements in fly ash can be determined with the modeling approach developed in this study. The adsorption of arsenic and selenium on bituminous coal fly ash was also successfully quantified with a speciation-based adsorption model. The speciation of arsenic and selenium in fly ash leachate varied with samples and was affected by the S/L ratio and leaching time.

ACKNOWLEDGMENTS

The endless support and help I received from faculty, staff, friends, and family has led me to where I am today. Many of them deserve further recognition, but to all of them I am very thankful.

I would like to express my sincere thanks to my advisor, Dr. Jianmin Wang, for his guidance, time, and support. Without these, I can't image how these projects and my dissertation would have been completed. Also, I would like to thank my committee – Drs. Craig Adams, Joel Burken, Glenn Morrison, Charles Chusuei and Mr. Ken Ladwig – for their time, guidance, and constructive comments.

Many thanks go to Ms. Honglan Shi and PerkinElmer technicians who have been invaluable in helping me on the method development for arsenic and selenium speciation analysis and to Mr. Gary for his remarkable work on maintaining laboratory instrumentations and fixing problems.

I would like to thank my colleagues in Dr. Wang' research group, Xiaohong Guan, Harmanjit Mallhi, Tingzhi Su and Shi Shu for their collaboration and hard work on the research projects and filling their sense of humor during tedious bottle-washing time. Special thanks to all other fellow students in the ERC for giving me a good time at UMR.

I am very grateful to my family in China and my friends both in the U.S. and back in China for their understanding, support, and friendship that helped me overcome so many difficulties in studying abroad. There is no word that can express my gratitude. Last but not least, I would like to thank my husband, Yu Liu, for always encouraging me and standing by me in all these years, for his love and support, no matter what.

TABLE OF CONTENTS

LIST OF ILLUSTRATIONS

LIST OF TABLES

SECTION

1. INTRODUCTION

Coal fly ash, a coal combustion product (CCP) of coal-fired power plants, is a pozzolanic material that can be classified into two classes, F and C, based on its chemical composition (ASTM C618). The primary inorganic components of fly ash are the oxides of Si, Al, Fe and Ca. Class F ash is generally produced from burning anthracite or bituminous coal, and contains at least 70% of SiO2+Al2O3+Fe2O3. class C ash is normally produced from lignite or subbituminous coals and contains less SiO2+Al2O3+Fe2O3 (>50%) but more calcium hydroxide or lime (ASTM C618; cockrell et al., 1970). Fly ash also contains less amount of Mg, Na, K and S and varying levels of trace elements (Kim and Cardone, 1997; Kim and Kazonich, 2001), among which, the potentially toxic elements Ag, As, B, Ba, Cd, Co, Cr, Cu, Hg, Ni, Pb, Se, and Zn can be released into soil, surface water and groundwater (EPRI, 1998; Mehnert and Hensel, 1996). In 2005, US generated more than 71 million short tons (6.4 × 1010 kg) of coal fly ashes, and 41% were further utilized as concrete products, road bases, etc (ACAA, 2006). Most of the remaining 59% were disposed of in landfills or impoundments. However, only slightly more than half of the landfills and a quarter of impoundments were lined. EPA has identified several damage cases with management of coal ash or waste co-management, contamination of groundwater or drinking water wells were reported in these cases (USEPA, 1988; USEPA, 1999). Therefore, the leaching potential of these trace elements from fly ash leading to possible contamination of ground and surface water is an environmental concern.

1.1. LEACHING METHODS TO EVALUATE THE LEACHING BEHAVIOR OF TRACE ELEMENTS FROM FLY ASH

There are a variety of leaching tests available to characterize the leaching behavior of trace elements from fly ash. The commonly used leaching procedures in the United States include those developed by U.S. Environmental Protection Agency (USEPA) and the American Society for Testing and Materials (ASTM), e.g. the extraction procedure (EP), the toxicity characteristic leaching procedure (TCLP), the synthetic precipitation leaching procedure (SPLP) (USEPA, 1992; 1994; 2004) and method ASTM-D3987. These standard methods, although widely used for regulatory purpose, environmental impact assessment, waste management and academic research, have deficiencies, such as modeling a single disposal scenario, not being intended to produce leachate representative of leachate generated in the field, etc. To address these deficiencies, The U.S. EPA Science Advisory Board (SAB) has recommended developing a leaching method that involve a better understanding of the mechanisms controlling leaching, multiple tests to address different disposal scenarios, and improved models to complement the leaching tests. (U.S. EPA SAB, 1991)

Kosson et al. (2002) and van der Sloot et al. (1994) proposed an integrated leaching framework to evaluate the leaching characteristics of inorganic constituents from various solids over a range of leaching conditions (e.g., pH, solid-to-liquid (S/L) ratio and waste form) in field management scenarios. This framework has improved our understanding on the leaching behavior of trace elements under a variety of field conditions. It would be beneficial, however, to develop a predictive capability based on fundamental parameters to quantify the leaching behavior. For those elements whose leaching is controlled by adsorption-desorption process, two intrinsic parameters, i.e. the

total leachable mass and the adsorption constant of the element of concern, determine the leaching behavior of these elements under various field conditions. With these two parameters, one can calculate the equilibrium concentration of the element in the leachate. Approaches such as long term or serial leaching, extraction with chelating agent or under extreme pH conditions have been developed to determine the total leachable mass of the element of concern in solid waste. However, these approaches are either very time consuming or only effective for specific elements. Even though we have the ability to determine the accurate value of the total leachable mass, we still need to know the adsorption constant in order to predict the leaching behavior of trace elements in solid media. Therefore, a simple, practical protocol is desired to determine the leaching parameters representing the availability and the stability of the elements of concern in solid media.

1.2. ARSENIC AND SELENIUM IN FLY ASH AND THEIR ENVIRONMENTAL CONCERN

Among all the trace elements in fly ash, arsenic and selenium are two oxyanionic elements of most concern because of their toxicity. Arsenic and certain arsenic compounds are known as carcinogenic to humans through both oral and inhalation routes. Long term exposure to arsenic can cause cancer of skin, liver, lung bladder and kidney (Smith et al., 1992). Effective January 2006, the Maximum Contaminant Level (MCL) for arsenic in drinking water was revised by USEPA from 50 $\mu g\ L^{-1}$ to 10 $\mu g\ L^{-1}$ (USEPA, 2002). The new MCL necessitates a more detailed evaluation of sources of arsenic that could potentially impact water quality, particularly anthropogenic sources that can be controlled. For bituminous coal fly ash, the arsenic concentrations are

typically below 200 ppmw (parts per million by weight) but can range from 1 to 1000 ppmw, depending on coal source and combustion technology (EPRI, 1987). Though selenium is an essential element for plant and animal nutrition at trace levels, it can cause severe respiratory and neurological problems if uptake exceeds threshold levels (ATSDR, 2003). USEPA regulated the MCL of selenium in drinking water to below 50 μg L^{-1} (USEPA, 2002). The Se concentration in coal fly ash can be as high as 200 ppmw (Kim, 2002), although it is usually less than 50 μg/g and is typically in the range of 10 to 20 μg/g (EPRI, 1987).

Previous studies demonstrated that the leaching behavior of arsenic and selenium from fly ash were affected by pH, solid-to-liquid (S/L) ratios, leaching time, temperature, the types of fly ash and presence of other cations/anions and (Otero-Rey et al., 2005; Baba and Kaya, 2004; Brunori et al., 1999; Jankowski et al., 2005; Iwashita et al., 2005,; EPRI, 2006a). U.S. EPA (2006) reported that under leaching conditions ranging from very acidic to very alkaline, the total leached arsenic was variable among different fly ashes, ranging from less than 5% in half of the ashes tested, to more than 30% in others. Iwashita et al. (2005) concluded that the leaching amount of selenium was essentially dependent upon its concentration in fly ash, while other studies have found no correlation between the total content of selenium in the ash and the concentration in the leachate (EPRI, 1987; U.S. EPA, 2006). van der Hoek et al. (1994) conducted leaching test with both acidic ash (bituminous coal ash) and alkaline ash (subbituminous coal ash) and found that the leaching behavior of arsenic and selenium from the two types of ashes are quite different. The acidic ash displayed elevated leaching of arsenic and selenium with increase of pH from 4 to 12, while the alkaline ash exhibited an opposite pH effect on the

leaching of both elements. Iwashita et al. (2005) also reported the decrease of Se leaching from an alkaline ash as pH was increased from 8 to 12. This difference was attributed to different phases controlling the leaching of arsenic and selenium from the two types of ashes.

1.3. MECHANISM AND MODELING STUDY ON LEACHING OF ARSENIC AND SELENIUM FROM FLY ASH

Several mechanisms have been proposed to interpret arsenic and selenium leaching behavior from fly ash. By comparing the leaching characteristics of arsenic and selenium from fly ash with their adsorption onto the major mineral compounds in fly ash, van der Hoek et al. (1994) concluded that arsenic and selenium leaching from acidic ash was likely to be controlled by surface complexation with iron oxide, while a calcium phase was shown to be responsible for alkaline ash. This conclusion is in agreement with that of Zielinski et al. (2006), who studied the mode of occurrence of arsenic in fly ash with XAFS spectroscopy, and reported that arsenic was associated with some combination of iron oxide, oxyhydroxide or sulfate in a highly acidic fly ash, but with a phase similar to calcium arsenate in a highly alkaline ash. Hassett et al. (1991) and Lecuyer et al. (1996) had attributed the stabilization of selenium in subbituminous coal ash to the formation of ettringite ($3CaO \cdot Al_2O_3 \cdot 3CaSO_4 \cdot 32H_2O$) at high pHs. Substitution for sulfate in the structure was suggested to be the relavant process. Aluminum oxide may also contribute to the adsorption of selenite in fly ash (Rajan, 1979; Hansen and Fisher, 1980; van der Hoek and Comans, 1996). Isabel and Annette (2003) reported that precipitation of $CaSeO_3$ could be another reason for the retention of selenite

in fly ash. In a word, the mechanism of arsenic and selenium leaching from fly ash is dependent on field conditions and fly ash characteristics.

Surface complexation models considering surface electrostatic effects have been used to quantify the adsorption/desorption of arsenic, selenium and other trace elements on various adsorbents (Goldberg, 1985; Goldberg and Glaubig, 1988; Dzombak and Morel, 1990, Hering and Dixit, 2005) and proved to be successful on laboratory studies. However, in natural systems, not all the parameters necessary for the surface complexation model are known, and its application is limited for systems with multiple adsorbents and heterogeneous surface sites (Honeyman and Santschi, 1988). Other researchers used a simplified surface complexation approach without surface charge correction to model the sorption of arsenic and selenium on iron hydroxide, and obtained the apparent adsorption constants comparable with literature data (Belzile and Tessier, 1990; van der Hoek and Comans, 1996). Based on Langmuir adsorption isotherm, Wang et al. (2004) also developed a modeling approach to determine the types and quantity of reactive surface sites on a class F fly ash and to quantify its capability on metal (cations) adsorption. This approach, although without incorporation of the electrostatic effect, was proved to be effective and accurate on modeling the adsorption of Cd(II), Cr(II), Cu(II), Ni(II) and Pb(II) on the fly ash, providing a valuable insight into the modeling the leaching/adsorption of anionic elements (e.g., arsenic and selenium) on fly ash.

1.4. SPECIATION OF ARSENIC AND SELENIUM IN FLY ASH AND THE GENERATED LEACHATE

The speciation of arsenic and selenium plays an important role on the toxicity and mobility of the elements of concern (Gerin et al., 1997). For example, arsenite (As(III))

generally has a higher toxicity and mobility than arsenate (As(V)), monomethylarsonic acid (MMA) and dimethylarsinic acid (DMA)) have been identified as less toxic than the inorganic forms, and arsenobetaine (AsB) is believed to be nontoxic (Hirata et al., 2006). For the two inorganic selenium species, selenite (Se(IV)) has been reported to be more toxic but less mobile in aqueous environment than selenate (Se(IV)) (Merrill et al., 2006; Goldberg and Glaubig, 1988; EPRI, 2006b; EPRI, 1994). With assistance of surface and aqueous analytical techniques, previous studies demonstrated that the predominant species of arsenic and selenium in fly ash and its liquid extracts from fly ash were As(V) and Se(IV), respectively (Wadge and Hutton, 1987; Jackson and Miller, 1999; Narukawa et al., 2005; Goodarzi and Huggins, 2001; Huggins et al., 2007).

Accurate measurements of arsenic and selenium species in fly ash leachate are desired for the environmental impact assessment. Coupled instrumental techniques are commonly used for the speciation analysis of As and Se in aqueous samples. Species separation can be achieved with ion chromatography (IC) (Jackson and Miller, 1999; Schlegel et al., 1994) or high performance liquid chromatography (HPLC) (Wadge and Hutton, 1987; Manning and Martens, 1997). Subsequent concentration detection can be performed using atomic adsorption spectrometry (AA) (Wadge and Hutton, 1987), inductively coupled plasma atomic emission spectrometry (ICP-AES) (Schlegel et al., 1994), and ICP-mass spectrometry (ICP-MS) (Lindermann et al., 2004; Orero Iserte et al., 2004;). The combination of HPLC with ICP-MS becomes more and more preferable for both academic research and industrial application due to its high sensitivity, minimal sample pretreatment, and the ability for simultaneous analysis of arsenic and selenium

(Lindermann et al., 2004; Orero Iserte et al., 2004; Martinez-Bravo et al., 2001). Therefore, the HPLC-ICP-MS system was selected for the speciation analysis of arsenic and selenium in this study.

2. PURPOSES AND OBJECTIVES

Arsenic, selenium and other potentially toxic elements pose a preeminent water quality problem and challenge facing environmental engineering in the world. Because of the large volumes of coal fly ash produced around the world, it is a potentially significant anthropogenic source of these elements. The leaching behavior of arsenic and selenium from fly ash, which is important for predicting potential impacts of fly ash on water quality is not well understood. A variety of leaching methods have been developed to determine the leaching characteristics of trace elements from fly ash. However, these methods had deficiencies such as modeling a single disposal scenario, not being intended to produce leachate representative of leachate generated in the field, time consuming or not suitable for all the elements of concern. Studies are lacking on how to determine the types and quantity of active surface sites, or the total availability and stability of specific element on fly ash. Surface complexation models had been widely used to quantify the adsorption/desorption of arsenic, selenium and other elements on various solid media. However, the incorporation of electrostatic effect had introduced more parameters than can be verified under field conditions. Therefore, the overall purpose of this study is to develop mechanistic understanding of the trace element leaching process in fly ash, and quantify their leaching behavior under various conditions with a simple and robust adsorption model. Specific objectives were as follows:

1. To date, few studies are available to evaluate the leaching potential of trace elements from fly ash under various conditions both qualitatively and quantitatively, hence, first objective of this work was to establish a practical protocol to determine the leaching parameters representing the availability

and the stability, i.e. the total leachable mass and the adsorption constant, for trace cationic elements in fly ash using model elements Cu(II), Cd(II), and Ni(II)

2. In order to fully understand the leaching behavior of arsenic and selenium from fly ash and their controlling mechanisms, the author launched a study to investigate arsenic and selenium leaching from and adsorption onto both bituminous and subbituminous coal ashes and their influence factors such as pH, presence of calcium and sulfate

3. Based on the qualitative results from the leaching and adsorption study of arsenic and selenium from and onto fly ash, a quantitative adsorption model is to be developed to describe the leaching/adsorption process of arsenic and selenium on fly ash under various pH conditions. This model will help predict the potential impact of arsenic and selenium leaching on ground water quality. Particularly, the effect of calcium on arsenic partitioning with fly ash will also be incorporated in the adsorption model. Since previous studies proved that the adsorption isotherm can be accurately simulated without surface charge correction, the surface electrostatic effect will not be considered in this model.

4. The speciation profile of arsenic and selenium largely determines their toxicity and mobility in the environment. Another objective of this research is to investigate the speciation of arsenic and selenium in fly ash under natural pH conditions. Various S/L ratios and different leaching time will be applied to evaluate their impact on the speciation variation. HPLC-ICP-MS

has been widely used for the speciation analysis of arsenic and selenium in aqueous samples. The suitability of this analytical technology being used for fly ash leachate samples will also be assessed.

3. MATERIAL AND EXPERIMENTAL

To fulfill the aforementioned objectives, the following experimental plan was implemented:

1. Batch equilibrium titration method was used to determine the densities and the acidity constants of surface sites on fly ash. Please refer to Paper I.
2. Batch leaching of raw ash was used to explore the leaching behavior of arsenic, selenium and other trace elements from fly ash. Please refer to Paper II.
3. Batch adsorption/partitioning experiment was used to investigate the adsorption behavior of trace elements onto fly ash, and to quantify their adsorption strength (adsorption constants) on fly ash surface. Please refer to Paper III.
4. Microwave assisted acid digestion was used to determine the total chemical composition of fly ash samples. Please refer to Paper IV.
5. Other experiments and approaches was used to determine the physical-chemical characteristics of fly ash samples, including loss-on-ignition (LOI), BET surface area, total elemental composition with XRF, pH at point of zero charge (pH_{pzc}). Please refer to Paper IV.
6. Speciation analysis for arsenic and selenium in fly ash leachate with HPLC-ICP-MS. Please refer to Paper V.

PAPER

I. QUANTIFYING THE AVAILABILITY AND THE STABILITY OF TRACE CATIONIC ELEMENTS IN FLY ASH *(Waste Management 2007, 27, 1345-1355)*

Tian Wang [a], Jianmin Wang [a,*], Heng Ban [b], Ken Ladwig [c]

[a] *Environmental Research Center; Dept. of Civil, Architectural and Environmental Engineering; Univ. of Missouri-Rolla, Rolla, MO 65409, United States*

[b] *Department of Mechanical Engineering, University of Alabama at Birmingham, Birmingham, AL 35294, United States*

[c] *Electric Power Research Institute (EPRI), 3412 Hillview Ave., Palo Alto, CA 94304, United States*

[*]Corresponding author: (phone) (573) 341-7503; (fax) (573) 341-4729; (email) wangjia@umr.edu

Abstract

For adsorption-desorption controlled leaching processes, the total leachable mass and the adsorption constant are parameters representing the availability and the stability of trace elements in solid media. With these parameters, one can predict the leaching behavior of trace elements from solids under various pH and solid-to-liquid ratio conditions. An approach was developed in this paper to determine these parameters for model elements Cu(II), Cd(II), and Ni(II) in fly ash. This approach consists of a batch equilibrium titration, a batch equilibrium leaching with and without target element addition, and mathematical modeling. Results indicated that the adsorption constant of a trace element can be determined by modeling the adsorption ratio of the added element to the system as a function of pH. Results also indicated that the trace element originally present in fly ash had similar adsorption-desorption behavior as that added externally. By modeling the batch leaching data with and without external element addition, the total leachable mass and adsorption constant of the target element can be determined simultaneously. The total leachable mass is in agreement with experimental data from 50 mM EDTA extraction.

Keywords: fly ash, metal, leaching, availability, stability

1. Introduction

Coal fly ash has the potential to release trace elements into soil, surface water and groundwater (Kim and Kazonich, 1999). It has been reported that potentially toxic elements Ag, As, B, Ba, Cd, Co, Cr, Cu, Hg, Ni, Pb, Se, and Zn can be leached from fly ash (EPRI, 1998; Mehnert and Hensel, 1996). Understanding the factors controlling the leaching behavior of trace elements is critical in predicting potential impacts of fly ash on the environment. A variety of leaching methods were used to investigate the leaching of trace elements from fly ash. These methods can be generally categorized as static tests (batch leaching) and dynamic tests (column leaching) depending on whether the leaching fluid is a single addition or is renewed (Kim, 2002). The U.S. Environmental Protection Agency (USEPA) published several standard leaching procedures, namely, the extraction procedure (EP), the toxicity characteristic leaching procedure (TCLP), and the synthetic precipitation leaching procedure (SPLP) (EPA, 1992; 1994; 2004). The EP and TCLP are expected to simulate the leaching of solid wastes placed in a municipal landfill. The SPLP is designed to simulate a monofill disposal scenario (Murarka, 1999). American Society for Testing and Materials (ASTM) has also proposed a standard method using water instead of acid solution as the leachant (ASTM-D3987). These standard methods have been widely used to assess the leaching behavior of trace elements for many types of solids, including fly ash, bottom ash, fly ash incorporated cement, and municipal solid waste incinerator ashes (Lo et al., 2000; Zhang et al., 2001; Egemen and Yurteri, 1996; Wang and Chiang, 1996; Maxwell, 1993). While these methods are simple to perform, the fixed pH conditions of leachants may not reflect the field management scenarios.

Therefore, the actual leaching behavior in field may be significantly different from that obtained in lab.

In order to overcome these limitations, Wang and his associates used a range of pH conditions to conduct batch leaching and partitioning experiments (Wang J., et al., 2004; 2005; Wang H. et al., 2003a; 2003b; Teng et al., 2003a; 2003b). Kosson and van der Sloot et al. also proposed an integrated leaching framework, which determines the leachability of trace elements for a range of pH conditions and solid-to-liquid (S/L) ratios, to evaluate the leaching characteristics for various solids in field management scenarios (Kosson et al., 2002; van der Sloot et al., 1994). These methods and results improved our understanding on the leaching behavior of trace elements under a variety of field conditions. However, it would be beneficial to develop a predicative capability based on fundamental parameters to quantify the leaching behavior. For elements whose leaching is controlled by adsorption-desorption processes, the total leachable mass, i.e. the intrinsic parameter determining the availability, and the adsorption constant, i.e. the intrinsic leaching parameter determining the binding strength or the stability, determine the leaching behavior of these elements under various field conditions. With these two parameters, one can calculate the equilibrium concentration of the element in the leachate.

Several methods have been used to directly determine the total leachable mass. However, these methods often have limitations. For example, long-term column leaching, sequential batch leaching, and serial batch leaching normally take weeks or months to complete (Zhang et al., 2001). Extractions using chelating agents such as ethylenediaminetetraacetic acid (EDTA) and sodium gluconate have also been used to determine the total leachable mass for some elements (Xu et al., 2001; Van Herck et al.,

1998; Garrabrants and Kosson, 2000). However, these extraction methods do not apply to elements that do not form complexes with chelating agents. Even for elements that form complexes with chelating agents, the metal complexes may also be adsorbable. As a result, not all metals are in the soluble phase. Some methods use extreme pH conditions to estimate the total leachable mass of trace elements. However, it is difficult to determine an appropriate pH for a specific solid medium, and it is possible that not all elements are released under a pre-selected pH condition. On the other hand, some solid particles may dissolve under extreme pH conditions. As a result, elements that are originally could not be released under field pH conditions (e.g. elements embedded in the structure of solids) could be dissolved into the liquid phase, which may result in high leachable mass fraction estimates. Even though we have the ability to determine the accurate value of the total leachable mass, we still need to know the adsorption constant in order to predict the leaching behavior of trace elements in solid media. The objective of this study is to establish a practical protocol to determine the leaching parameters representing the availability and the stability, i.e. the total leachable mass and the adsorption constant, for trace cationic elements in fly ash using model elements Cu(II), Cd(II), and Ni(II).

2. Theoretical aspects

For the trace cationic elements of which the leaching is controlled by adsorption-desorption, the following equation can be used to describe their partitioning (i.e. the adsorption ratio) in fly ash under low metal loading conditions (Wang et al., 2004):

$$R = \frac{\alpha_H K_S S_T}{1 + \alpha_H K_S S_T} \quad (1)$$

where R is the adsorption ratio (i.e. the ratio of the adsorbed element to the total element in the system); α_H is the ratio of free surface site to the total non-metal-complexed surface site, $\alpha_H = \frac{K_H}{[H^+] + K_H}$; K_H is the surface acidity constant (M); K_S is the adsorption constant (M^{-1}); S_T is the total surface site concentration (M), $S_T = \Gamma_m \times SS$; Γ_m is the surface site density (mol/g); SS is the concentration of fly ash (g/L); and $[H^+]$ is the proton concentration in the bulk solution (M).

The adsorption ratio R can be calculated using the measured element concentration in solution and the total element concentration in the system (if known). By modeling R – pH relationship, the adsorption constant, K_S, can be determined. It should be noted that the application of Equation 1 requires knowledge of the total element concentration in the system. Therefore, this equation is more suitable for describing adsorption/partitioning in a system that uses relatively clean solids where the amount of the target element carried to the system by solids can be ignored or estimated without causing significant error during R calculation.

For raw ash with unknown background element concentration, the partitioning of the trace element can not be directly calculated. However, an experiment with external element addition can be conducted. By modeling the adsorption ratio of the added element using Equation 1, the adsorption constant can also be determined.

The adsorption ratio of the added element can be calculated using the following equation:

$$R = 1 - \frac{\Delta M_d}{M_{add}} \qquad (2)$$

where ΔM_d is the difference between the dissolved element concentration for the experiment with the external element addition and that without external element addition (baseline data) for the same pH condition (mg/L), and M_{add} is total added element concentration (mg/L).

It should be noted that this method of determining the adsorption constant only valid when the total element concentration in the system is very low compared to the surface site concentration, so that the adsorption of the element is in the linear range of the Langmuir isotherm. Previous research indicated that as long as the total element concentration is less than 10% of the total surface site concentration, the adsorption is in the linear range of the Langmuir isotherm (Wang et al., 2004). This criterion can be easily met for most environmental media including fly ash.

The overall adsorption ratio of the target element in the system can be expressed as a function of the total dissolved element concentration and the total element addition:

$$R = 1 - \frac{M_d}{M_b + M_{add}} \tag{3}$$

where M_d is the total dissolved element concentration (mg/L), and M_b is the background element concentration carried into the system by solids under a specific S/L ratio (mg/L).

Combining Equations 1 and 3 yields the following equation:

$$M_d = \frac{M_b + M_{add}}{1 + \alpha_H K_S S_T} \tag{4}$$

Equation 4 indicates that the total soluble element concentration is a function of pH and added element concentration. By fitting experimental M_d – (pH, M_{add}) data using a multiple variable nonlinear regression program, the total background element concentration (M_b) and the adsorption constant (K_S) can be determined. M_b can be

converted to the total leachable mass of the element (TLM) in mg element/kg ash, or ppmw, based on the solids concentration (SS) in kg/L, shown in the following equation:

$$TLM = \frac{M_b}{SS} \quad (5)$$

The fly ash surface site density (Γ_m) and acidity constant (K_H), which are essential parameters for adsorption modeling, can be determined using a method developed by Wang et al. in previous publications (Wang et al., 2000; 2004).

3. Materials and methods

3.1. Fly ash

Two ash samples were used in this study. Sample AN/Col #2 was collected from the cold side electrostatic precipitator (ESP) of a facility burning eastern bituminous coal. Sample AN/NRT #2 was collected from the same facility when it was burning a different eastern bituminous coal with slightly higher calcium content. Table 1 lists the loss on ignition (LOI), BET surface area, and total elemental composition for Cu(II), Cd(II) and Ni(II).

Washed ash samples were used for surface characterization, i.e. the determination of surface site density and acidity constant. The purpose of washing was to reduce the interferences of soluble materials on acid or base consumption. All washing was performed with deionized water at the S/L ratio of 1:5 (200 g/L), and was repeated for five times. Aeration was used to agitate the ash – water mixture, and each washing lasted for 20 hours. Washed ash was dried in an oven at 105 °C for at least 24 hours before use. Washed AN/Col #2 sample was also used in adsorption experiments to determine the adsorption behavior of trace elements under ideal conditions.

Raw AN/Col #2 and AN/NRT #2 ash samples were used in batch leaching experiments, with and without external element addition, to determine the total leachable mass and the adsorption constant of trace elements. All samples were dried at 105 °C for at least 24 hours before use.

3.2. Batch partitioning of washed ash

A batch method established previously was employed in this study to determine element adsorption behavior under ideal conditions, using washed ash samples (Wang et al., 2004). The procedure was as follows: for the set of experiments with S/L ratio of 1:10, 10 g fly ash samples were added into each of several 125-mL LDPE bottles. There were two or three groups of bottles, corresponding to two or three initial element concentrations to be tested. One bottle in each group was kept empty as a blank. Then 100 mL water that contains 0.01 M of $NaNO_3$ and the pre-selected concentrations of elements were added to each bottle including the blank. $NaNO_3$ was used to adjust the ion strength. All bottles in the same group had the same initial element concentration. Nitric acid (HNO_3) or sodium hydroxide (NaOH) were used to adjust the pH value in each group of bottles to a desired pH distribution in the range from 2 to 12. No acid or base was added to the blank. All bottles were loaded on a shaker and shaken for 24 hr. After shaking, samples were settled for overnight, and the supernatant was collected and acidified for measurement of the element of concern. Final pH values were measured with the rest sample in bottles.

3.3. Batch Leaching of Raw Ash

The procedures for this experiment were the same as those described above except that raw ash samples were used, and the ionic strength was not adjusted. For both

ashes, TDS was determined to be approximately 500 - 750 mg/L in pH range of 4-10 at S/L of 1:10. Therefore, the ionic strength was estimated to be in the range between 0.013 – 0.019 M, based on the equation $I = 2.5 \times 10^{-5} \times TDS$, where I is in (M) and TDS is in (mg/L) (Fair et al., 1968). Samples were divided into 3 groups for the background leaching experiment (no external metal addition), and the leaching experiments with 2 mg/L and 5 mg/L of target element addition, respectively.

3.4. EDTA extraction

An EDTA extraction method used by Kosson et al. was modified and applied in this experiment (Kosson et al., 2002). Ten grams of fly ash was leached with 100 mL of 50 mM EDTA at different pH value within pH range from 4 to 9. After shaking for 24 hours, the samples were centrifuged for 15 min at 3000 rpm, and supernatants were collected and analyzed for dissolved metal concentrations.

3.5. Analytical method

Flame Atomic Absorption Spectrophotometer (FLAA model 3110; Perkin-Elmer Corp., Norwalk, Connecticut, USA) were used to determine concentrations of Cu(II), Cd(II), and Ni(II) in the solution. The detection limits for the three elements of concern are in range from 0.03 mg/L to 0.1 mg/L. Triplicate measurements were applied for each sample and the average values were taken as final results. Duplicates and spiking checks were conducted for quality control, and 90-110% of recovery was obtained for all the samples. An Orion PerpHecT Triode pH electrode (model 9207BN) and a pH meter (PerpHecT LoR model 370) were used for pH measurement.

3.6. Data analysis

A single variable non-linear regression program, Kaleidagraph™ (Synergy Software, 2002) was used to fit batch equilibrium titration data for the determination of the surface site density and acidity constant. A multiple-variable non-linear regression program, NLREG (Sherrod, 2005), was used to fit batch partitioning and batch leaching data for the determination of the total leachable mass and the adsorption constant. NLREG performs statistical regression analysis to estimate the values of parameters for nonlinear functions with least-squares algorithm. The regression analysis determines the values of the parameters that cause the function to best fit the experimental data.

4. Results and discussion

4.1. Surface site characterization

Batch equilibrium titration method was used to determine the surface site density and the acidity constant. Figure 1 shows net titration data (points) for ash samples AN/Col #2 and AN/NRT #2, which are differences between the overall acid/base consumption (by ash and water) and that by blank (by water only). An equation developed in a previous study was used to fit the net titration data (Wang et al., 2004). The solid curves in Figure 1 are curve fitting results. Based on the curve fitting, it was found that both samples have three types of acid sites, α, β, and γ. Table 2 shows the site density and the acidity constant of each site. Based on a previous investigation (Wang et al., 2004), the deprotonated form of site α is neutrally charged and has negligible adsorption constant to cationic elements. Therefore, it is not considered for cationic element adsorption. Site γ has very high acidity constant (pK_H). Therefore, when free surface site γ are available, all cationic metal species are in negatively charged hydroxide

form which are no longer adsorbable by negatively charged free site γ. The free site β is the only reasonable one for cationic metal adsorption. The modeling results based on only site β also fit the experimental data very well. Therefore, the free site β is responsible for the adsorption of cationic elements.

4.2. Metal partitioning with washed ash

Figure 2 shows the experimental and modeling results for Cu(II), Cd(II) and Ni(II) partitioning with washed ash AN/Col #2. The results indicate that the maximum concentrations of Cu(II) and Ni(II) in solution were slightly greater than the concentrations added, which indicates that the washed ash still has residual elements and contributes some dissolved Cu(II) and Ni(II). For Cd(II), the maximum concentrations in solution are similar with those added externally due to the low background Cd(II) concentration in the ash sample. Based on the above information, the background concentrations (M_b) of Cu(II), Cd(II) and Ni(II) in washed ash were estimated to be 2 mg/L, 0 mg/L and 0.5 mg/L, respectively, and the adsorption ratios were calculated using Equation 3. Figure 2(d) shows the adsorption ratios of Cu(II), Cd(II) and Ni(II) as a function of pH. For each element, data points with different initial concentrations were combined together. It can be seen that the adsorption ratios of all elements increase with the increase of pH. Almost all Cu(II) is adsorbed by the fly ash when pH is greater than 6; for Cd(II) and Ni(II), the complete adsorption occurs when pH is above 8.

Equation 1 was used to fit the partitioning data in Figure 2(d). Previously determined parameters including the surface site density and the acidity constant for site β were applied to the model. The modeling results, shown as solids curves, agree with experimental data. Since all data points fit well with the same curve, it proved that the

metal partitioning process is controlled by adsorption/desorption and in the linear range of Langmuir adsorption isotherm (Wang et al., 2004). Model results indicate that adsorption constants ($\log K_S$) of Cu(II), Cd(II), and Ni(II) on the washed ash are, respectively, 6.4, 4.6, and 5.1. The correlation coefficients (R^2) of the curve fittings are, respectively, 0.991, 0.997, and 0.994. These values are similar to those obtained using an ash generated in a different power plant burning the similar type of coal (Wang et al., 2004).

4.3. Batch leaching of raw ash with and without external element addition

Background leaching and leaching with two levels of external element additions for Cu(II), Cd(II), and Ni(II) were investigated using raw ash. Figures 3(a) – 3(c) show dissolved concentrations of Cu(II), Cd(II) and Ni(II) as a function of pH (experimental data shown as points). Figure 3(d) plots the adsorption ratio of the added elements as a function of pH (points), calculated using Equation 2. Equation 1 was used to fit these data. The solid curves in Figure 3(d) are the curve fitting results. Results indicate that adsorption constants ($\log K_S$) of Cu(II), Cd(II), and Ni(II) on the raw ash are, respectively, 6.1, 4.5, and 5.0. The correlation coefficients (R^2) of the curve fittings are, respectively, 0.982, 0.998, and 0.997. These results are almost identical to those for washed ash. Therefore, the method to determine the adsorption constant by modeling the adsorption ratio of the added element as a function of pH is validated. The agreement of these results also indicates that the adsorption of the three elements in this experiment is in the linear range of the Langmuir isotherm. Since the metal leaching from raw ash has similar performance as metal adsorption by washed ash, and both fit Equation 1 that was derived

on by adsorption hypothesis, the leaching of the three elements is also mainly controlled by adsorption–desorption.

Although the adsorption constant values from the raw ash and those from the washed ash are same in this study, the results obtained using raw ash are considered more practical than those obtained using washed ash, since no background estimation was made during adsorption ratio calculation for the raw ash. In addition, by using the differences between soluble element concentrations for the experiment with external element addition and that without external element addition (baseline), the concentration error caused by particle dissolution can be eliminated. Moreover, constants obtained using raw ash without ionic strength adjustment can better reflect the field condition.

4.4. The total leachable mass

In this study, we define the total leachable mass as the total amount of trace elements available for leaching, or the availability. Equation 4 was used to fit experimental data in Figures 3(a) – 3(c) to determine the total element concentration carried to the reactor by solids, or the background concentration. With previously determined parameters such as the surface site density, acidity constant, and adsorption constant, the only unknown parameter in Equation 4 is M_b. It was determined using non-linear regression programs. Since M_b was determined after K_S was known, this method is defined as "step method". Table 3 summarizes the background concentrations of Cu(II), Cd(II), and Ni(II) at S/L = 1:10 and their adsorption constants. Table 3 also listed the values for total leachable mass in mg element/kg ash (or ppmw) calculated from the M_b.

The solid curves in Figures 3(a) – 3(c) are modeling results, which are in agreement with overall experimental data. However, it is observed that, for the

background leaching data, the measured soluble Cu and Ni concentrations are slightly greater than modeling results when pH is less than 3. This difference is caused by the dissolution of ash particles when pH is less than 3, which may release extra elements to the soluble phase. Since this low pH is considered not practical in field, the calculated background value could better represent the total leachable mass under practical conditions.

4.5. Simultaneous determination of M_b and K_S

Both the background concentration (M_b) and the adsorption constant (K_S) can be determined simultaneously by fitting the experimental M_d - (pH, M_{add}) relationship using Equation 4. Table 3 also shows the calculated K_S and M_b results, denoted as the "integrated method", as well as the converted total leachable mass values. These values are comparable with the results obtained earlier when M_b and K_S were determined separately. Therefore, it can be concluded that elements originally present on fly ash surface have the same adsorption-desorption behavior as those added externally, and the simultaneous determination of M_b and K_S can simplify the modeling efforts without causing significant error.

It is obvious that the step method is more complex than the integrated method for the determination of the total leachable mass and the adsorption constant. However, the K_S value determined using the step method is considered more accurate than that based on the integrated method. This is because that the step method uses the adsorption ratio of the added element to calculate K_S. By using the difference of the dissolved element concentrations between the experimental data with external element addition and the baseline data for the determination of element adsorption ratio, the interferences of extra

elements released from solids as a result of particle dissolution under extreme pH conditions can be eliminated.

Theoretically, K_S and M_b can be simultaneously determined using Equation 4 based on only the background leaching data. However, since relatively large amount of extra elements can be released to the solution under very low pH conditions as a result of particle dissolution, using only one set of background leaching data to determine both K_S and M_b could result in large error. By conducting experiments with external element addition, more experimental data can be generated, and more reliable modeling results can be obtained. For example, if only the background leaching data (S/L =1:10) were used for determining the total leachable mass and the logK_S of Ni in ash AN/Col #2, the results were 0.7±0.1 mg/kg and 5.9±0.2, respectively. Both calculated values have greater standard errors than those obtained using all three groups of data, and the correlation coefficient R^2 is also decreased from 0.98 to 0.91.

4.6. Method verification with a different S/L ratio

Since the total leachable mass and the adsorption constant are intrinsic parameters of fly ash, their values are independent of the S/L ratio. The effectiveness of above method was verified using a S/L ratio of 1:5. Figure 4 shows experimental data (points) and modeling results (solid curves) when M_b and K_S are determined separately. Table 3 lists the adsorption constants and background concentrations obtained from both the step method and the integrated method. The total leachable mass and the adsorption constant values are almost identical to those obtained under S/L = 1:10 condition. Therefore, the approach developed in this study can be effectively used to determine the total leachable mass and the adsorption constant for trace cationic elements in fly ash.

4.7. Method verification using a different fly ash

A second raw fly ash sample, AN/NRT #2, was used to verify the effectiveness of the method for the determination of total leachable mass and the adsorption constant. All experiments were conducted at S/L ratio of 1:10 using the same procedure described above. Figure 5 shows the experimental data and curve fitting results, and Table 3 lists the curve fitting parameters for both step and integrated methods. Curve fitting results show that the approach developed in this study also works well for ash AN/NRT #2, and parameters determined from the integrated method are very close to those from the step method.

4.8. EDTA extraction experiment

EDTA is a strong chelating agent which has been frequently used for soil remediation and heavy metal extraction (Van Herck et al., 1998; Song and Greenway, 2004). Kosson et al. used an EDTA extraction method to determine the potentially extractable content of wastes and secondary materials (Kosson et al., 2002; Garrabrants and Kosson, 2000). The method was modified here to determine the total leaching mass of Cu(II), Cd(II), and Ni(II) in fly ash.

Figure 6 shows the extraction results for both AN/Col #2 and AN/NRT #2 ashes. Results indicate that the pH does not significantly affect the soluble element concentrations. The average concentration is taken as the background value, assuming that all elements were extracted to the soluble phase by EDTA. These values are converted to the total leachable mass in mg/kg ash.

Figure 7 shows the total leachable mass for Cu(II), Cd(II), and Ni(II) determined using different methods and under different S/L ratios. It indicates that there is no

significant difference between them. It was noticed that the results of Cd(II) from step method and integrated method (S/L =1:10) are negative numbers for both ashes. This is because that the total leachable mass of Cd(II) in both ashes is close to zero, while the nonlinear regression program tried different value to fit the experimental data from both directions. Therefore, it is no surprise to come out a small negative value. Compared to the EDTA extraction method, the approach developed in this study has the advantage of determining the total leachable mass for elements that do not form complex with EDTA or other chelating agents. In addition, it can be used to determine the adsorption constant of trace elements, which is a parameter quantifying the stability. With these two parameters, one can predict the equilibrium concentration of trace elements in solution under various pH and S/L ratio conditions. This approach may also be appropriate to determine the intrinsic leaching characteristics of other trace cationic elements in fly ash. It is also expected that this approach could be normalized to determine the intrinsic leaching parameters of trace cationic elements in other solid media.

5. Conclusions

The batch leaching results with and without external element addition indicate that the trace elements originally present in fly ash have the similar adsorption-desorption behavior as those added externally. The total leachable mass and the adsorption constant are parameters representing the availability and the stability of trace elements in fly ash, which play an important role on their leaching behavior under various pH and S/L ratio conditions. These parameters for Cu(II), Cd(II), and Ni(II) in fly ash are determined by modeling batch leaching data with and without external element addition. The values of these parameters obtained under different S/L ratios are consistent. The total leachable

mass values also agree with those determined using the EDTA extraction method, indicating that it is an appropriate approach to determine the intrinsic leaching characteristics of Cu(II), Cd(II), Ni(II) and other trace cationic elements with similar leaching mechanisms.

Acknowledgements

This work was supported by the Electric Power Research Institute (EPRI) and the Environmental Research Center (ERC) for Emerging Contaminants at the University of Missouri-Rolla (UMR). Authors also wish to thank Dr. Glenn Morrison, Dr. David Drain, and Dr. Eliot Atekwana for their comments. Conclusions and statements made in this paper are those of the authors, and in no way reflect the endorsement of the funding agencies.

References

Egemen, E., Yurteri, C., 1996. Regulatory leaching tests for fly ash: A case study. Waste Management & Research 14, 43-50.

EPA, 1992. Toxicity Characteristic Leaching Procedure. US Environmental Protection Agency, Method 1311, Test Methods for Evaluating Solid Waste: Physical/Chemical Methods (SW-846).

EPA, 1994. Synthetic Precipitation Leaching Procedure. US Environmental Protection Agency, Method 1312, Test Methods for Evaluating Solid Waste: Physical/Chemical Methods (SW-846).

EPA, 2004. Extraction Procedure Toxicity Test Method. US Environmental Protection Agency, Method 1310B, Test Methods for Evaluating Solid Waste: Physical/Chemical Methods (SW-846).

EPRI, 1998. Leaching of inorganic constituents from coal combustion by-product under field and laboratory conditions. EPRI Report TR-111773-V1. EPRI: Palo Alto, CA.

Fair, G.M., Geyer, J.C., and Okun, D.A., 1968. Water and Wastewater Engineering. Volume 2 Water Purification and Wastewater Treatment and Disposal. Wiley, New York.

Garrabrants, A. C., Kosson, D.S., 2000. Use of a chelating agent to determine the metal availability for leaching in soils and wastes. Waste Management 20, 155-165.

KaleidagraphTM (version 3.52) Copyright 2002 by Synergy Software.

Kim, A.G., Kazonich, G., 1999. Mass release of trace elements from coal combustion by-products. International Ash Utilization Symposium, Center for Applied Energy Research, University of Kentucky: Lexington, KY.

Kim, A.G., 2002. CCB Leaching summary: survey of methods and results. Coal Combustion By-Products and Western Coal Mines, a technical interactive forum: Golden, CO.

Kosson, D.S., van der Sloot, H.A., Sanchez, F., Garrabrants, A.C., 2002. An integrated framework for evaluating leaching in waste management and utilization of secondary materials. Environmental Engineering Science 19, 159 – 204.

Lo, I.M., Tang, C. I., Li, X.D., Poon, C.S., 2000. Leaching and microstructural analysis of cement-based solidified wastes. Environ. Sci. Technol. 34, 5038-5042.

Maxwell, D.P., Cox, H.B., Flora, H.B., 1993. Evaluation of test procedures to determine bulk and surface composition of selected metals on fly ash particles. Annual Meeting - Air & Waste Management Association (86th): Salt Lake City, Utah.

Mehnert, E., Hensel, B.R., 1996. Coal combustion by-products and contaminant transport in groundwater. Coal Combustion By-Products Associated with Coal Mining Interactive Forum: Southern Illinois University at Carbondale, Carbondale, IL.

Murarka, I.P., 1999. Importance of leaching tests. EPA Public Meeting on Waste Leaching: Crystal, VA. Available at [http://www.epa.gov/epaoswer/hazwaste/test/pdfs/import.pdf].

Sherrod, P. H. NLREG: Nonlinear Regression Analysis Program (version 6.3). Copyright 2005 by P. H. Sherrod.

Song, Q. J., Greenway, G. M., 2004. A study of the elemental leachability and retention capability of compost. Environ. Monit. 6, 31-37.

Teng, X., Wang, H., Ban, H., Wang, J., 2003a. Effect of ammonia on metal leaching from fly ash. WEFTEC'2003: Los Angeles, CA.

Teng, X., Wang, H., Wang, J., Ban, H., Golden, D., Ladwig, K., 2003b. The effect of ammonia on mercury release from coal fly ash. 28th International Technical Conference on Coal Utilization & Fuel Systems: Clearwater, FL.

van der Sloot, H.A., Kosson, D.S., Eighmy, T.T., Comans, R.N.J., Hjelmar, O., 1994. Approach towards international standardization: a concise scheme for testing of granular waste leachability. In Environmental aspects of construction waste materials; Goumans J.J.J.M., van der Sloot H.A., Aalbers Th.G., eds; Elsevier: Amsterdam, The Netherlands. pp453-466.

Van Herck, P., Vandecasteele,C., Wilms, D., 1998. The use of EDTA to increase the leachability of heavy metals from municipal solid waste incineration fly ash. Environmental Science Research 55, 181-192.

Wang, J., Huang, C. P.; Allen, H.E., Poesponegoro, I., Poesponegoro, H., Takiyama, L. R., 1999. Effects of dissolved organic matter and pH on heavy metal uptake by sludge particulates exemplified by copper(II) and nickel(II): three-variable model. Water Environment Research 71(2), 139-147.

Wang, H., Teng, X., Wang, J., Ban, H., Golden, D., Ladwig, K., 2003a. Environmental impact of metal leaching from ammoniated power plant fly ash. 2003 SWE (The Society of Women Engineers) Annual Conference: Birmingham, AL.

Wang, H., Teng, X., Wang, J., Ban, H., Golden, D., Ladwig, K., 2003b. The effect of ammonia on nickel leaching from coal ashes. 15th International Symposium on Management & Use of Coal Combustion Products (CCPs), American Coal Ash Association (ACAA): Tampa, FL.

Wang J., Huang, C. P., Allen, H.E., 2003c. Modeling heavy metal uptake by sludge particulates in the presence of dissolved organic matter. Water Research, 37(20), 4835-4842.

Wang J., Huang, C. P., Allen, H.E., 2000. Surface physical-chemical characteristics of sludge particulates. Water Environ. Res. 72, 545-553.

Wang, J., Teng, X., Wang, H., Ban, H., 2004. Characterizing the metal adsorption capability of a class f coal fly ash. Environ. Sci. Technol. 38, 6710 – 6715.

Wang, J., Ban, H., Teng, X., Ladwig, K., 2005. The effect of ammonia on the leaching of cu(ii) and cd(ii) from fly ash. 2005 World of Coal Ash: Lexington, KY.

Wang, K.S., Chiang, K.Y., 1996. Metal leachability and species analysis in municipal solid waste incinerator ashes. International Conference on Solid Waste Technology and Management: Philadelphia, PA.

Xu, Y.H., Nakajima, T., Ohki, A., 2001. Leaching of arsenic from coal fly ashes 2. Arsenic pre-leaching with sodium gluconate solution. Toxicological and Environmental Chemistry 81, 69-80.

Zhang, M.H., Blanchette, M.C., Malhotra, V. M., 2001. Leachability of trace metal elements from fly ash concrete: results from column-leaching and batch-leaching tests. ACI Materials Journal 98, 126-136.

Table 1. Sample composition and specific surface area

Sample	Cu (µg/g)	Cd (µg/g)	Ni (µg/g)	LOI (%)	BET Surface Area (m^2/g)
AN/Col #2	193±2	0.89±0.02	187±3	6.7	7.6
AN/NRT #2	165±4	0.56±0.01	91±2	9.8	8.7

Table 2. Site density (Γ_m) and acidity constant (pK_H) for ash AN/Col #2 and AN/NRT #2

Sample	Site	α	β	γ	R^2
AN/Col #2	Γ_m (mol/g)	2.3×10^{-4}	3.2×10^{-5}	1.1×10^{-4}	0.997
	pK_H	2.8	8.3	12.0	
AN/NRT #2	Γ_m (mol/g)	4.5×10^{-4}	2.7×10^{-5}	4.1×10^{-5}	0.998
	pK_H	3.4	8.8	12.1	

Table 3. Intrinsic leaching parameters of ash AN/Col #2 and AN/NRT #2 for Cu(II), Cd(II) and Ni(II) determined under different conditions

Ash	Method	Element	M_b (mg/L)	SE*	$logK_S$	SE*	TLM** (mg/kg)
AN/Col #2	Step Method (S/L=1:10)	Cu(II)	1.84	0.10	6.1	0.1	18.4
		Cd(II)	-0.05	0.02	4.5	0.05	-0.5
		Ni(II)	0.59	0.03	5.0	0.06	5.9
	Integrated Method (S/L=1:10)	Cu(II)	2.05	0.09	6.4	0.06	20.5
		Cd(II)	-0.05	0.02	4.4	0.04	-0.5
		Ni(II)	0.62	0.03	5.2	0.05	6.2
	Step Method (S/L=1:5)	Cu(II)	3.80	0.14	6.1	0.05	19.0
		Cd(II)	0.04	0.02	4.2	0.03	0.2
		Ni(II)	1.04	0.06	4.6	0.07	5.2
	Integrated Method (S/L=1:5)	Cu(II)	4.12	0.13	6.3	0.04	20.6
		Cd(II)	0.02	0.02	4.1	0.02	0.09
		Ni(II)	1.0	0.06	4.5	0.06	5.0
AN/NRT #2	Step Method (S/L=1:10)	Cu(II)	1.39	0.08	7.2	0.07	13.9
		Cd(II)	-0.07	0.03	5.1	0.05	-0.7
		Ni(II)	0.17	0.04	5.0	0.05	1.7
	Integrated Method (S/L=1:10)	Cu(II)	1.16	0.07	6.5	0.04	11.6
		Cd(II)	-0.09	0.02	4.4	0.02	-0.9
		Ni(II)	0.17	0.05	4.5	0.05	1.7

*SE = Standard Error;
**TLM = Total Leachable Mass.

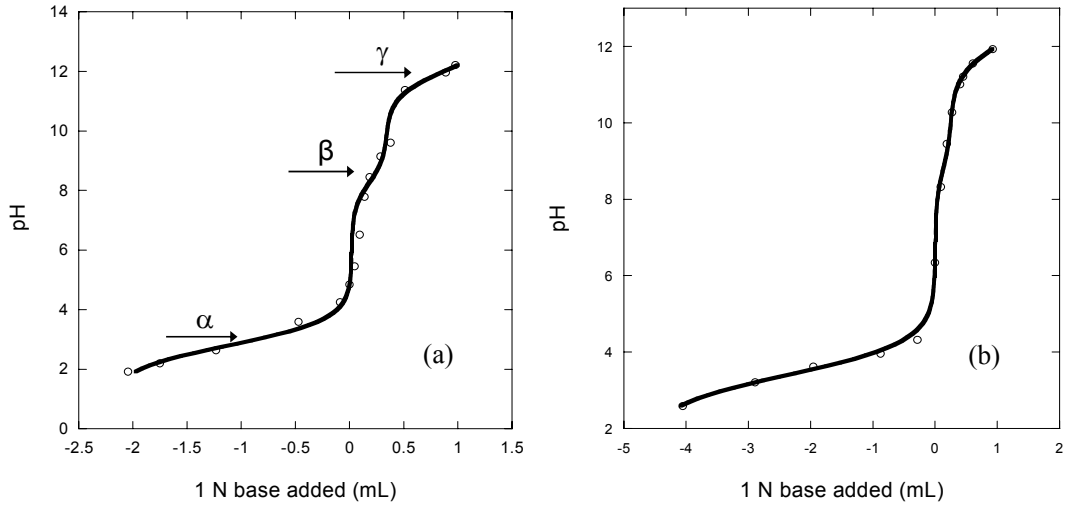

Figure 1. Titration and curve fitting results for washed ashes. (a) AN/Col #2; (b) AN/NRT #2. Ionic strength = 0.01 M ($NaNO_3$), temperature = 20-25 °C; equilibration time = 24 hours (negative values were used for acid consumption on X axis).

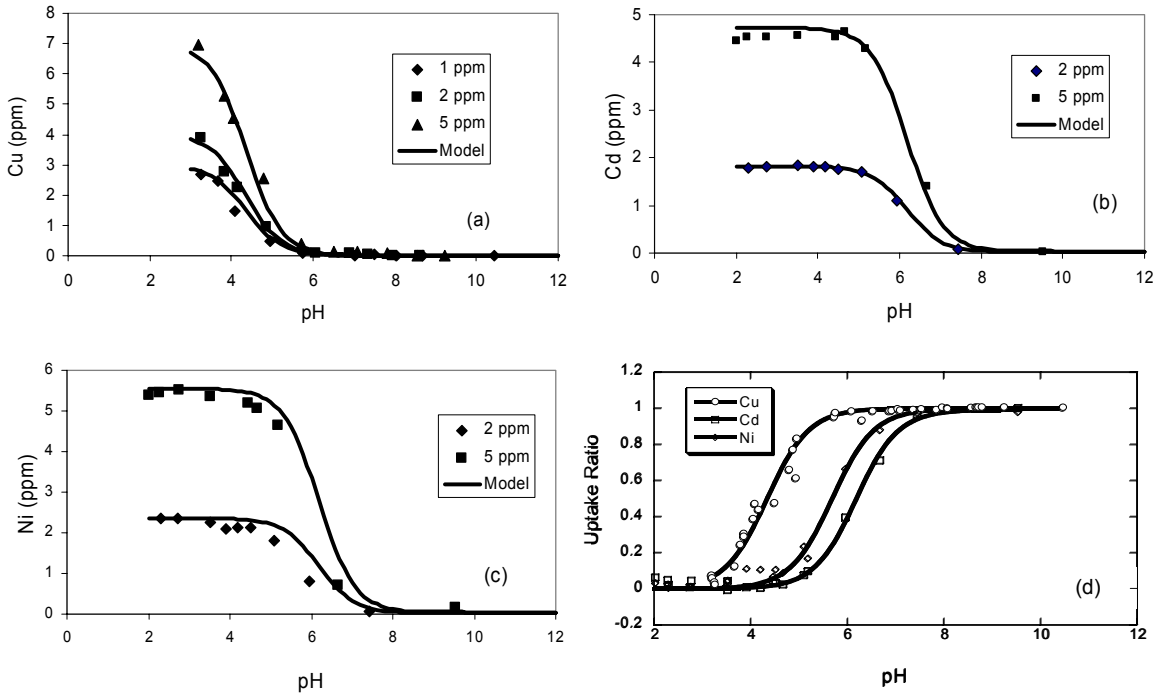

Figure 2. Batch experimental data and modeling results for washed ash AN/Col #2. (a) – (c) soluble concentrations of Cu(II), Cd(II), and Ni(II) as a function of pH; and (d) adsorption ratio as a function of pH. Experimental conditions: Added element concentrations = 1, 2, 5 mg/L for Cu(II), and 2, 5 mg/L for Cd(II) and Ni(II); S/L = 1:10; ionic strength = 0.01M ($NaNO_3$); temperature = 20-25 °C; equilibration time = 24 hours.

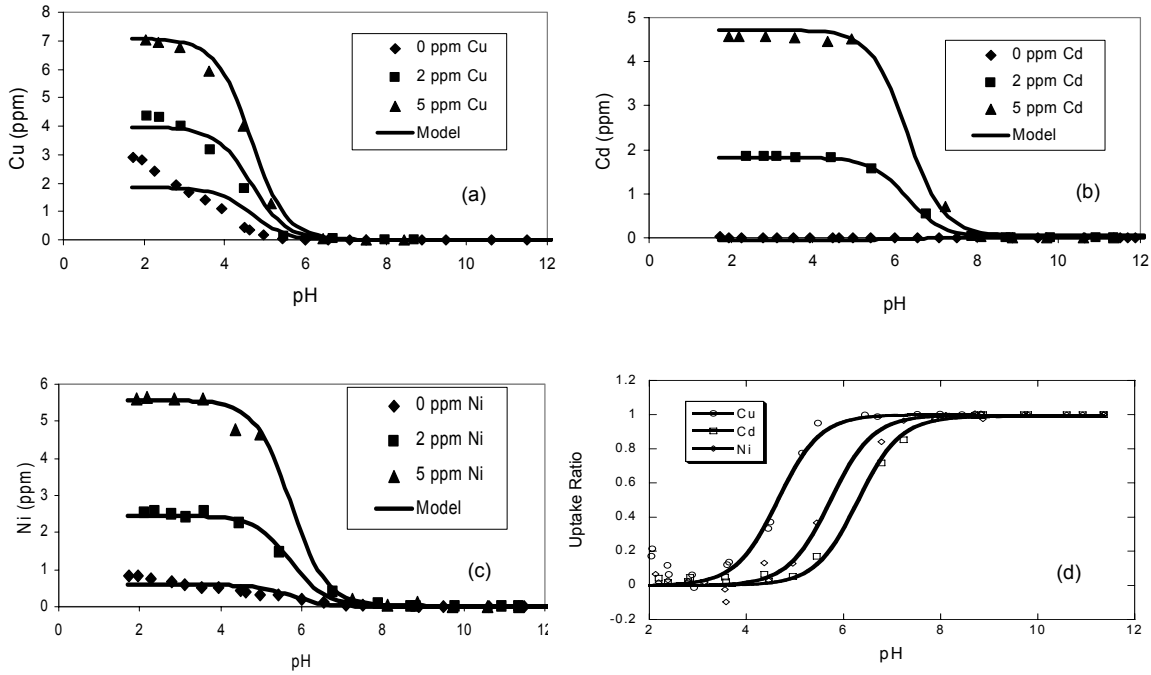

Figure 3. Batch experimental data and modeling results for raw ash AN/Col #2 at S/L ratio of 1:10. (a) – (c) soluble concentrations of Cu(II), Cd(II), and Ni(II) as a function of pH; and (d) adsorption ratio of the added elements as a function of pH. Experimental conditions: temperature = 20-25 °C; equilibration time = 24 hours.

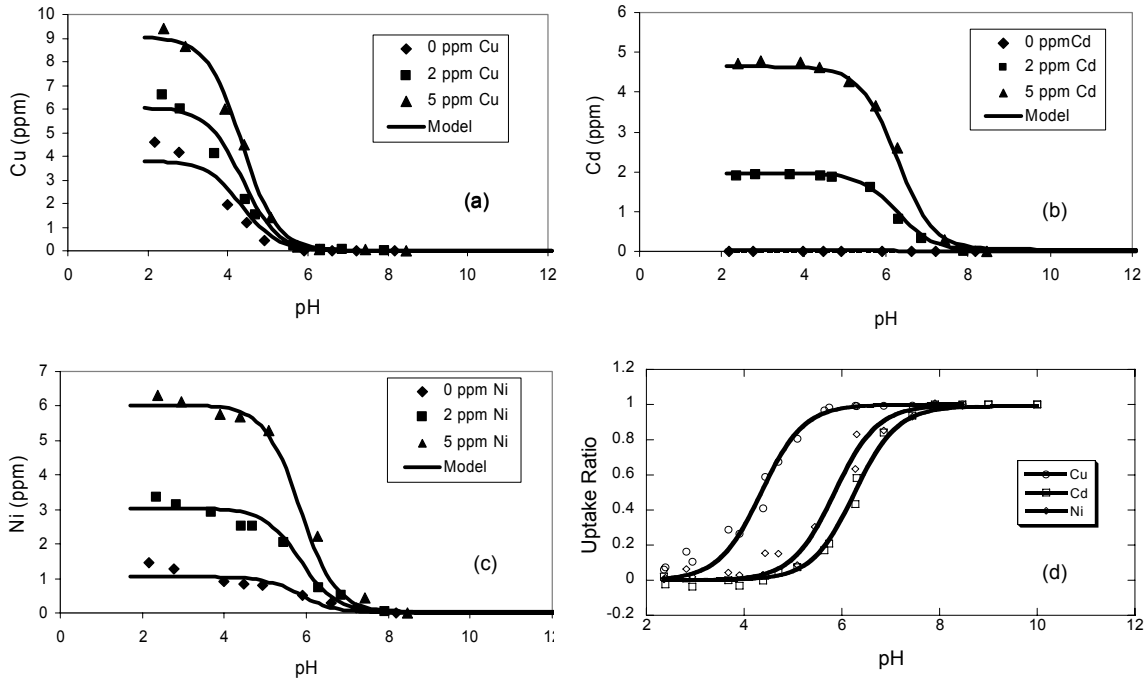

Figure 4. Batch experimental data and modeling results for raw ash AN/Col #2 at S/L ratio of 1:5. (a) – (c) soluble concentrations of Cu(II), Cd(II), and Ni(II) as a function of pH; and (d) adsorption ratio as a function of pH. Experimental conditions: temperature = 20 – 25 °C; equilibration time = 24 hours.

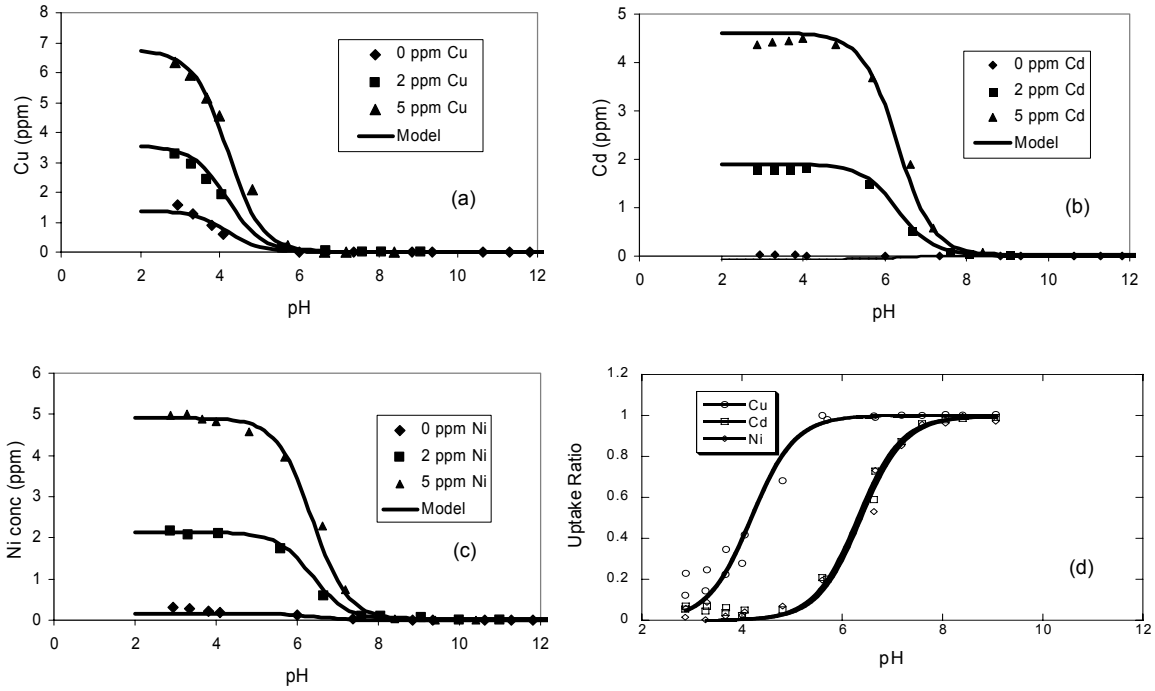

Figure 5. Batch experimental data and modeling results for raw ash AN/NRT#2 at S/L ratio of 1:10. (a) – (c) soluble concentrations of Cu(II), Cd(II), and Ni(II) as a function of pH; and (d) adsorption ratio as a function of pH. Experimental conditions: temperature = 20-25 °C; equilibration time = 24 hours.

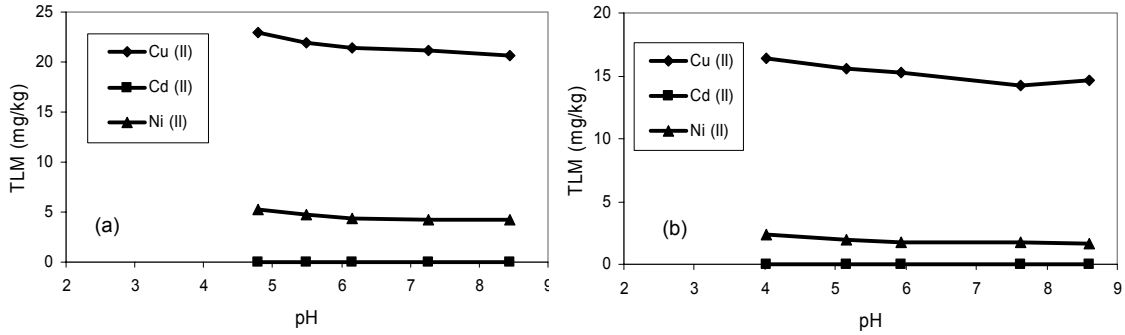

Figure 6. Total extractable element concentration using EDTA. (a) ash AN/Col #2; (b) ash AN/NRT #2.

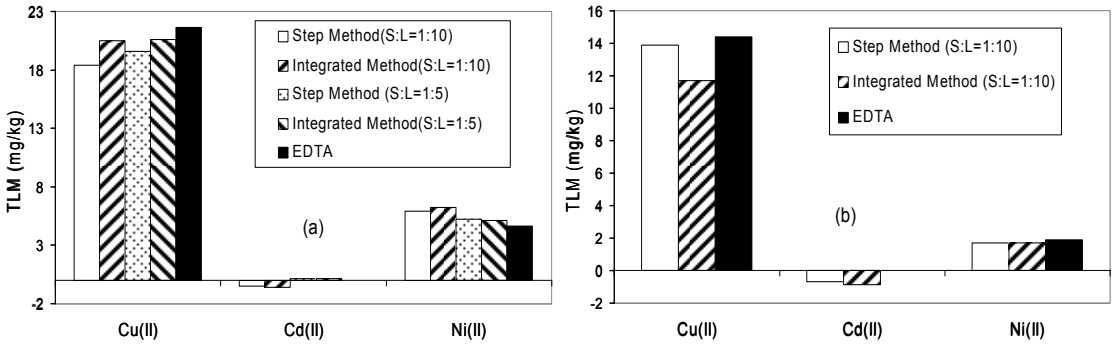

Figure 7. Total leachable mass results determined using different methods or under different conditions. (a) AN/Col #2; and (b) AN/NRT #2.

II. The Leaching Characteristics of Selenium from Coal Fly Ashes *(Journal of Environmental Quality 2007, accepted)*

Tian Wang [a], Jianmin Wang [a,*], Heng Ban [b], Ken Ladwig [c]

[a] *Environmental Research Center; Dept. of Civil, Architectural and Environmental Engineering; Univ. of Missouri-Rolla, Rolla, MO 65409, United States*

[b] *Department of Mechanical Engineering, University of Alabama at Birmingham, Birmingham, AL 35294, United States*

[c] *Electric Power Research Institute (EPRI), 3412 Hillview Ave., Palo Alto, CA 94304, United States*

[*]Corresponding author: (phone) (573) 341-7503; (fax) (573) 341-4729; (email) wangjia@umr.edu

ABSTRACT

The leaching characteristics of selenium from several bituminous and subbituminous coal fly ashes under different pH conditions were investigated using batch methods. Results indicated that pH had significant effect on selenium leaching from bituminous coal ash. The minimum selenium leaching occurred in the pH range between 3 and 4, while the maximum selenium leaching occurred at pH 12. The release of selenium from subbituminous coal ashes was very low for the entire experimental pH range, possibly due to the high content of calcium which can form hydration or precipitation products as a sink for selenium. The adsorption results for different selenium species indicated that Se(VI) was hardly adsorbable on either bituminous coal ashes or subbituminous coal ashes at any pH. However, Se(IV) was highly adsorbed by bituminous coal ashes under acidic pH conditions and was totally removed by subbituminous coal ashes across the entire pH range. This result suggests that the majority of selenium released from the tested fly ashes was Se(IV). A speciation-based model was developed to simulate the adsorption of Se(IV) on bituminous coal fly ash, and the pH-independent adsorption constants of $HSeO_3^-$ and SeO_3^{2-} were determined. The

modeling approach is useful for understanding and predicting the release process of selenium from fly ash.

Keywords Selenium; Leaching; Coal fly ash; pH; Modeling

INTRODUCTION

Selenium is an essential element for plant and animal nutrition at trace levels, but it can cause severe respiratory and neurological problems if uptake exceeds threshold levels (ATSDR, 2003). U.S. EPA set both the maximum contaminant level (MCL) and the maximum contaminant level goal (MCLG) for selenium in drinking water at 50 μg/L (U.S. EPA, 2002). Such contamination may originate from coal fly ash which contains selenium and various other trace elements. The content of selenium in coal fly ash can be as high as 200 mg/kg (Kim, 2002), although it is usually less than 50 mg/kg and is typically in the range of 10 to 20 mg/kg (EPRI, 1987). According to the American Coal Ash Association (ACAA), US power facilities produced more than 71 million short tons (6.4×10^{10} kg) of coal fly ashes in 2005, and 41% were further utilized as concrete products, road bases, etc (ACAA, 2006). Most of the remaining 59% were disposed of in landfills or impoundments. Therefore, the leaching potential of selenium from fly ash leading to possible contamination of ground and surface water is an environmental concern is an environmental concern. Understanding the leaching behavior of selenium from coal fly ash is significant for assessing the potential environmental impact of fly ash.

Selenium leaching from coal fly ash has been investigated previously by various researchers (EPRI, 1987; van der Hoek and Comans, 1996; Jankowski et al., 2004; Iwashita et al., 2005; EPRI, 2006a; and 2006b; U.S. EPA, 2006). Most of these studies indicated that pH is a key factor affecting selenium leaching from fly ash. Se leaching

tends to increase as pH of the aqueous phase is raised, although it may not always be the case. van der Hoek and Comans (1996) have recorded the least leaching of Se an at pH 5-6 for an acidic ash, and Iwashita et al. (2005) reported decrease of Se leaching from an alkaline ash as pH was increased from 8 to 12 for an alkaline ash with high Ca composition. Iwashita et al. (2005) also concluded that the leaching amount of selenium was essentially dependent upon its concentration in fly ash, while other studies have found no correlation between the total content of selenium in the ash and the concentration in the leachate (EPRI, 1987; U.S. EPA, 2006). In addition, it has been widely observed that selenate (Se(VI)) is less adsorbable than selenite (Se(IV)) by various minerals such as goethite, iron oxyhydroxide, and montmorillonitic soil (Merrill et al., 1986; Goldberg and Glaubig, 1988; EPRI, 1994, 2006a). Several previous studies have reported that selenium in fly ash and fly ash leachate exists predominantly as Se(IV) (Wadge and Hutton, 1987; Jackson and Miller, 1999; Narukawa et al., 2005).

Several mechanisms have been proposed to interpret selenium leaching behavior from fly ash. Research indicates that the leaching of selenium from bituminous coal ashes is controlled primarily by iron hydroxide adsorption and that from subbituminous coal ash is controlled by calcium precipitation (van der Hoek et al., 1994; van der Hoek and Comans, 1996), the latter generally has a greater content of calcium oxide. Hassett et al. (1991) and Lecuyer et al. (1996) attributed the stabilization of selenium in subbituminous coal ash to the formation of ettringite ($3CaO \cdot Al_2O_3 \cdot 3CaSO_4 \cdot 32H_2O$). Aluminum oxide may also contribute to the adsorption of selenite in fly ash (Rajan, 1979; Hansen and Fisher, 1980; van der Hoek and Comans, 1996). Surface complexation models considering surface electrostatic effects have been used to quantify the

adsorption/desorption of selenium and other trace elements on various adsorbents (Goldberg, 1985; Goldberg and Glaubig, 1988; Dzombak and Morel, 1990) and proved to be successful on laboratory studies. However, in natural systems, not all the parameters necessary for the surface complexation model are known, and its application is limited for systems with multiple adsorbents and heterogeneous surface sites (Honeyman and Santschi, 1988). Other researchers used a simplified surface complexation approach without surface charge correction to model the sorption of arsenic and selenium on iron hydroxide, and obtained the apparent adsorption constants comparable with literature data (Belzile and Tessier, 1990; van der Hoek and Comans, 1996). Nonetheless, studies are lacking on how to determine the types and quantity of reactive surface sites in field samples for use in surface-complexation modeling.

The objectives of this study were to investigate the overall leaching behavior of selenium from both bituminous coal fly ash and subbituminous coal fly ash, determine the major factors affecting selenium leaching, and develop a simplified surface complexation approach without considering the electrostatic effect, to quantify the reactive surface sites on fly ash and the adsorption of selenium onto fly ash for better understanding the selenium leaching process.

MATERIALS AND METHODS

Materials

A total of seven ash samples were used in this study. Ashes #1004, #33, #1008 and #1009 were all collected from one pulverized coal power plant (Plant ID 33106) burning eastern bituminous coal. The plant uses cold-side electrostatic precipitators (ESPs) to capture fly ash. Ashes #1004 and #1009 were collected from the same unit but

at different times, when different eastern bituminous coals were being burned; #1008 and #1009 had the same coal source with a calcium content (Table 1), while #1008 was sampled when an ammonia-based selective non-catalytic reduction (SNCR) system was being tested. Ash #33 was collected from a separate unit burning the same coal as Ash #1004, but with ammonia-based flue gas conditioning for the ESP. Ashes #1015, #1018, and #7 were collected from power plants burning primarily subbituminous coal. Ashes #1015 and #1018 came from a cyclone boiler power plant (Plant ID 25410) with cold-side ESPs and burning a blend of 80% subbituminous and 20% bituminous coal. Ash #1018 was sampled when SNCR system was tested. Sample #7 came from a pulverized coal power plant (Plant ID 50213) with hot-side ESPs and burning 100% subbituminous coal.

The basic physical/chemical characteristics of these ashes, including BET surface area (analyzed using Quantachrome Autosorb-1-C high performance surface area and pore size analyzer, Quantachrome Instruments, FL, USA), pH_{pzc} (denoted as the pH at which the surface charge, surface potential and ξ potential are zero), loss-on-ignition (LOI) (determined using gravimetric methods), and total concentrations of selenium, calcium and sulfur are shown in Table 1. ξ potential of fly ash as a function of pH was analyzed using Zetasizer 3000 (Malvern Instruments, Worcestershire, UK) to determine pH_{pzc} because the surface potential can not be directly measured. The total Se in fly ash was determined using microwave-assisted acid digestion (0.4 g fly ash + 10 mL HNO_3 + 5 mL HF + 5 mL HCl) followed by graphite furnace atomic absorption (GFAA) measurement. The accuracy of the metal determination was demonstrated by using a certified reference material, NIST-1633a (National Institute of Standards and Technology,

USA; certified Se = 10.3±0.6 mg/kg, measured Se = 10.2±0.7 mg/kg,). Total Ca and S concentration was determined using X-Ray Fluorescence Spectroscopy (X-LAB 2000, SPECTRO Analytical Instruments GmbH & Co. KG).

Se(IV) and Se(VI) stock solutions were prepared from sodium selenite (MP Biomedicals, Inc.) and sodium selenate (Alfa Aesar). Sulfate stock solution was prepared from sodium sulfate (Fisher Scientific). All solutions were prepared using 18.2 MΩ deionized (DI) water.

Batch Leaching of Raw Ash

A batch leaching experiment was performed to determine the leaching behavior of selenium from raw fly ash (as obtained from the electrostatic precipitator in power plant) under different pH conditions. Raw ash was dried at 105 °C for at least 24 hours before use. Ten grams of ash and 100 mL of DI water were added to each of a series of 125 mL LDPE bottles to create a solid/solution ratio (S/L) of 1:10. Different volumes of 1 M HNO_3 or NaOH stock solution were added to these bottles to yield final pH values distributed in a range between 2 and 12, and pH was not adjusted during the leaching process and no replicates were made since many pH points were selected in the range. The bottles were sealed and shaken at 180 oscillation/min using an EBERBACH 6010 shaker for 24 hours to achieve equilibrium (EPRI, 2005), then allowed to settle overnight. The supernatant was collected and acidified using concentrated HNO_3 for selenium analysis using GFAA spectrometer (AAnalyst 600, Perkin-Elmer Corp., Norwalk, Connecticut, USA). The final pH in the remaining slurry was measured using an Orion pH meter (perpHecT LoR model 370) equipped with an Orion PerpHecT Triode pH electrode (model 9207BN).

Equilibrium Fly Ash Titration and Selenium Adsorption Experiments

Batch equilibrium titration and Se adsorption experiments were conducted using washed ash. The washing process was used to obtain a relatively clean surface by removing soluble constituents, including selenium, from the fly ash. The washing was conducted using a 0.2 M NaOH solution to remove readily soluble and adsorbed selenium from bituminous coal ashes (#1004, #33, and #1009). For subbituminous coal ashes (#1015, #1018, and #7), only DI water was used as a washing solution because natural pH of these ashes in DI water was already greater than 11. Washing was performed with a solid-to-liquid ratio of 1:5, and repeated 5 times. Each washing cycle lasted for 20 hours. Air bubbling was used to agitate the ash-water mixture. At the end of each washing cycle, the mixture was allowed to settle for 2-3 hours, and the supernatant was decanted. The washed ash was dried at 105 °C for at least 24 hours before use.

The procedures for fly ash titration and Se adsorption experiments were similar to the batch leaching experiments. Batch titration experiments were conducted with a liquid phase of 0.01 M $NaNO_3$ as a supporting electrolyte. The volume of acid or base used, and the corresponding final pH in each bottle were recorded to plot the overall titration curve. The 0.01 M $NaNO_3$ solution was also titrated as a blank. The net titration curve was obtained by subtracting the acid/base consumption by the blank (0.01 M $NaNO_3$ solution) from the overall titration curve for the same pH condition. For the adsorption experiments, the liquid phase contained pre-selected concentrations of selenium in 0.01 M $NaNO_3$ solution. For study on sulfate impact on selenium adsorption, pre-selected concentrations of sulfate were also added into the aqueous phase. All other conditions were the same with those of the batch leaching experiment (Wang et al., 2004).

RESULTS AND DISCUSSION

Selenium Leaching from Raw Ash

Figure 1 shows the batch leaching results of selenium for six ashes used in this research. For bituminous coal ashes (Ashes #1004, #33, and #1009), the lowest release occurred in pH range 3-4. When pH was greater than 4, selenium leaching increased with the increase of pH, whereas at pH below 3, the leaching increased with the decrease of pH. The maximum release occurred at pH close to 12, with concentrations of 2500 μg/L, 1700 μg/L and 2000 μg/L, corresponding to 55%, 69% and 67% of total Se, for ashes #1004, #33, and #1009, respectively. By contrast, at their natural pH (4.4 for #1004, 4.5 for #33 and 6.0 for #1009), only 2%, 2% and 25% of total Se were released from these ashes, respectively. Ash #1008 was not selected for batch leaching because of the limit amount of this sample.

Se(IV) was reported as the main selenium species in leachate from both bituminous and subbituminous fly ashes (Wadge and Hutton, 1987; Jackson and Miller, 1999; Narukawa et al., 2005), although Narukawa et al. found a higher fraction of Se(VI) in bituminous ash leachate. The pKa values of selenious acid (H_2SeO_3) are 2.64 and 8.36, respectively (NEA, 2005). Therefore, when pH is less than 2.6, the neutral H_2SeO_3 species dominates in the system. Selenium leaching was increased with the decrease of pH below 2.6, indicating that the neutral selenium species may not be readily adsorbed by the ash surface, an alternative explanation is that the low pH might trigger dissolution of some oxidic surfaces, which can also result in the increase of selenium leaching. With the increase of pH, the total concentrations of anionic species $HSeO_3^-$ and SeO_3^{2-} would also increase. These anions can be adsorbed to ash surface sites. When pH was further

increased, more and more surface species were deprotonated and hindered the adsorption of negatively charged selenium species for the same surface sites, resulting in the increase of selenium leaching.

Figure 1 also shows that the selenium leaching from subbituminous coal Ashes #1015, #1018, and #7 was very low at all pH values compared with that from the bituminous coal ashes. The subbituminous coal ashes contained less selenium compared with the bituminous coal ashes (Table 1), but the releases do not appear to be proportional to the total selenium content. The subbituminous coal ashes contained significantly more calcium than bituminous coal ashes, which may reduce selenium leaching through the formation of ettringite under high pH conditions (Hassett et al., 1991; Lecuyer et al., 1996) or precipitation of calcium selenite (Isabel and Annette, 2003).

Impact of Selenium Speciation on Adsorption

Se(VI) Adsorption in Single Species System. Washed bituminous Ash #1004 was selected for this experiment. Adsorption experiments were conducted using two Se(VI) additions, 1 mg/L and 2 mg/L, plus the background leaching (without Se(VI) addition). Results are shown in Figure 2a. The background leaching curve of washed ash indicated that less than 500 μg/L (5 mg/kg ash) of selenium were leached at all pH levels, the reduced leaching was due to selenium elimination by washing process. Comparing soluble selenium concentrations from curves with and without (background) external Se(VI) addition at the same pHs, slight adsorption of Se(VI) was observed at acidic pHs. This behavior might be interpreted with the outer-sphere (Hayes et al. 1987;) or even inner-sphere complexation (Fukushi and Sverjensky, 2007; Rietra et al., 2001) between selenate and surface oxides, which is positively charged at lower pHs. Nonetheless, the

adsorption of Se(VI), compared with Se(IV) (See next section), was not significant in the entire experimental pH range from 2 to 12. This result is consistent with previous studies on Se (IV) and Se(VI) adsorption on soils (Goldberg and Glaubig, 1988; EPRI, 1994) and goethite (Rietra et al., 2007)

Se(IV) Adsorption in Single Species System. Washed Ash #1004 was also used to determine the adsorption of Se(IV) on fly ash under two addition conditions, 1 mg/L and 2 mg/L. Results are shown in Figure 2b, along with the background leaching results. Se(IV) was much more adsorbed than Se(VI) in the acidic pH range, with the maximum adsorption occurred at pH of approximately 4. Based on pKa values, when pH was less than 2.5 the dominant species of Se (IV) would have been the neutral species (H_2SeO_3), the decrease of adsorption in this pH range may be due to the poor adsorbability of H_2SeO_3 or dissolution of ash particles at very low pHs. When pH was greater than 6, the negatively charged different selenium species ($HSeO_3^-$ and SeO_3^{2-}) dominate in the system. Due to the decrease of protonated surface sites with the increase of pH, these Se species would have less sorption sites to bind to and thus less Se (IV) was adsorbed as the pH increased. Similar results were also observed for Se(IV) adsorption onto soils and minerals (Goldberg and Glaubig, 1988; EPRI, 1994; Rietra et al., 2007). The similarity between the background leaching curve and the Se(IV) adsorption curve indicated that Se(IV) is likely to be the dominant species in the background leachate.

Selenium Adsorption in Mixed Species System. To determine interactive effects of selenium species during adsorption, batch studies adding mixed species were performed using washed Ash #1009 (bituminous coal ash) and Ash #1018 (subbituminous coal ash). The test solution contained 2 mg/L Se(VI) and 2 mg/L Se(IV). For each ash, the

adsorption in single species systems was also determined as a reference. Figure 3 shows the adsorption results plotted as the total soluble selenium concentration as a function of pH.

The adsorption behavior of Se(IV) and Se(VI) for Ash #1009 (Figure 3a) was similar to that for Ash #1004 (see Figure 2 for comparison). Se(IV) adsorption was at the maximum at pH 3-4, and decreased with the increase of pH. Se(VI) adsorption was not significant across the entire experimental pH range. The background leaching curves for both raw ash and washed ash were also plotted in the same graph. Comparing all the soluble selenium concentration curves, selenium leaching from the raw ash followed the same trend as the Se(IV) added to washed ash, suggesting that the predominant selenium species of the released Se from fly ash was Se(IV), in agreement with conclusions from previous studies for other ashes (Wadge and Hutton, 1987). These data are also in agreement with field leachate data from bituminous coal ash ponds (EPRI, 2006b). The total selenium concentration in the mixed species system was approximately equal to the sum of selenium concentrations for two single species systems after subtracting the background leaching concentration. Therefore, the adsorption of one selenium species was not affected by the other in the mixed system under the experimental loading condition.

Selenium concentrations in batch solutions for the raw Ash #1018 (primarily subbituminous coal ash) and those for the experiment with only Se(IV) addition were negligible compared to that with Se(VI) addition across the entire pH range (Figure 3b). The leaching curve for the experiment with mixed selenium species addition and that with single Se(VI) species addition overlapped. Therefore, this ash acted as a sink for

Se(IV), possibly due to high concentrations of calcium in the fly ash, which can trap Se(IV) through ettringite formation or precipitation (Hassett et al., 1991; Lecuyer et al., 1996; Isabel and Annette, 2003). However, as shown in Figure 3b, almost all added Se(VI) stayed in the soluble phase in the entire pH range. Therefore, Se(VI) does not adsorb to this fly ash. In terms of adsorption, Se(IV) and Se(VI) did not affect each other during the experiment".

Field leachates collected from subbituminous coal ash landfills, including the landfill serving the power plant where Ash #7 was collected, exhibit high selenium concentrations, with almost all of it present as Se(VI) species (EPRI, 2006b). Since the fresh subbituminous ash, including Ash #7, exhibited low leaching potential consistent with Se(IV) in these lab studies, the field data may indicate conversion of Se(IV) to Se(VI) under landfill conditions.

Impact of Sulfate on Selenium Adsorption. Sulfate is a common component in coal fly ash, and was reported to compete with selenium for adsorption on several media including goethite, manganese dioxide and soils (Balistrieri and Chao, 1987, 1990; Goh and Lim, 2004; EPRI 2006a). Experiments were conducted to evaluate the sulfate impact on selenium adsorption on washed Ashes #1009 and #1018 under different sulfate concentrations. All solutions contained 2 mg/L Se(IV), 2 mg/L Se(VI), and 0.01 M $NaNO_3$. For Ash #1009, the sulfate concentrations added to the contacting solution were 0, 200, and 500 mg/L. For Ash #1018, the sulfate concentrations added to the leaching solution were 0, 500, and 1000 mg/L. The experimental data plotted in Figure 4 shows soluble selenium and sulfate concentrations as a function of pH for both ashes. No significant impact of sulfate on selenium adsorption was observed since all selenium

concentration curves overlap, with exception of one single point in Figure 4a around pH 2, which could hardly affect the general conclusion. Apparently, Ash #1018 had a higher soluble sulfate background after washing than ash #1009. For Ash #1009, most sulfate added into the system remained in soluble phase in the entire experimental pH range. Sulfate does not appear to compete with selenium for adsorption on Ash #1009 at the concentration levels studied in this research. For Ash #1018, results indicated that the external sulfate tended to be trapped on surface at lower pHs, which might be due outer-sphere adsorption. In spite of the adsorption potential of sulfate on ash #1018, selenium adsorption was not affected. This conclusion is at odds with previous studies which have found sulfate to influence Se adsorption onto other materials (such as goethite, soil and manganese dioxide) (Glasauer et al., 1995; Wu et al., 2002; Goldberg, 1985; Goldberg 1988; Balistrieri and Chao, 1990; EPRI, 2006a). However, fly ash has different properties and characteristics to these materials and this may explain the different outcome observed here.

Modeling Se(IV) Adsorption on Bituminous Coal Ash

Surface Site Characterization. The surface site density and acidity constant of fly ash are essential parameters for metal adsorption modeling. A previously developed titration method (Wang, et al., 2004) was used to determine these parameters. Unlike the widely used surface complexation models (Stumm and Morgan, 1996; Dzombak and Morel, 1990), this method assumes that the solid surface contains more than one monoprotic weak acid site, with independent surface site densities and acidity constants. Based on the relationship between the mass of acid or base used and the corresponding pH in

equilibrium, the surface site concentration and acidity constant for each site can be determined through modeling. The model is expressed as:

$$\Delta V_{SS} = \sum_i \frac{V_0 S_{Ti} K_{Hi}}{C} \left\{ \frac{1}{[H^+] + K_{Hi}} - \frac{1}{[H^+]_0 + K_{Hi}} \right\} \quad (1)$$

where ΔV_{SS} is the net volume of stock acid/base (negative value for acid) solution consumed by surface sites (mL); V_0 is total volume of the ash mixture (mL); S_{Ti} is the total acid site concentration of species i (M); K_{Hi} is the acidity constant of the species i (M); C is the concentration of the acid/base stock solution (M); and $[H^+]_0$ is the hydrogen ion concentration of the control unit (without acid or base addition) (M). Note that the total surface site concentration $S_{Ti} = \Gamma_i \times SS$, where Γ_i is the surface site density for species i (mol/g-SS) and SS is the solids concentration (g/L).

After correction using the titration data for blanks, the net titration data for 0.2 M NaOH washed Ash #1004 with S/L ratio of 1:10 were plotted as the equilibrium pH as a function of the volume of acid (negative value) or base consumed by fly ash (mL), shown in Figure 5a. A nonlinear regression program Kaleidagraph™ (Synergy Software, 2002) was employed for the curve fitting. Results showed that using three surface sites can best fit the experimental data. Table 2 lists the surface site density (Γ) and acidity constant (pK_H) for each site, α, β, and γ. Since the pH_{pzc} of this ash was 6.4 (Table 1), which is between the pK_Hs of the site α and site β (3.5 and 7, respectively), the protonated surface sites α is positively charged, denoted as $\underline{S_1}OH_2^+$, while the protonated species of the other two surface sites are in neutral form. Titration was also performed with another DI water washed ash #1008, results were displayed in Figure 5b and Table 1.

Modeling Se(IV) Adsorption. The protonated surface site α was hypothesized to be responsible for the adsorption of anionic Se(IV) species. The concentration of the protonated surface site α is expressed as:

$$[\underline{S_1}OH_2^+]=\alpha_+ S_T \quad (2)$$

where S_T is the total site (protonated and unprotonated) concentration, and α_+ is the fraction of the protonated surface site:

$$\alpha_+ = \frac{[H^+]}{[H^+]+K_H}. \quad (3)$$

The updated acidity constants of selenious acid, pK_{a1} and pK_{a2}, are 2.64 and 8.36, respectively (NEA, 2005). Therefore,

$$[HSeO_3^-] = \alpha_1 [Se(IV)]_D \quad (4)$$

$$[SeO_3^{2-}] = \alpha_2 [Se(IV)]_D \quad (5)$$

where α_1, and α_2 are the fractions of Se(IV) as $HSeO_3^-$ and SeO_3^{2-}, respectively;

$$\alpha_1 = \frac{[H^+]K_{a1}}{[H^+]^2+[H^+]K_{a1}+K_{a1}K_{a2}}, \text{ and } \alpha_2 = \frac{K_{a1}K_{a2}}{[H^+]^2+[H^+]K_{a1}+K_{a1}K_{a2}}; \text{ and } [Se(IV)]_D$$

is the total dissolved Se(IV) concentration.

Assuming 1:1 stoichiometry between selenium species and the responsible surface sites, the adsorption reactions of selenium species are expressed as:

$$\underline{S_1}OH_2^+ + HSeO_3^- = \underline{S_1}\text{-}HSeO_3 + H_2O;\ K_{S1} \quad (6)$$

$$\underline{S_1}OH_2^+ + SeO_3^{2-} = \underline{S_1}\text{-}SeO_3^- + H_2O;\ K_{S2} \quad (7)$$

where K_{S1} and K_{S2} are adsorption constants of $HSeO_3^-$ and SeO_3^{2-} species, respectively.

The concentration of surface site α (obtained from batch titration) was 0.024 M at S/L = 1:10 (100 g/L solids), whereas the 2 mg/L of Se(IV) (equivalent to 0.024 mM) was

only 0.1% of the total site concentration, it is reasonable to assume that the adsorption is in the linear range of the Langmuir isotherm, the concentrations of adsorbed Se(IV) species are expressed as:

$$[\underline{S}_1 - HSeO_3] = K_{S1}\alpha_+ S_T \alpha_1 [Se(IV)]_D \quad (8)$$

$$[\underline{S}_1 - SeO_3^-] = K_{S2}\alpha_+ S_T \alpha_2 [Se(IV)]_D \quad (9)$$

Therefore, the adsorption ratio of Se(IV) is expressed as:

$$R = \frac{[Se(IV)]_{ads}}{[Se(IV)]_D + [Se(IV)]_{ads}} = \frac{\alpha_+ \Gamma SS(K_{S1}\alpha_1 + K_{S2}\alpha_2)}{1 + \alpha_+ \Gamma SS(K_{S1}\alpha_1 + K_{S2}\alpha_2)} \quad (10)$$

where $[Se(IV)]_{ads}$ is total concentration of adsorbed Se(IV) species.

The Se(IV) adsorption ratio R_{exp} (experimental data) was calculated using the following equation:

$$R_{exp} = 1 - \frac{[Se(IV)]_D}{[Se(IV)]_{add} + [Se(IV)]_b} \quad (11)$$

where $[Se(IV)]_{add}$ and $[Se(IV)]_b$ represent concentrations of added Se(IV) and background Se(IV), respectively.

Based on Figure 2b, the total background Se(IV) concentration of ash #1004 was estimated to be 0.50 mg/L. The adsorption ratio of Se(IV) under different selenium addition conditions was calculated using Equation 11, shown as squares in Figure 6a. Results indicated that the adsorption ratio curves for different Se(IV) additions overlap, indicating the adsorption was in the linear range of the Langmuir isotherm. The parameters for surface site α, including the site density and the acidity constant (Table 2), were substituted into Equation 10 and KaleidaGraph was used to fit the experimental data.

The solid line in Figure 6a is the modeling results. The adsorption constants of $HSeO_3^-$ and SeO_3^{2-} ($logKs_1$ and $logKs_2$) on ash #1004 were determined and listed in Table 3, together with the correlation coefficient R^2. As a verification, another ash #1008 was also applied in the adsorption test, the curve fitting results and adsorption constants are shown in Figure 6b and Table 3, respectively. The modeling results showed reasonable agreement with the experimental data, especially for ash #1008. The deviation between the experimental and modeling data in Figure 6a may be due to the insufficient data points in certain pH range, or a larger experimental error. Nonetheless, the imperfection of the modeling might also be an indication of other mechanism involved in the adsorption. i.e. Hayes et al. (1987) showed with x-ray adsorption fine structure analysis (EXAFS) that selenite forms binuclear complex on goethite in aqueous suspension. Further study is desired to improve the accuracy of this model while maintaining its simplicity.

Since the soluble Se(IV) concentration curves for the washed bituminous coal ash with Se(IV) addition had the same trend as those for the raw ash with no Se(IV) addition, and the washed ash was successfully modeled using only an adsorption approach, it can be concluded that the leaching of Se(IV) from raw bituminous coal Ash #1004 is mainly controlled by adsorption. On the other hand, the leaching of selenium from the subbituminous coal ash was very low and did not demonstrate any characteristics typically related to adsorption. It is hypothesized that the high concentrations of calcium in the subbituminous coal ash may control selenium leaching through the formation of ettringite or calcium selenite precipitate (Hassett et al., 1991; Lecuyer et al., 1996; Isabel and Annette, 2003).

CONCLUSIONS

This research demonstrates that pH is the most important factor affecting selenium leaching from bituminous coal fly ashes, with the lowest release occurring in the pH range 3-4. When pH increased above 4, selenium release increased concomitantly. As the pH approached 12, approximately 50-70% of the total selenium in the fly ash was released. Adsorption/desorption processes were found to be the main mechanisms controlling selenium leaching from these materials. For subbituminous coal ashes, very little selenium was leached, which may be due to the high calcium content in these ashes. Results from adsorption experiments suggest that Se(IV) was the predominant species in the released selenium from both types of ashes. In addition, Se(VI) was hardly adsorbed by either type of fly ash. Also, sulfate added in solution was found not to significantly impact upon the adsorption of selenium by either type of ash. A speciation-based adsorption model was capable of predicting Se(IV) adsorption by bituminous coal fly ash, and determining the adsorption constants ($\log K_S$) of $HSeO_3^-$ and SeO_3^{2-} This model is robust and simpler than other models reported in the literature for quantifying selenium adsorption.

ACKNOWLEDGEMENTS

This work was supported by the Electric Power Research Institute (EPRI), the Missouri Water Resources Research Center (MWRRC), and the Environmental Research Center (ERC) for Emerging Contaminants at the University of Missouri-Rolla (UMR). The authors also thank Dr. C.P. Huang and Mr. Minghua Li at the University of Delaware for providing the zeta potential measurement, and Mr. Lenin Kasthuri for providing the adsorption data for ash #1008. Conclusions and statements made in this

paper are those of the authors, and in no way reflect the endorsement of the aforementioned funding agencies.

REFERENCES

ACAA, 2006. 2005 Coal Combustion Product (CCP) Production and Use Survey. American Coal Ash Association. http://www.acaa-usa.org/CCPSurveyShort.htm.

Agency for Toxic Substances and Disease Registry (ATSDR). 2003. Toxicological Profile for Selenium. http://www.atsdr.cdc.gov/toxprofiles/tp92.html.

Balistrieri, L.S., Chao, T.T.,1987. Selenium adsorption by goethite. Soil Sci. Soc. Am. j. 51, 1145-1151.

Balistrieri, L.S., Chao, T.T. 1990. Adsorption of selenium by amorphous iron oxyhydroxide and manganese dioxide. Geochimica et Cosmochimica Acta. 54, 739-751.

Belzile N., Tessier A., 1990. Interactions between arsenic and iron oxyhydroxides in lacustrine sediments. Geochimica et Cosmochimica Acta. 54, 103-109.

Dzombak, D. A.; Morel, F. M. M. Surface Complexation modeling: Hydrous ferric oxide; John Wiley: New York, 1990.

EPRI, 1987. Chemical Characterization of Fossil Fuel Combustion Wastes. EPRI, Palo Alto, CA. EA-5321.

EPRI, 1994. Chemical Attenuation Reactions of Selenium. EPRI, Palo Alto, CA. TR-103535.

EPRI, 2005. Effects of Ammonia on Trace Element Leaching from Coal Fly Ash. EPRI, Palo Alto, CA. 1010063.

EPRI, 2006a. Chemical Attenuation Coefficients for Selenium Species Using Soil Samples Collected from Selected Power Plant Sites. EPRI, Palo Alto, CA. 1012585.

EPRI, 2006b. Characterization of Field Leachates at Coal Combustion Product management Sites: Arsenic, Selenium, Chromium, and Mercury Speciation. EPRI, Palo Alto, CA. 1012578.

Fukushi, K., Sverjensky, D. A., 2007. A surface complexation model for sulfate and selenate on iron oxides consistent with spectroscopic and theoretical molecular evidence. Geochimica et Cosmochimica Acta, 71(1), 1-24.

Glasauer, S., Doner, H.E., Gehring, A.U., 1995. Adsorption of selenite to goethite in a flow-through reaction chamber. European Journal of Soil Science, 46(1), 47-52.

Goh, K.H., Lim, T.T., 2004. Geochemistry of inorganic arsenic and selenium in a tropical soil: effect of reaction time, pH, and competitive anions on arsenic and selenium adsorption. Chemosphere, 55(6), 849-859.

Goldberg, S., 1985. Chemical modeling of anion competition on goethite using the constant capacitance model. Soil Sci. Soc. Am. j. 49(4), 851-6.

Goldberg, S., Glaubig, R.A., 1988. Anion sorption on a calcareous, montmorillonitic soil - selenium. Soil Sci. Soc. Am. j. 52(4), 954-8.

Hansen, L.D. and Fisher, G.L., 1980. Elemental distribution in coal fly ash particles. Environ. Sci. Technol., 14(9) 1111-1117.

Hassett, D.J., Pflughoeft-Hassett, D.F., McCarthy, G.J., 1991. Ettringite formation in coal ash as a mechanism for stabilization of hazardous trace elements. Proc: 9th Int. Ash Use Symp., 2, 31-1to 31-17.

Hayes, K., Roes, A., Brown, G., Hodgson, K., Leckie, J., Parks, G., 1987. In situ x-ray absorption study of surface complexes: Se oxyanions on alpha FeOOH. Science, 238, 783-86.

Honeyman, B. D., Santschi, P. H., 1988. Metals in aquatic systems. Environmental Science and Technology, 22(8), 862-71.

Isabel, B., Annette, J. C., 2003. Sorption of selenite and selenate to cement minerals. Environ. Sci. Technol., 37, 3442,-3447

Iwashita, A., Sakaguchi, Y., Nakajima, T., Takanashi, H., Ohki, A., Kambara, S., 2005. Leaching characteristics of boron and selenium for various coal fly ashes. Fuel, 84(5), 479-485.

Jackson, B.P., Miller W.P., 1999. Soluble arsenic and selenium species in fly ash/organic waste-amended soils using ion chromatography-inductively coupled plasma mass spectrometry. Environ. Sci. Technol., 33(2), 270 – 275.

Jankowski, J., Ward, C.R., French, D., Groves, S., 2004. Leachability of heavy metals from selected Australian fly ashes and its implications for groundwater contamination. Proceedings, 21st Annual International Pittsburgh Coal Conference, 22, 2-1 to 2-23.

Kim, A.G., Kazonich G., 2001. Release of trace elements from CCB: maximum extractable fraction. Proceedings, 14th International Symposium on Management and Use of Coal Combustion Products (CCPs), 1, 20-1 to 20-15.

Kim, A.G., 2002. Physical and chemical characteristics of CCB. Proc: Coal Combustion By-Products and Western Coal Mines: a Technical Interactive Forum, Golden, CO, 25-42.

Merrill, D.T., Manzione, M., Parker, D., Petersen, J., Crow, W., Hobbs, A., 1986. Field evaluation of As and Se removal by iron coprecipitation. J. Water Pollut Control Fed. 58(1), 18-26.

Miller, G.P., 2001. Arsenic Partitioning: Making predictions using PHREEQC. Extended Abstracts, USGS Workshop on Arsenic in the Environment. Denver, CO. February 21-22, 2001.

Narukawa, T., Takatsu, A., Chiba, K., Riley, K.W., French, D.H., 2005. Investigation on chemical species of arsenic, selenium and antimony in fly ash from coal fuel thermal power stations. J. Environ. Monit. 7, 1342 – 1348.

NEA (Nuclear Energy Agency), 2005. Thermochemical database project (TDB) selected data: Selenium formation data. (http://www.nea.fr/html/dbtdb/tdbdata/tdbdata.html)

Rajan, S.S.S., 1979. Adsorption and desorption of sulfate and charge relationships in allophanic clays. Soil Sci. Soc. Am. j. 43, 65–69.

Rietra, R. P. J. J., Hiemstra, T., van Riemsdijk, W. H., 2001. Comparison of selenate and sulfate adsorption on goethite. Journal of Colloid and Interface Science, 240(2), 384-390.

Stumm, W., Morgan, J.J., 1996. Aquatic Chemistry. 3rd Ed. John Wiley & Sons.

U.S. EPA, 2002. National Primary Drinking Water Standards. EPA 816-F-02-013.

U.S. EPA., 2006. Characterization of mercury-enriched coal combustion residues from electric utilities using enhanced sorbents for mercury control. EPA/600/R-06/008.

van der Hoek, E.E., Bonouvrie, P.A., Comans, R.N.J., 1994. Sorption of As and Se on mineral components of fly ash: relevance for leaching processes. Applied Geochemistry, 9, 403-412.

van der Hoek, E.E., Comans, R.N.J., 1996. Modeling arsenic and selenium leaching from acidic fly ash by sorption on iron (hydr)oxide in the fly ash matrix. Environ. Sci. Technol., 30(2), 517-523.

Wadge, A., Hutton, M., 1987. The leachability and chemical speciation of selected trace elements in fly ash from coal combustion and refuse incineration. Environ. Pollut. 48(2), 85-99.

Wang, J., Teng, X., Wang, H., Ban, H., 2004. Characterizing the metal adsorption capability of a class F coal fly ash. Environ. Sci. Technol., 38(24), 6710-6715.

Wu, C.H., Kuo, CY., Lin, C.F., Lo, S.L., 2002. Modeling competitive adsorption of molybdate, sulfate, selenate, and selenite using a Freundlich-type multi-component isotherm. Chemosphere, 47(3), 283-292.

Table 1. Sample characterization

Sample ID	Coal Type	Natural pH (S/L = 1:10)	Se (mg/kg)	Ca (g/kg)	S (g/kg)	BET Area (m^2/g)	pH_{pzc}	LOI (g/kg)
Ash #1004	Bituminous	4.5	45.6	5.9	2.2	7570	6.4	67
Ash #33	Bituminous	4.4	24.7	5.5	2.9	10910	6.7	144
Ash #1008	Bituminous	6.5	30.5	11.0	2.7	6480	6.2	85
Ash #1009	Bituminous	6.0	30.0	10.0	2.2	8710	7.4	98
Ash #1015	Subbituminous	10.6	4.6	143	19.9	25650	7.6	148
Ash #1018	Subbituminous	10.6	5.7	129.8	20.2	15680	6.8	97
Ash #7	Subbituminous	12.3	17.8	161.5	5.5	1240	6.6	2

Table 2. Surface site density and acidity constants of 0.2 M NaOH-washed Ash #1004 and DI water washed Ash #1008.

Sample ID	Site	α	β	γ
# 1004	Site density (10^{-5}mol/g)	24 ± 1	8.2 ± 1.3	6.4 ± 2.8
	Acidity constant (pK_H)	3.5 ± 0.1	7.0 ± 0.3	10.6 ± 0.4
# 1008	Site density (10^{-5}mol/g)	39 ± 1	2.1 ± 2.1	22 ± 5
	Acidity constant (pK_H)	3.2 ± 0.1	8.9 ± 2	12.2 ± 1.5

Table 3. Adsorption constants of $HSeO_3^-$ and SeO_3^{2-} for Ash #1004 and Ash #1008

Species	$\log K_S$		R^2	
	#1004	#1008	#1004	#1008
$HSeO_3^-$	2.6±0.1	3.6±0.1	0.89	0.99
SeO_3^{2-}	6.3±0.1	6.3±0.1		

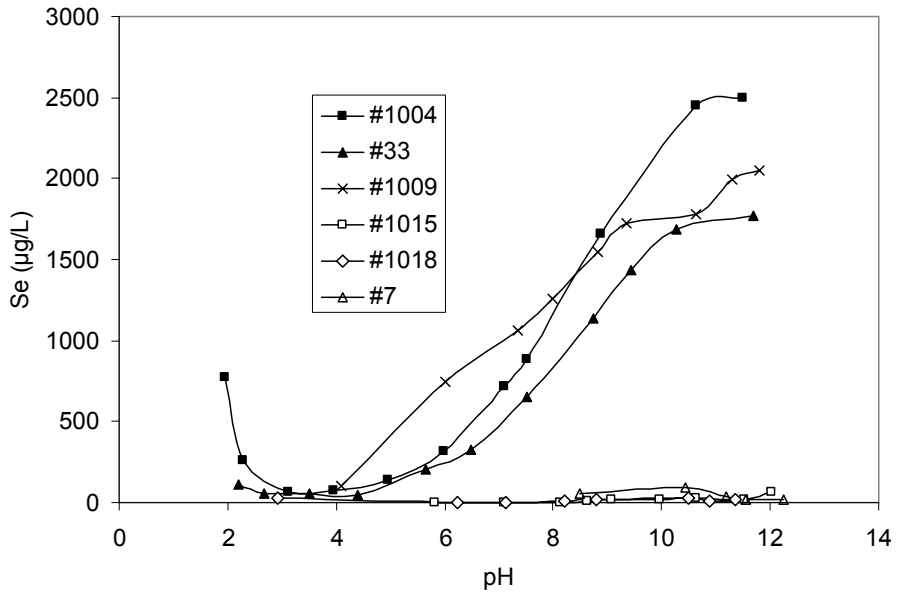

Figure 1. Selenium leaching from bituminous and subbituminous coal fly ashes. Experimental conditions: S/L = 1:10; temperature = 20 – 25 °C ; equilibration time = 24 hours.

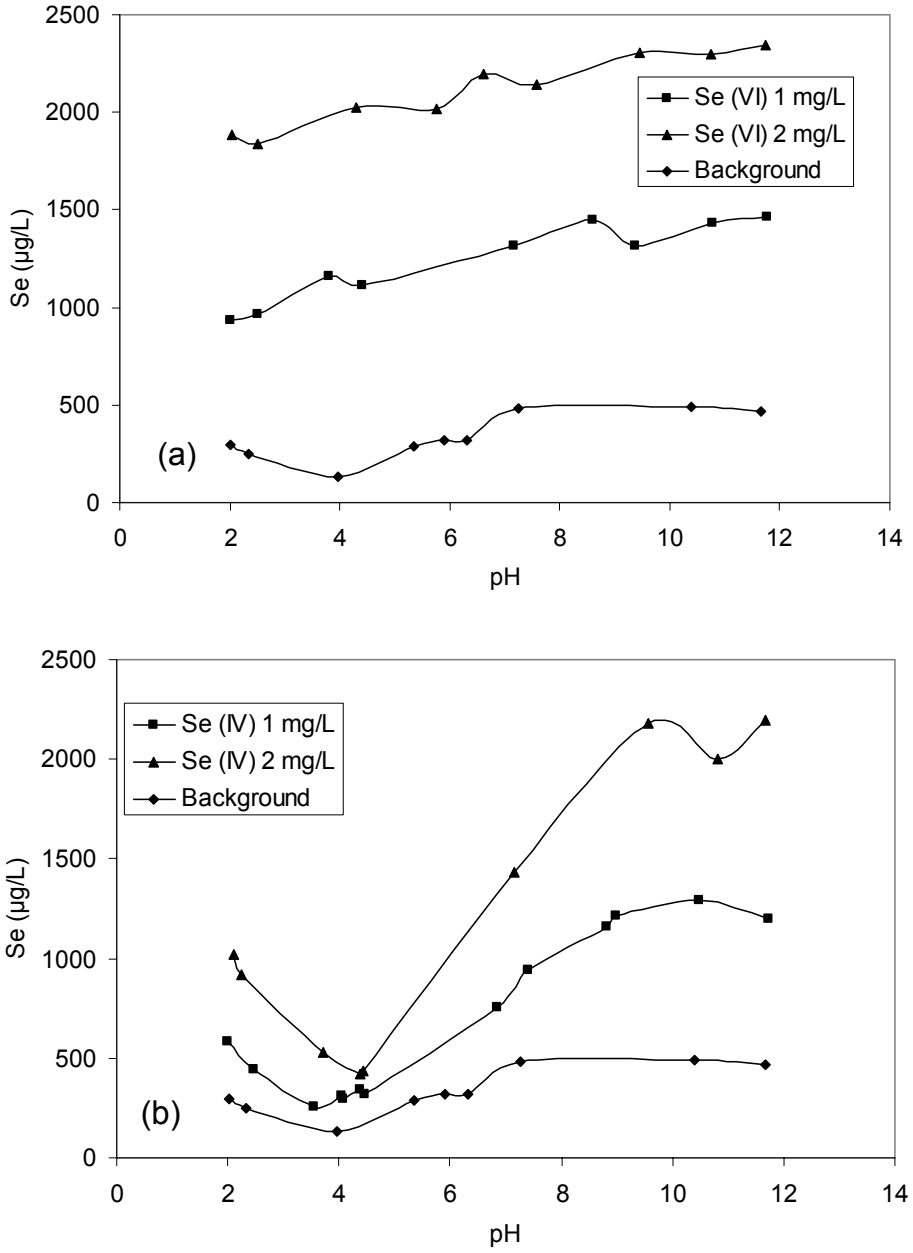

Figure 2. Soluble selenium concentrations as a function of pH under different selenium addition conditions for 0.2 M NaOH washed Ash #1004. (a) Se(VI); (b) Se(IV). Experimental conditions: S/L = 1:10; ionic strength = 0.01 M $NaNO_3$; temperature = 20 – 25 °C ; equilibration time = 24 hours.

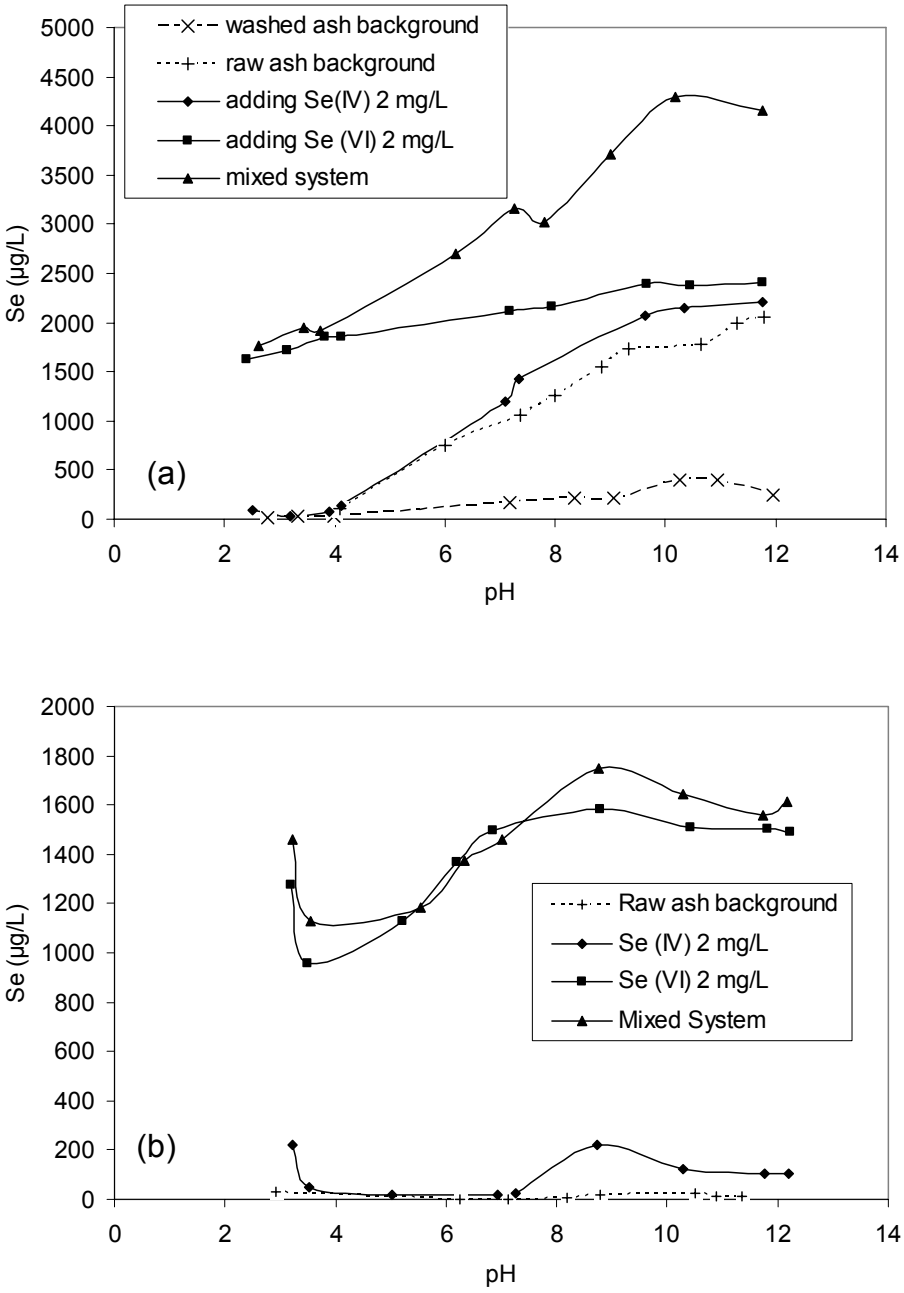

Figure 3. Selenium adsorption results in single and mixed species systems for different types of ashes. (a) 0.2 M NaOH washed bituminous coal ash # 1009; and (b) DI water washed subbituminous coal Ash #1018. Experimental conditions were same as Figure 2.

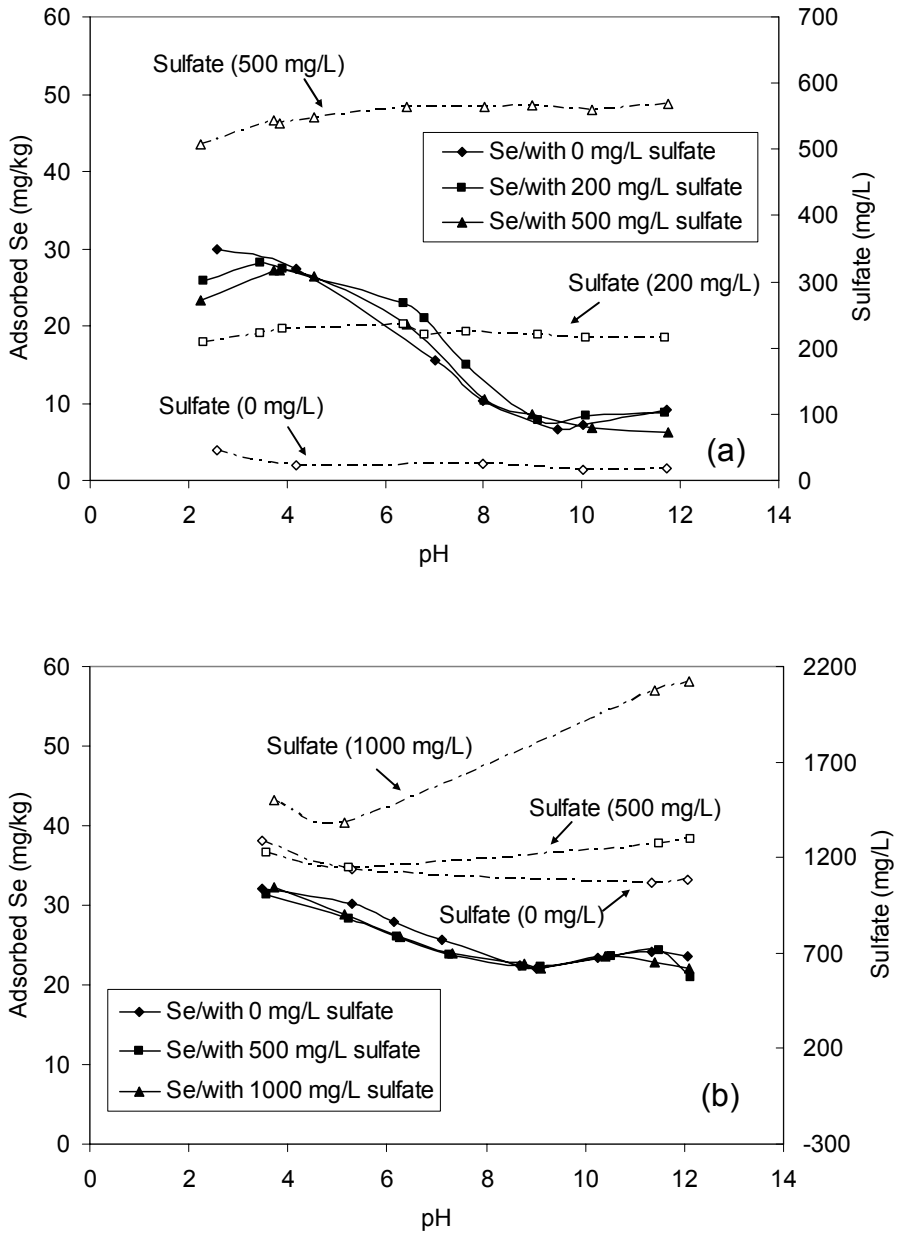

Figure 4. Sulfate impact on selenium adsorption for different types of ashes. (a) 0.2 M NaOH washed bituminous coal ash # 1009; and (b) DI water washed subbituminous coal Ash #1018. Experimental conditions were same as Figure 2.

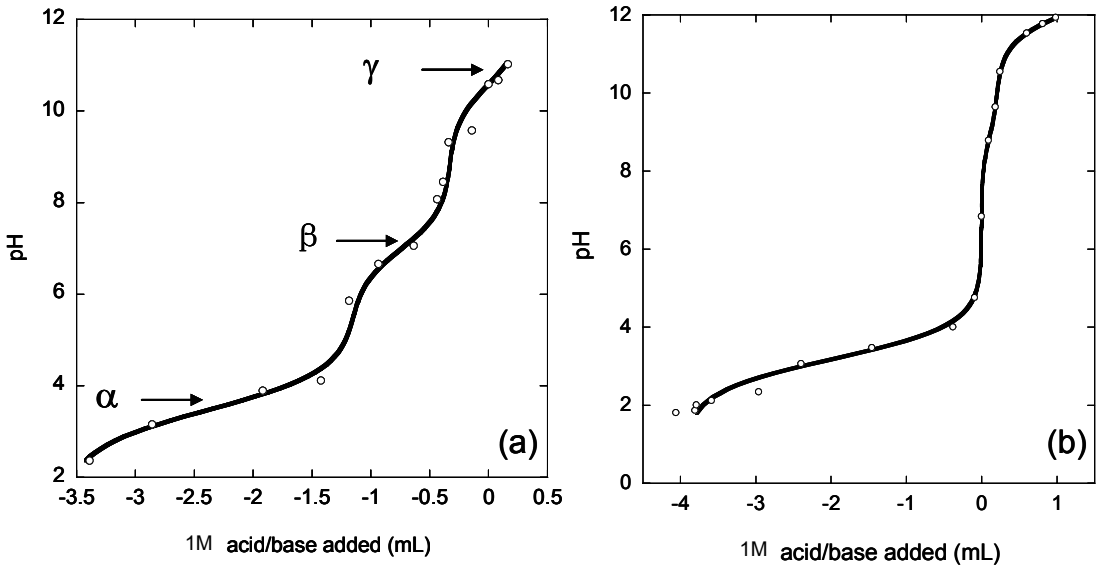

Figure 5. Titration and curve fitting results for two ashes. (a) 0.2 M NaOH washed Ash #1004 and (b) DI water washed ash #1008. Experimental conditions: S/L = 1:10; ionic strength = 0.01 M ($NaNO_3$); temperature = 20 – 25 °C; equilibration time = 24 hours (negative values were used for acid consumption on X axis).

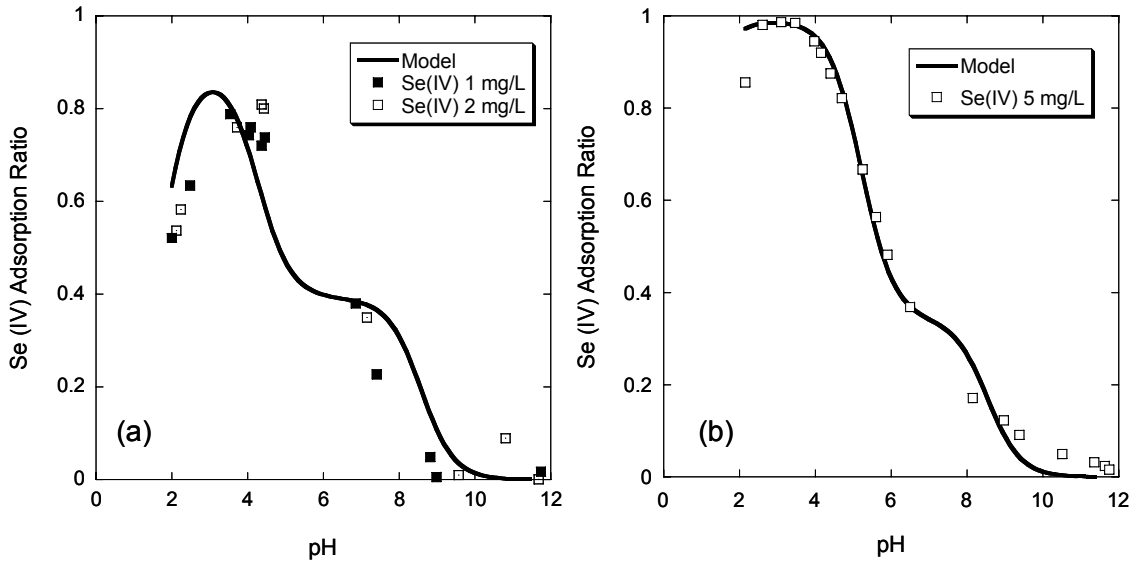

Figure 6. Se(IV) partitioning results – experimental data and modeling result for two ashes. (a) 0.2 M NaOH washed Ash #1004 and (b) DI water washed ash #1008. Experimental conditions were same as Figure 2.

III. Adsorption Characteristics of Arsenic(V) onto a Class F Fly Ash *(to be submitted to Chemosphere, 2007)*

Tian Wang [a], Jianmin Wang [a,*], Charles C. Chusuei [b], Heng Ban [c], Ken Ladwig [d], C. P. Huang [e]

[a] *Environmental Research Center; Dept. of Civil, Architectural and Environmental Engineering; Univ. of Missouri-Rolla, Rolla, MO 65409, United States*

[b] *Departments of Chemistry, University of Missouri – Rolla, Rolla, MO 65409, United States*

[c] *Department of Mechanical Engineering, University of Alabama at Birmingham, Birmingham, AL 35294, United States*

[d] *Electric Power Research Institute (EPRI), 3412 Hillview Ave., Palo Alto, CA 94304, United States*

[e] *Department of Civil and Environmental Engineering, University of Delaware, Newark, DE 19716, United States*

[*]Corresponding author: (phone) (573) 341-7503; (fax) (573) 341-4729; (email) wangjia@umr.edu

Abstract

Arsenic (As) poses a preeminent water quality problem and challenge facing environmental engineering in the world. Because of the large volumes of coal fly ash produced around the world, it is a potentially significant anthropogenic source of arsenic. The leaching behavior of arsenic from fly ash, which is important for predicting potential impacts of fly ash on water quality, is not well understood. This research focused on the adsorption aspect of the leaching process. Batch methods were used to investigate arsenic leaching using a raw ash, and arsenic adsorption using a clean, washed ash. Experimental results indicated that pH had a significant effect on arsenic leaching and adsorption. Between pH 3 and 7, less arsenic was in the dissolved phase. When pH was less than 3 or greater than 7, increasing amounts of arsenic were leached and desorbed from the fly ash. The adsorption behavior of arsenic was interpreted with the speciation of surface sites and arsenic, and a speciation-based model was developed to quantify the arsenic adsorption as a function of pH. This work is important in offering insight into the

leaching mechanism of arsenic from coal fly ash, and providing a robust model to quantify arsenic adsorption by a solid media such as fly ash.

Keywords Arsenic, Adsorption, Fly Ash, pH, Speciation-based Model

1. Introduction

In January 2006, the USEPA reduced the Maximum Contaminant Level (MCL) for arsenic in drinking water to 10 μg L^{-1} from 50 μg L^{-1} (EPA, 2003). The new MCL necessitates a more detailed evaluation of sources of arsenic that could potentially impact water quality, particularly anthropogenic sources that can be controlled. Coal fly ash, a coal combustion product (CCP) of coal-fired power plants, contains varying levels of arsenic and other trace elements (Kim and Cardone, 1997; Kim and Kazonich, 2001). For bituminous coal fly ash (class F fly ash), the arsenic concentration ranges from 1 to 1000 ppmw (parts per million by weight) (EPRI, 1987). In 2005, US generated a total of 123 million short tons (1.12×10^{11} kg) of CCPs, and 58% of which was fly ash (ACAA, 2006). The amount of coal fly ash production is unlikely to be substantially reduced in the near future due to the continued increase in the use of coal for power production (EIA, 2007). Therefore, understanding the leaching process of arsenic in fly ash during ash disposal and reuse is important in developing novel methods to control arsenic leaching and protecting water quality.

According to previous research, arsenic is enriched on the fly ash surface (Silberman and Harris, 1984; Xu et al., 2001a). Both As(III) and As(V) were detected in fly ash, but the latter was present in a much greater fraction (Silberman and Harris, 1984; Goodarzi and Huggins, 2001). Various leachants, including HNO_3, H_2SO_4, sodium citrate, geopolymer, and EDTA have been used to determine the total arsenic leaching

potential from fly ash (Silberman and Harris, 1984; Sakaguchi et al., 2002; Bankowski et al., 2004; U.S. EPA, 2006). Silberman and Harris (1984) found that as much as 78-97% of the total arsenic could be leached from fly ash with a 0.5 N H_2SO_4 or a 1 M sodium citrate at pH 5. U.S. EPA (2006), using leaching conditions ranging from very acidic to very alkaline, found that total leached arsenic was variable among different fly ashes, ranging from less than 5% in half of the ashes tested, to more than 30% in others. Under typical environmental conditions, significantly lower leaching is expected than under extreme acid or alkaline conditions.

Many factors can influence the leaching of arsenic from fly ash, such as pH, calcium, magnesium, reducing or oxidizing conditions, solid-to-liquid (S/L) ratio, leaching time, temperature and anionic constituents such as sulfate and phosphate (Lecuyer et al., 1996; Qafoku et al., 1999; Xu et al., 2001b; Praharaj et al., 2002). Several mechanisms have been proposed to interpret arsenic leaching behavior. It was reported that the leaching of arsenic from acidic ash was sorption controlled with iron oxide acting as the controlling sorbent (van der Hoek et al., 1994). A model incorporating the electrostatic effect was used to quantify the adsorption of arsenic onto fly ash (van der Hoek and Comans, 1996). However, modeling results were strongly dependent on the initial assumptions, namely that amorphous iron oxide was the lone reactive site and the calculated adsorption constant was pH dependent. Similar models were also used to quantify arsenic adsorption onto other solid media such as soil mineral and metal oxides (Goldberg, 1985; 1986; Goldberg and Glaubig, 1988a; 1988b; Hering and Dixit, 2005). However, studies are lacking on how to determine the types and quantity of reactive

surface sites in field samples for use in these models, and very little is known regarding the field application of laboratory derived adsorption constants (Miller, 2001).

The overall objective of this study was to understand the adsorption process that affects the arsenic leaching. Specifically, this research was to characterize the reactive surface sites of a class F ash pertinent to arsenic adsorption, develop mechanistic understanding of arsenic adsorption behavior, and quantify arsenic adsorption onto fly ash using a robust, speciation-based model.

2. Materials and Methods

2.1. Fly Ash Sample

A class F fly ash (sample ID 10633-1004) was selected as the model ash for this study. It was collected from the cold-side electrostatic precipitator (ESP) of a power plant burning eastern bituminous coal. Loss-on-ignition (LOI), an indicator for unburned carbon content in ash, was determined to be 6.7% based on a gravimetric method. Specific surface area, determined using a Quantachrome Autosorb-1-C high performance surface area and pore size analyzer, was 7.57 $m^2\ g^{-1}$. The pH at which the surface charge is zero (pH_{zpc}) of this fly ash was determined to be 6.5 using a Zetasizer 3000 (Malvern Instruments, Worcestershire, UK). The total arsenic concentration in the fly ash was 48.1 $\pm$ 0.5 $\mu g\ g^{-1}$ based on EPA total digestion protocol (method 3052).

The raw ash sample was used for the background leaching experiments under various pH conditions. It was dried at 105 °C for at least 24 hours to remove moisture before the experiment. A washed ash sample was used for batch equilibrium titration and batch As(V) adsorption experiments. The washing process was employed to remove some soluble constituents to obtain a relatively clean surface for the mechanistic study. A

0.2 M NaOH solution was used for washing. The washing was performed with an S/L ratio of 1:5, and was repeated 5 times. Each washing cycle lasted for 20 hours. For each washing cycle, the ash-water mixture was agitated with air for approximately 18 hours, and allowed to settle for approximately 2 hours. The supernatant was then decanted. The washed ash was dried at 105 °C for at least 24 hours before use.

2.2. Background Leaching

The background leaching experiment was performed to determine the pH effect on the leaching of arsenic from raw fly ash. Deionized (DI) water was used as the leaching solution. The leaching procedure consisted of: (a) distributing 10.0 g of dried raw ash and 100 mL of DI water to each of a series of 125 mL LDPE bottles (S/L = 1:10); (b) adding different volumes of 1 M HNO_3 or NaOH stock solution to these bottles to yield final pH values distributed in a range between 2 and 12; (c) sealing and shaking the bottles at 180 strokes/min using a reciprocating shaker (Eberbach 6010) for 24 hours; (d) filtering 20 mL supernatant with 0.45 μm syringe membrane filter; (e) acidifying the filtrate for arsenic analysis; (f) measuring the final pH of the remaining mixture in bottles. An Orion pH electrode (model 9207BN) and Orion pH meter (perpHecT LoR model 370) were used for pH measurements.

2.3. Batch Equilibrium Titration

A batch equilibrium titration method was employed to determine the surface acidity (site density and acidity constant) of the NaOH-washed ash. Two S/L ratios, 1:10 and 1:20, were used in this study. The procedure was similar to the background leaching experiment, except that 0.01 M $NaNO_3$ solution (instead of DI water, for ionic strength adjustment) was used as the leaching solution. The volume of acid or base used, and the

corresponding final pH in each bottle were recorded to plot the overall titration curve. The 0.01 M $NaNO_3$ solution was also titrated as a blank. The net titration curve was obtained by subtracting the acid/base consumption by the blank from the overall titration curve for the same pH condition. The net titration curve was then modeled using a non-linear regression program, Kaleidagraph™ (Synergy Software, Reading, PA), based on a titration equation to determine the surface acidity.

2.4. As(V) Adsorption

Batch adsorption experiments were conducted to examine the adsorption behavior of As(V) onto NaOH-washed ash. Two S/L ratios, 1:10 and 1:20, were used in this research. The experimental procedure was similar to the background leaching experiment, except that the leaching solution contained 0.01 M $NaNO_3$ (for ionic strength adjustment) and different concentrations of spiked As(V). Equilibrium concentrations of arsenic and the final pH for all bottles were measured.

2.5. Chemical Analysis

A graphite furnace atomic absorption spectrometer (AAnalyst 600, Perkin-Elmer Corp., Norwalk, Connecticut, USA) with an instrumental detection limit (IDL) for arsenic of 0.3 μg L^{-1} was used to determine arsenic concentrations in solution. The operating conditions were optimized based on the recovery of spiked samples.

3. Results and Discussion

3.1. Effect of pH on Arsenic Leaching from Raw Ash

The soluble arsenic concentration was clearly a function of pH for the raw ash, as shown in Figure 1. The minimum arsenic release was observed in the pH range between 3

and 7. At pH 2.8 and below, arsenic release increased significantly. On the other hand, at pH values above 7, soluble arsenic concentration was also increased. Since the arsenic concentration in fly ash was 48.1 μg g^{-1} fly ash, the total concentration of arsenic in the system under the experimental condition (S/L ratio = 1:10, or 100 g L^{-1} of fly ash) was 4.8 mg L^{-1}. Therefore, approximately 25% of total arsenic was released at pH 12.

The major arsenic species in fly ash was reported to be As(V) (Silberman and Harris, 1984; Goodarzi and Huggins, 2001). Since the acidity constants (pK_a) of arsenious acid (H_3AsO_4) are 2.26, 6.76, and 11.29, respectively (Lide, 2003), the neutral H_3AsO_4 species dominate the speciation when pH < 2.3. Since arsenic release was significant under very acidic pH conditions, neutrally charged H_3AsO_4 species appears to have a low affinity for adsorption by the ash surface. The dissolution of ash particles under very acidic conditions might also contribute to the high soluble arsenic concentration. When pH is above 2.3, anionic arsenic species ($H_2AsO_4^-$, $HAsO_4^{2-}$, and AsO_4^{3-}) dominate the system. Between pH 3 and 7, these anionic arsenic species were mostly adsorbed. At pH values greater than 7, arsenic release increased, possibly caused by the decrease of protonated surface sites that are responsible for arsenic anion adsorption.

3.2. Surface Characterization

Detailed study of ash surface characterization and arsenic adsorption using NaOH-washed ash resulted in better insight on the arsenic leaching behavior from raw ash. The resulting net titration data (open circles) for 0.2 M NaOH-washed ash under two S/L ratios, 1:10 and 1:20 are shown Figure 2. The following equation was used to fit the net titration data to determine the acid site concentration and the acidity constant, based

on the assumption that multiple monoprotic acid sites were present on ash surface (Wang et al., 2004):

$$\Delta V_{SS} = \sum_i \frac{V_0 \underline{S}_{Ti} K_{Hi}}{C} \left\{ \frac{1}{[H^+] + K_{Hi}} - \frac{1}{[H^+]_0 + K_{Hi}} \right\} \quad (1)$$

where ΔV_{SS} is the net volume of standard acid or base (negative value for acid) solution consumed by surface sites (mL); V_0 is total volume of the ash mixture (mL); $\underline{S}_{Ti}$ is the total acid site concentration of species i (M); K_{Hi} is the acidity constant of the species i (M); C is the concentration of the acid or base standard solution (M); and $[H^+]_0$ is the hydrogen ion concentration of the control unit (without acid or base addition) (M).

Kaleidagraph™ was employed for curve fitting, and the most appropriate fit was achieved when considering 3 types of sites on the ash surface, denoted as α, β, and γ. The curve fitting results (solid lines) agree with the experimental data as shown in Figure 2. The total surface site concentration ($\underline{S}_T$) and acidity constant (pK_H) for each type of surface site were determined. Based on the total surface site concentration and fly ash concentration, the surface site density (Γ) was determined. The surface site density and acidity constant values obtained for two S/L ratios, shown in Table 1, were consistent. Based on the surface acidity parameters, the surface site speciation diagram was developed, shown in Figure 3.

The protonated surface sites α, β and γ were hypothesized to be responsible for arsenic anion adsorption. In an S/L = 1:10 system, the ash concentration = 100 g L^{-1}. Since the density of the surface site β is 8.2×10^{-5} mol g^{-1} ash, the total concentration of surface site β, $\underline{S}_{T2} = 8.2 \times 10^{-3}$ M. In addition, since the acidity constant of site β, pK_{H2} = 7.0, the fraction of the protonated surface site β at pH 9 is 0.01. Therefore, the total

concentration of protonated surface site β at pH 9 is 8.2×10^{-5} M. Assuming one site can bind one arsenic anion, these protonated surface sites β can adsorb 6.2 mg L^{-1} of arsenic, more than the total arsenic concentration in the system of 4.8 mg L^{-1} (48 μg g^{-1} ash x 100 g L^{-1}). Therefore, if the protonated surface site β is responsible for arsenic adsorption, no arsenic would be in the soluble phase when pH approaches to 9. This hypothesis was not supported by the leaching data in Figure 1, which showed that significant fraction of arsenic is in the soluble phase when pH approaches 9. Based on the same rationale, the protonated surface site γ is not responsible for arsenic adsorption. As a result, the protonated surface site α is believed to be the dominant site for the adsorption of anionic arsenic species. Under strongly acidic pH condition, the less adsorbable neutrally charged arsenic species, H_3AsO_4, dominated the system. Therefore, the adsorption of the overall arsenic was low. Under neutral and slight acidic pH conditions, the protonated surface site α was available for adsorbing anionic arsenic species, resulting in the minimum arsenic release. When pH was increased to greater than 7, much less protonated surface site α was available, resulting in the decrease in arsenic adsorption.

As shown in Table 1, the pK_H values of the site α, site β, and site γ are 3.5, 7.0, and 10.6, respectively. Since the ash has the pH_{zpc} of 6.5, between the two pK_Hs for sites α and β, the protonated surface sites α are positively charged, while the protonated surface sites β and sites γ are neutral. Since arsenic was adsorbed when pH was greater than pH_{zpc} of 6.5, where both the arsenic species and the ash surface were negatively charged, the adsorption of arsenic by fly ash was predominantly a chemisorption process, i.e. the surface charge or surface electrostatic effect played an insignificant role in arsenic adsorption.

Please note that Figure 3 indicates that when pH is greater than 5, the concentration of the protonated surface site α is relatively low, which could be thought that its arsenic adsorption capacity is also low when pH is greater than 5. However, the adsorption of arsenic and occupation of free protonated surface sites will stimulate the protonation of more surface sites to maintain a constant ratio of the protonated surface sites to total sites at certain pH, which will further increase the adsorption of arsenic until no more protonated surface sites available. Therefore, arsenic adsorption ratio at pH between 5 and 7 can still be significant since the total amount of site α was much higher than total arsenic concentration, and the ratio of protonated sites was not extremely low within this pH range.

3.3. As(V) Adsorption onto NaOH-Washed Ash

As(V) adsorption experiments were conducted using NaOH-washed ash under S/L ratios of 1:10 and 1:20, to obtain data for mechanistic understanding of the arsenic leaching behavior. The washing process removed easily soluble components in fly ash, and thus created ideal conditions for adsorption experiments. Four different As(V) additions (1, 2, 5, and 10 mg L^{-1}) were applied for the adsorption experiment under the S/L ratio of 1:10. In addition, an equilibrium experiment without arsenic addition was performed. Soluble arsenic concentrations (points in Figure 4a) under different arsenic additions increased at pH conditions < 3 and > 7, as was observed for raw ash. Some arsenic, estimated to be 1.2 mg L^{-1} at the maximum, was also released from the washed ash particles. Comparison with Figure 1 (raw ash leaching data) reveals that both the washed ash and raw ash behave similarly with respect to soluble arsenic concentration.

Therefore, the adsorption results using washed ash provided benchmark data for understanding arsenic leaching from raw ash.

Figure 4(b) shows the arsenic adsorption ratio (i.e. the ratio of adsorbed arsenic to the total available arsenic in the system) as a function of pH (points). The adsorption ratio was calculated based on the equilibrium arsenic concentration shown in Figure 4(a), the added arsenic concentration, and an estimated maximum background arsenic concentration of 1.2 mg L^{-1}. To calculate the arsenic adsorption ratio R, the following equation was used:

$$R=1-\frac{[As(V)]_D}{[As(V)]_{add}+[As(V)]_b} \quad (2)$$

where $[As(V)]_D$, $As(V)]_{add}$, and $As(V)]_b$ are the soluble, added, and background arsenic concentrations, respectively. All adsorption ratio data for different arsenic additions fall in the same line**,** as shown in Figure 4(b), suggesting that the adsorption is in the linear range of the Langmuir isotherm.

To further investigate the arsenic adsorption behavior under a broader arsenic loading range, a lower ash concentration of 50 g L^{-1} (S/L = 1:20) was used to conduct the adsorption experiment with arsenic additions of 1, 2, 5, 10 and 100 mg L^{-1}. An equilibrium experiment without arsenic addition was also performed. Figure 5(a) shows the soluble arsenic concentration data (points). Compared with Figure 4a, the maximum arsenic concentration released from the washed ash decreased by 50%, to 0.6 mg L^{-1}. The overall arsenic adsorption ratio was calculated, shown as points in Figure 5(b). Unlike the other four groups of data, the arsenic adsorption ratio for 100 mg L^{-1} As(V) addition were significantly lower, indicating that arsenic adsorption under 100 mg L^{-1} addition was not in the linear range of the Langmuir isotherm.

3.4. Modeling As(V) Adsorption onto Washed Ash

3.4.1. Surface Site Speciation

Surface site density and acidity constant are essential parameters for adsorption modeling. It was hypothesized that the protonated surface site α is responsible for arsenic adsorption. Its deprotonation reaction is expressed as:

$$\underline{S_1}OH_2^+ = \underline{S_1}OH + H^+;\ K_H \quad (3)$$

where K_H is the acidity constant of the protonated surface site α, or $\underline{S_1}OH_2^+$.

The concentration of the protonated surface site α is expressed as:

$$[\underline{S_1}OH_2^+] = \alpha_+ S_T \quad (4)$$

where S_T is the total surface site α (protonated and unprotonated) concentration, and α_+ is the fraction of the protonated surface site, $\alpha_+ = \frac{[H^+]}{[H^+] + K_H}$.

3.4.2. Arsenic Speciation

Different arsenic species co-exist in aqueous solutions, depending on the pH. The concentrations of different As(V) species can be calculated based on the following equations:

$$[H_2AsO_4^-] = \alpha_1 [As(V)]_D \quad (5)$$

$$[HAsO_4^{2-}] = \alpha_2 [As(V)]_D \quad (6)$$

$$[AsO_4^{3-}] = \alpha_3 [As(V)]_D \quad (7)$$

where α_1, α_2 and α_3 are the fractions of As(V) as $H_2AsO_4^-$, $HAsO_4^{2-}$, and AsO_4^{3-}, respectively.

3.4.3. Arsenic Adsorption Equations

The adsorption of different arsenic species by the protonated surface site α can be expressed as:

$\underline{S_1}OH_2^+ + H_2AsO_4^- = \underline{S}\text{-}H_2AsO_4 + H_2O;\ K_{S1};$ (8)

$\underline{S_1}OH_2^+ + HAsO_4^{2-} = \underline{S}\text{-}HAsO_4^- + H_2O;\ K_{S2};$ (9)

$\underline{S_1}OH_2^+ + AsO_4^{3-} = \underline{S}\text{-}AsO_4^{2-} + H_2O;\ K_{S3};$ (10)

where K_{S1}, K_{S2} and K_{S3} are adsorption constants of $H_2AsO_4^-$, $HAsO_4^{2-}$, and AsO_4^{3-}, respectively.

The concentrations of adsorbed arsenic species are expressed using the following equations:

$$[\underline{S_1} - H_2AsO_4] = K_{S1}[\underline{S_1}OH_2^+]\alpha_1[As(V)]_D \quad (11)$$

$$[\underline{S_1} - HAsO_4^-] = K_{S2}[\underline{S_1}OH_2^+]\alpha_2[As(V)]_D \quad (12)$$

$$[\underline{S_1} - AsO_4^{2-}] = K_{S3}[\underline{S_1}OH_2^+]\alpha_3[As(V)]_D \quad (13)$$

3.4.4. Speciation Based Langmuir Isotherm

The total site concentration, $\underline{S}_T$ is expressed as:

$$\underline{S}_T = [\underline{S_1}OH_2^+] + [\underline{S_1}OH] + [\underline{S_1}\text{-}H_2AsO_4] + [\underline{S_1}\text{-}HAsO_4^-] + [\underline{S_1}\text{-}AsO_4^{2-}] \quad (14)$$

The $[\underline{S_1}OH]$ is expressed as:

$$[\underline{S_1}OH] = \frac{[\underline{S_1}OH_2^+][K_H]}{[H]} \quad (15)$$

From equations (11) to (15), the following equation is obtained:

$$[\underline{S_1}OH_2^+] = \frac{\alpha_+ \underline{S}_T}{1 + \alpha_+(K_{S1}\alpha_1 + K_{S2}\alpha_2 + K_{S3}\alpha_3)[As(V)]_D} \quad (16)$$

Therefore, the total adsorbed As(V) concentration is expressed as:

$$[\mathrm{As(V)}]_{ads} = [\underline{S_1} - H_2AsO_4] + [\underline{S_1} - HAsO_4^-] + [\underline{S_1} - AsO_4^{2-}]$$
$$= \frac{\underline{S}_T \alpha_+ (K_{S1}\alpha_1 + K_{S2}\alpha_2 + K_{S3}\alpha_3)[\mathrm{As(V)}]_D}{1 + \alpha_+ (K_{S1}\alpha_1 + K_{S2}\alpha_2 + K_{S3}\alpha_3)[\mathrm{As(V)}]_D} \quad (17)$$

Compared with the original Langmuir isotherm, Equation 17 includes the pH effect on the surface site speciation and arsenic speciation, and the competition effect of different arsenic species for the same adsorption site.

When adsorption ratio R is considered, Equation 17 is re-written to:

$$R = \frac{[\mathrm{As(V)}]_{ads}}{[\mathrm{As(V)}]_D + [\mathrm{As(V)}]_{ads}}$$
$$= \frac{\alpha_+ \underline{S}_T (K_{S1}\alpha_1 + K_{S2}\alpha_2 + K_{S3}\alpha_3)}{1 + \alpha_+ \underline{S}_T (K_{S1}\alpha_1 + K_{S2}\alpha_2 + K_{S3}\alpha_3) + \alpha_+ (K_{S1}\alpha_1 + K_{S2}\alpha_2 + K_{S3}\alpha_3)[\mathrm{As(V)}]_D} \quad (18)$$

If $[\mathrm{As(V)}]_D$ is significantly lower than $\underline{S}_T$, the adsorption is in the linear range of Langmuir isotherm, and Equation 18 is simplified to:

$$R = \frac{\alpha_+ \underline{S}_T (K_{S1}\alpha_1 + K_{S2}\alpha_2 + K_{S3}\alpha_3)}{1 + \alpha_+ \underline{S}_T (K_{S1}\alpha_1 + K_{S2}\alpha_2 + K_{S3}\alpha_3)} \quad (19)$$

Equation 19 indicates that the adsorption ratio is a function of pH, and independent of the total concentration in the system.

3.4.5. Modeling As(V) Adsorption Data

As shown in Figure 4(b), the adsorption ratios calculated for different arsenic additions fall along the same curve. The same scenario was observed in Figure 5(b) when arsenic addition was equal to or less than 10 mg L^{-1}. These results indicate that at arsenic concentrations below 10 mg L^{-1}, the adsorption is in linear range of Langmuir isotherm, and the adsorbed arsenic concentration is proportional to the total arsenic concentration.

When the arsenic addition was increased to 100 mg L^{-1} for the S/L ratio of 1:20, the adsorption ratio decreased significantly.

According to previous research, if the relative metal concentration is low (i.e. less than 10% of the surface site concentration), adsorption is in the linear range of the Langmuir isotherm (Wang et al., 2004). The concentration of surface site α determined by batch equilibrium titration was 0.012 M at S/L = 1:20 (50 g L^{-1} solids). The 100 mg L^{-1} As(V) was equivalent to 0.0013 M, which was approximately equal to 10% of the total site concentration. Therefore, the arsenic adsorption for the 100 mg L^{-1} addition is expected to be in the linear range of the Langmuir isotherm if the all surface α sites served as the arsenic adsorption sites. But experimental data clearly show the contrary. It is suspected that only a fraction of the surface site α determined from acid/base titration were responsible for arsenic adsorption.

Equation 18 was employed to model the experimental data obtained with S/L ratio of 1:20 in Figure 5(b). Since the AsO_4^{3-} species is not significant under low and neutral pH conditions where protonated surface sites α are available, its adsorption was not considered during modeling. A multi-variable nonlinear regression program NLREG (Phillip H. Sherrod, 6430 Annandale Cove, Brentwood, TN) was used for curve fitting. The acidity constant of the surface site α determined from titration was applied to the model. The density of arsenic adsorption sites (denoted as Γ_{As}), and the adsorption constants for $H_2AsO_4^-$ and $HAsO_4^{2-}$ (K_{S1} and K_{S2}) were treated as unknown constants. The solid lines in Figure 5(b) show the curve fitting results. Modeling data showed that the maximum arsenic adsorption density (Γ_{As}) is 0.75×10^{-5} mol g^{-1} ash; i.e. only 3.1% of the acid sites (determined based on the titration) are arsenic adsorption sites. The

adsorption constants ($\log K_S$) for $H_2AsO_4^-$ and $HAsO_4^{2-}$ are, respectively, 4.4 and 7.9. The regression coefficient for the curve fitting (R^2) is 0.895. Solid lines in Figure 5(a) are calculated arsenic concentration results based on the model parameters.

As shown in Figure 5, the modeling results agree with the experimental data. When arsenic addition was less than 10 mg L^{-1}, the model-calculated adsorption ratio and experimental data fell onto the same curve, indicating that the adsorption was in the linear range of the Langmuir isotherm. Although larger errors were observed for calculated adsorption ratios under the 100 mg L^{-1} As(V) addition, the model calculation still reasonably reflects the trend of the experimental data.

The experimental data with S/L ratio of 1:10 were used for verification of the speciation-based arsenic adsorption model. Using the parameters (maximum arsenic adsorption density and the adsorption constants) determined based on the S/L ratio of 1:20 data, the arsenic adsorption behavior under the S/L ratio of 1:10 was calculated. Figure 4 shows the predicted soluble arsenic concentration and adsorption ratio results (solid lines). The predictions are in good agreement with the experimental data (points). The match between model prediction and the experimental data successfully demonstrates the validity of this speciation-based adsorption model on predicting arsenic adsorption onto fly ash.

Comparison between arsenic leaching data for raw ash (Figure 1) and arsenic adsorption data for washed ash (Figures 4 and 5) indicates that soluble arsenic concentrations for both systems followed the same trend, especially when pH is less than 7. Therefore, adsorption-desorption is one of the main processes affecting arsenic leaching. However, when pH is greater than 7, the soluble arsenic concentration curve for

the leaching experiment using raw ash is below than what was expected for the adsorption experiment using washed ash. For example, washed ash showed maximum soluble arsenic concentration when pH is less than 10, while for the raw ash, the maximum soluble arsenic concentration was not achieved when pH is approximately 12. As a result, some other factors or ash components which were removed through the washing process contributed to the low arsenic solubility for the raw ash under the alkaline pH condition. Future research is scheduled to identify quantify the impact of these components on arsenic leaching.

4. Conclusions

The pH significantly impacts the leaching of arsenic from fly ash. Between pH 3 and 7, arsenic leaching was at minimum. However, when pH was less than 3 or greater than 7, more arsenic was leached. The arsenic adsorption by NaOH-washed ash showed similar behavior as the arsenic leaching from raw ash especially when pH is less than 7, suggesting that adsorption is one of the main mechanisms affecting arsenic leaching from the tested class F ash. Results indicate that there are three types of acid sites on fly ash surface. A speciation-based model was developed to quantify the adsorption behavior of arsenic onto the washed ash. Based on the modeling, only a small fraction of the protonated surface sites α was responsible for arsenic anion adsorption. The arsenic adsorption site density (Γ_{As}) was determined to be 0.75×10^{-5} mol g^{-1} ash through curve fitting. The adsorption constants ($\log K_{S1}$ and $\log K_{S2}$) of $H_2AsO_4^-$ and $HAsO_4^{2-}$ were determined to be 4.4 and 7.9. This research offers a substantial simplification of modeling arsenic(V) adsorption onto solid particles by eliminating insignificant surface electrostatic effect, and providing insights on the arsenic leaching mechanism from class

F fly ash. It contributes to the development of models for field leaching process prediction, which can be used to assess the potential impact of fly ash on groundwater quality and to develop methods to minimize the arsenic leaching.

Acknowledgements

This work was supported by the Electric Power Research Institute (EPRI), the Missouri Water Research Center (MWRC), and the Environmental Research Center (ERC) for Emerging Contaminants at the University of Missouri-Rolla (UMR). The authors thank Mr. Minghua Li at the University of Delaware for providing the zeta potential measurement. Conclusions and statements made in this paper are those of the authors, and in no way reflect the endorsement of the aforementioned funding agencies.

References

ACAA, 2006. 2005 Coal Combustion Product (CCP) Production and Use Survey. American Coal Ash Association. http://www.acaa-usa.org/CCPSurveyShort.htm.

Bankowski P., Zou L., and Hodges R., 2004. Reduction of Metal Leaching in Brown Coal Fly Ash Using Geopolymers. J. Hazard. Mater. 114(1-3), 59-67.

Energy Information Administration (EIA), 2007. Annual Energy Outlook 2007. www.eia.doe.gov.

EPRI, 1987. Chemical Characterization of Fossil Fuel Combustion Wastes. EPRI report EA-5321.

Goldberg, S., 1985. Chemical modeling of anion competition on goethite using the constant capacitance model. Soil Sci. Soc. Am. J. 49(4), 851-6.

Goldberg, S., 1986. Chemical modeling of arsenate adsorption on aluminum and iron oxide minerals. Soil Sci. Soc. Am. J. 50(5), 1154-1157.

Goldberg, S., Glaubig, R.A., 1988a. Anion sorption on a calcareous, montmorillonitic soil - arsenic. Soil Sci. Soc. Am. J. 52(5), 1297-300.

Goldberg, S., Glaubig, R.A., 1988b. Anion sorption on a calcareous, montmorillonitic soil - selenium. Soil Sci. Soc. Am. J.l, 52(4), 954-8.

Goodarzi F., Huggins F.E., 2001. Monitoring the Species of Arsenic, Chromium and Nickel in Milled Coal, Bottom Ash and Fly Ash from a Pulverized Coal-fired Power Plant in Western Canada. J. Environ. Monit. 3(1), 1-6.

Hering, J.G., Dixit, S., 2005. Contrasting sorption behavior of arsenic(III) and arsenic(V) in suspensions of iron and aluminum oxyhydroxides. In: O'Day, et al. (Eds), Advances in Arsenic Research. Oxford University Press, 2005. pp 8 – 24.

Kim A.G., Cardone C., 1997. Preliminary Statistical Analysis of Fly Ash Disposal in Mined Areas. Proc: 12th International Symposium on Coal Combustion By-Product Management and Use. American Coal Ash Association. 1, 11-1 to 11-13.

Kim A.G., Kazonich G., 2001. Release of Trace Elements from CCB: Maximum Extractable Fraction. Proceedings 14th International Symposium on Management and Use of Coal Combustion Products (CCPs). 1, 20-1 to 20-15.

Lecuyer I., Bicocchi S., Ausset P., Lefevre R., 1996. Physico-Chemical Characterization and Leaching of Desulphurization Coal Fly Ash. Waste Manage. Res. 14(1), 15-28.

Lide D.R., 2003. Handbook of Chemistry and Physics. 84th Ed. CRC Press.

Miller G.P., 2001. Arsenic Partitioning: Making Predictions Using PHREEQC. Extended Abstracts, USGS Workshop on Arsenic in the Environment. Denver, CO. February 21-22, 2001.

Praharaj T., Powell M.A., Hart B.R., Tripathy S., 2002. Leachability of Elements from Sub-bituminous Coal Fly Ash from India. Environment International. 27(8), 609-615.

Qafoku N.P., Kukier U., Sumner M.E., Miller W.P., Radcliffe D.E., 1999. Arsenate Displacement from Fly Ash in Amended Soils, Water, Air, and Soil Pollut.. 114, 185-198.

Sakaguchi Y., Nakajima T., Takanashi H., Ohki A., 2002. Analysis of Coal Fly Ash by X-ray Photoelectron Spectroscopy. Sekitan Kagaku Kaigi Happyo Ronbunshu. 39, 133-134.

Silberman D., Harris W.R., 1984. Determination of Arsenic(III) and Arsenic(V) in Coal and Oil Fly Ashes. International Journal of Environmental Analytical Chemistry. 17(1), 73-83.

U.S. EPA, 2003. National Primary Drinking Water Standards. EPA 816-F-03-016.

U.S. EPA., 2006. Characterization of Mercury-Enriched Coal Combustion Residues from Electric Utilities Using Enhanced Sorbents for Mercury Control. EPA/600/R-06/008.

van der Hoek E.E., Bonouvrie P.A., Comans R.N.J., 1994. Sorption of As and Se on Mineral Components of Fly Ash: Relevance for Leaching Processes. Appl. Geochem.. 9, 403-412.

van der Hoek E.E., Comans R.N.J., 1996. Modeling Arsenic and Selenium Leaching from Acidic Fly Ash by Sorption on Iron (Hydr)oxide in the Fly Ash Matrix. Environ. Sci. Technol. 30(2), 517-523.

Wang J., Teng X., Wang H., Ban H., 2004. Characterizing the Metal Adsorption Capability of a Class F Coal Fly Ash. Environ. Sci. Technol. 38(24), 6710-6715.

Xu Y., Nakajima T., Ohki A., 2001a. Leaching of Arsenic from Coal Fly Ashes 1. Leaching Behavior of Arsenic and Mechanism Study. Toxicol. Environ. Chem.. 81(1-2), 55-68.

Xu Y., Nakajima T., Ohki A., 2001b. Leaching of Arsenic from Coal fly Ashes 2. Arsenic Pre-leaching with Sodium Gluconate Solution. Toxicol. Environ. Chem. 81(1-2), 69-80.

Table 1. Surface site densities and acidity constants of 0.2 M NaOH-washed ash.

S/L ratio	Surface Site Parameter	α	β	γ
1:10	Γ (10^{-5} mol g^{-1})	24 ± 1	8.2 ± 1.3	6.4 ± 2.8
	pK_H	3.5 ± 0.1	7.0 ± 0.3	10.6 ± 0.4
1:20	Γ (10^{-5} mol g^{-1})	24 ± 1	7.0 ± 1.1	7.2 ± 0.9
	pK_H	3.3 ± 0.1	7.1 ± 0.4	8.9 ± 0.4

Note: +/- values indicate the standard error.

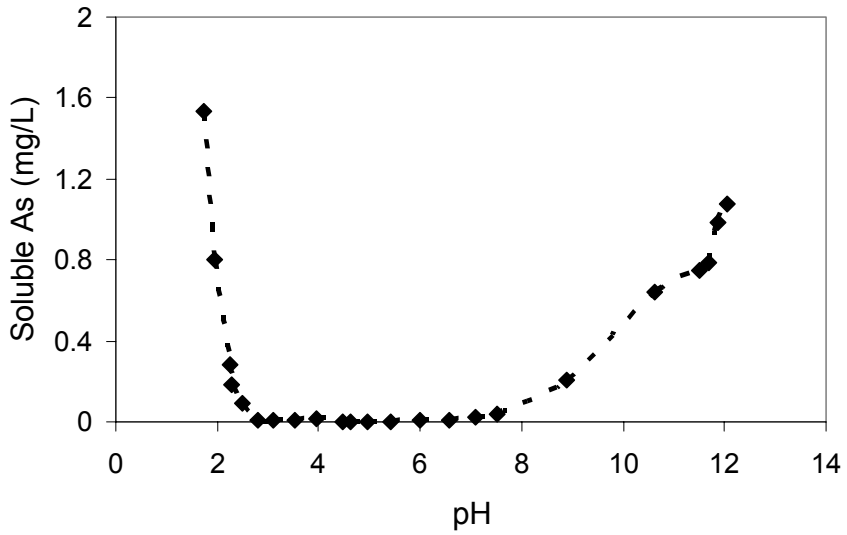

Figure 1. Batch leaching results for the raw ash. Experimental conditions: S/L = 1:10; temperature = 20 – 25 °C; equilibration time = 24 hours.

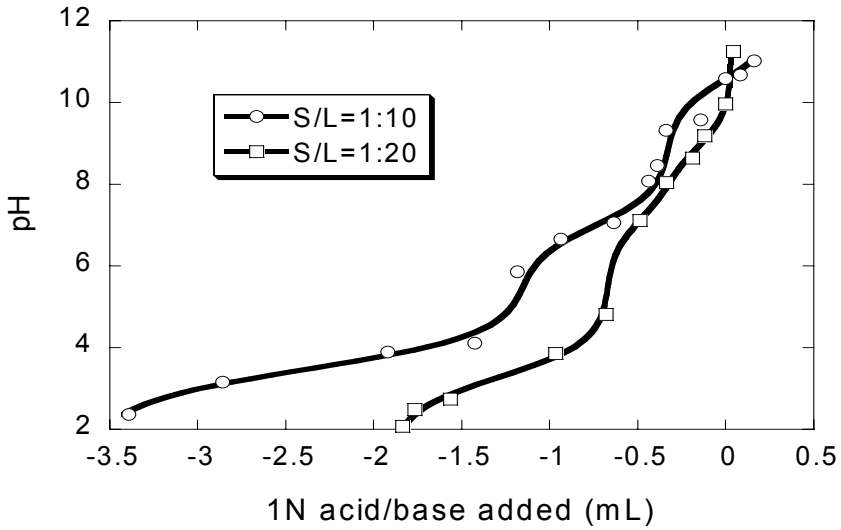

Figure 2. Titration and curve fitting results for 0.2 M NaOH-washed ash. S/L = 1:10 and 1:20; ionic strength = 0.01 M ($NaNO_3$); room temperature = 20 – 25 °C; equilibration time = 24 hours (negative values were used for acid consumption on X axis).

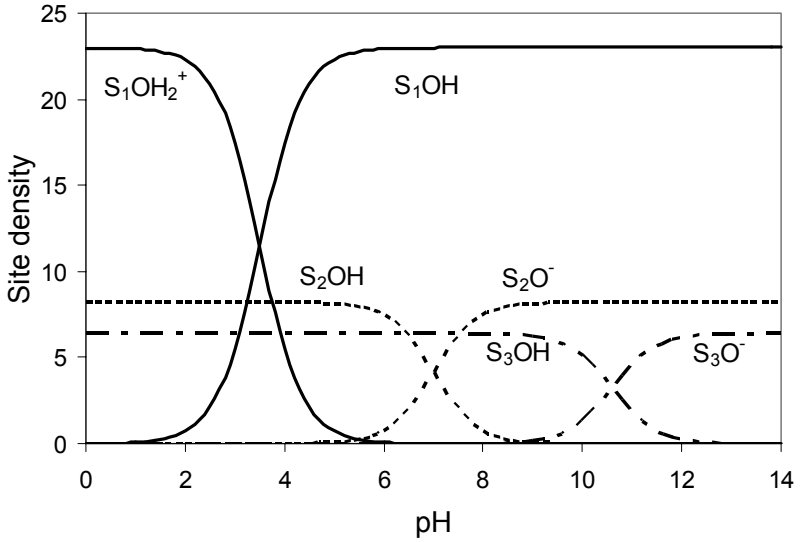

Figure 3. Speciation diagram of 0.2 M NaOH-washed ash. Site densities and acidity constants were obtained from titration with S/L=1:10. Sites S_1, S_2 and S_3 correspond to sites α, β and γ, respectively.

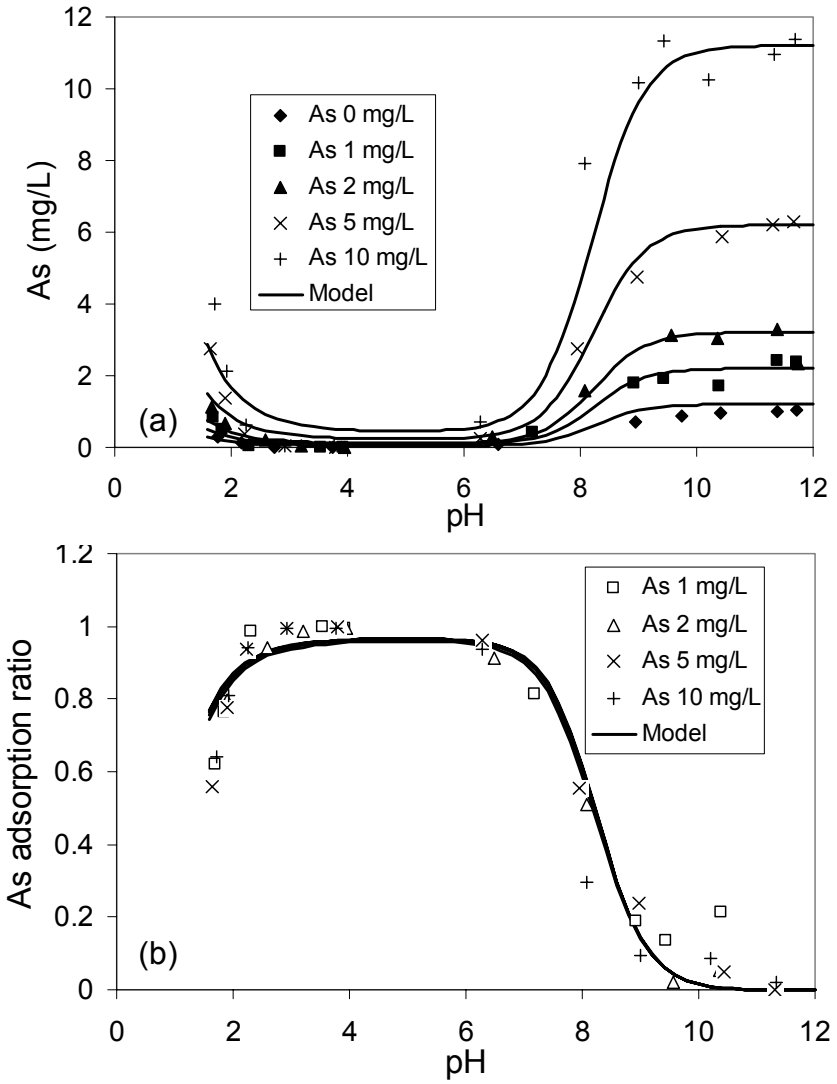

Figure 4. As(V) adsorption data for 0.2 M NaOH-washed ash with S/L ratio of 1:10. (a) soluble concentration as a function of pH; and (b) As(V) adsorption ratio as a function of pH. The solid lines denote modeling results. Ionic strength = 0.01 M ($NaNO_3$); temperature = 20 – 25 °C; equilibration time = 24 hours.

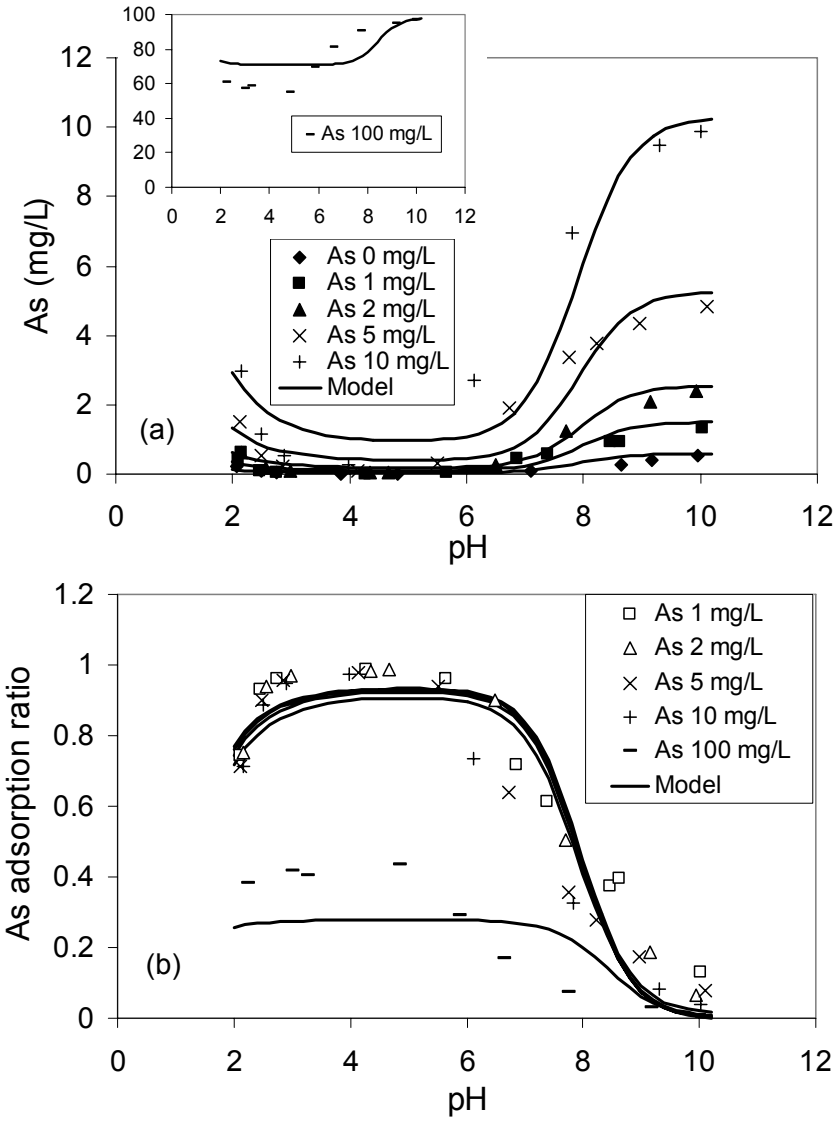

Figure 5. As(V) adsorption data for 0.2 M NaOH-washed ash with S/L ratio of 1:20. (a) soluble concentration as a function of pH; and (b) As(V) adsorption ratio as a function of pH. The solid lines denote modeling results. Ionic strength = 0.01 M NaNO3; temperature = 20 – 25 °C; equilibration time = 24 hours.

IV. Understanding the Leaching Behavior of Arsenic and Selenium for Different Types of Coal Fly Ashes Plants *(to be submitted to Environmental Science and Technology)*

TIAN WANG,[†] JIANMIN WANG,[*,†] HONGLAN SHI[†], KEN LADWIG[‡]

[†] Department of Civil, Architectural & Environmental Engineering, University of Missouri – Rolla, Rolla, MO 65409

[‡] Electric Power Research Institute (EPRI), 3420 Hillview Ave., Palo Alto, CA 94304

[*] Corresponding author phone: (573) 341-7503; email: wangjia@umr.edu

ABSTRACT

Batch leaching experiments were employed to investigate the leaching behavior of arsenic (As) and selenium (Se) for three different types of fly ash samples. The effects of pH, solid-to-liquid (S/L) ratio, presence/absence of air, and leaching time on the leaching and speciation of As and Se were studied. For bituminous coal ash, the leaching of arsenic and selenium is mostly controlled by adsorption/desorption and slow diffusion processes. However, for subbituminous coal ash, the high calcium content may form precipitation with both arsenic and selenium and control their leaching. Results also indicated that As(V) and Se(IV) are major arsenic and selenium species in all ash leachate, and the presence of air did not alter the speciation of arsenic and selenium in the leachate for the 1-day leaching experiment. Substantially more arsenic and selenium were leached from both bituminous coal ash and subbituminous coal ash in 30-day leaching experiment compared to the normally used 1-day leaching experiment due to the slow diffusion process of arsenic and selenium and the decrease of calcium concentration in the leachate of the subbituminous coal ash resulted from the slow minimization process.

This study also demonstrated that HPLC-ICP-MS is an appropriate method for determining As and Se speciation in fly ash leachates.

KEYWORDS: Arsenic, Selenium, Leaching, Speciation, Fly Ash

Introduction

The concentrations of As and Se in coal fly ash are often greater than those in background soils (1, 2). For bituminous coal fly ash, the As concentrations are typically below 200 ppmw (parts per million by weight) but can be as high as 1000 ppmw, depending on coal source and combustion technology (3). The Se concentration can be as high as 200 ppmw (4), although it is typically in the range of 10 to 20 ppmw (3). US power facilities produced more than 71 million short tons (6.4 x 1010 kg) of coal fly ashes in 2005 (5). Therefore, understanding the leaching mechanism of As and Se in coal fly ash is significant in evaluating the potential impacts of fly ash on groundwater quality and developing novel methods to control As and Se leaching from fly ash.

Previous studies demonstrated that the leaching behavior of As and Se from fly ash were affected by pH, solid-to-liquid (S/L) ratios, leaching time, temperature and the types of fly ash (6-11), among which pH was reported to be the key factor. Jankowski et al. (9) conducted a long term (144 h) batch leaching test with four Australian fly ashes and found that As leaching from both acidic and alkaline ashes was increased with time, whereas after reaching a maximum concentration, As leaching from alkaline ash was decreased. Se mobility showed a similar pattern with that of As. van der Hoek et al. (12) concluded that As and Se leaching from acidic ash was likely to be controlled by surface complexation with iron oxide, while a calcium phase was shown to be responsible for the leaching in alkaline ash. Because speciation plays an important role on the toxicity and

mobility of the elements of concern, more emphasis has recently been placed on measuring the chemical speciation of As and Se in environmental samples (13). For example, As(III) is generally more toxic and more mobile than As(V), the methylated forms (monomethylarsonic acid (MMA) and dimethylarsinic acid (DMA)) have been identified as less toxic than the inorganic forms, and arsenobetaine (AsB) is believed to be nontoxic (14). With respect to the two common inorganic Se species, Se(VI) has been reported to be less toxic and more mobile in aqueous environment than Se(IV) (15-18). Previous studies also demonstrated that the predominant species of As and Se in both solid fly ash and the liquid extracts from fly ash were As(V) and Se(IV), respectively (19-23).

Accurate measurement of As and Se speciation in fly ash leachate is desired for the assessment of their mobility and environmental impact. Coupled instrumental techniques have been developed for the speciation analysis of As and Se in aqueous samples, which combines a separation process with suitable detection technique. Separation of different As and Se species can be achieved with ion chromatography (IC) (20, 24) or high performance liquid chromatography (HPLC) (19, 25). Commonly used detectors are atomic adsorption spectrometry (AA) (19), inductively coupled plasma atomic emission spectrometry (ICP-AES) (24), and ICP-mass spectrometry (ICP-MS) (20). The combination of HPLC with ICP-MS has become more and more preferable for both academic research and industrial application because of its high sensitivity, minimal sample pretreatment, and the ability for simultaneous analysis of As and Se (26-29).

The overall objective of the present study is to understand the leaching behavior of As and Se in 3 different types of fly ash samples under different conditions such as pH, S/L

ratio, presence/absence of air, and leaching time, based on the speciation analyses of As and Se in the leachate. The conditions of the HPLC-ICP-MS method for the speciation analysis of As and Se in fly ash leachate are also discussed.

Methods

Fly Ash Samples. Three different types of fly ash samples, denoted as 33103-110 (Ash #110), 33106-1005 (Ash #1005) and 50213-7 (Ash #7) were used in this study. Ashes #110 was collected from a power plant burning a blend of 75% bituminous coal and 25% subbituminous coal. Ash #1005 was collected from one pulverized coal power plant burning an eastern bituminous coal, and #7 was collected from a power plant burning a subbituminous coal. Other physical and chemical properties including total content of As, Se and Ca, loss-on-ignition (LOI), and BET specific surface area are shown in Table 1.

Reagents and Standards. Laboratory pure 18 MΩ deionized water was used throughout the experiment. Other reagents, including As(III), As(V), Selenium(IV) and Selenium(VI) standard solutions, solid cacodylic acid (dimethylarsenic acid, DMA), and solid arsenobetaine were obtained from Sigma-Aldrich (St. Louis, MO, USA). Monosodium acid methane was purchased from ChemService (West Chester, PA USA). Reagents used for the HPLC mobile phases including ammonium phosphate (monobasic), nitric acid and ammonium hydroxide (hi-purity), and HPLC grade methanol were purchased from Fisher Scientific. The 5 mg/L intermediate As and Se standards were made from the stock solutions with deionized water. Calibration standards (5, 10, 50 and 100 μg/L) were freshly prepared by serial dilution of the intermediate standards with mobile phase. The mobile phase was filtered with 0.2 μm membrane filter before use.

Batch Leaching Experiments. Two types of background leaching experiments were conducted in this study. One was conducted under a consistent S/L ratio of 1:10 (100 g/L) but with different pH conditions from 2 to 12, while the other one was conducted under the natural pH but with different S/L ratios from 1:20 to 1:2. The objectives were to test effects of pH and S/L on the leaching separately. For Type I experiments, pH was adjusted with 1 N HNO_3 or NaOH. Samples were mixed for 24 hours on a mechanical shaker at 180 osc/min. After shaking, all bottles were allowed to settle for 30 minutes. The supernatant was collected and filtered through a 0.45 μm syringe filter, acidified with 1% HNO_3 before analysis using ICP-MS for total As and Se concentration. The pH was measured using the remaining mixture. For Type II experiments, four S/L ratios (1:20; 1:10, 1:5 and 1:2) were applied for each sample. The pH was not adjusted before or during the leaching process. In order to examine if the speciation of As and Se changes during the leaching experiment under the natural conditions, a comparison experiment using Ash #110 were carried out under the N_2 gas environment. All sample bottles were set up in a glove box that was continuously purged with high purity nitrogen. The oxygen level in glove box was monitored with dry anaerobic indicator strips (Becton Dickinson Company, Sparks, MD). Deionized water and fly ash were purged within the glove box for at least 2 hours before mixing. The tightly sealed bottles were taken to a shaker and shaken for 24 hours at 180 osc/min. After shaking, all bottles were brought back to the continually N_2-purged glove box. The supernatants were collected and filtered inside the glove box and transferred to polypropylene tubes for speciation analysis using HPLC-ICP-MS right away without acidification. Thirty-day long term leaching experiments were also conducted to

determine effects of leaching time and the slow mineralization process on the leaching of As and Se from all ashes.

Instrument. HPLC–ICP-MS system was used for speciation analysis. Isocratic methods were used for As and Se separation. The HPLC system consisted of a PerkinElmer Series 200 Micro Pump and series 200 auto sampler, with a Hamilton PRP-X100 (4.1 mm x 150 mm, 3 μm particle size) anion exchange column. The isocratic mobile phase contained 10 mM ammonium nitrate and 10 mM ammonium phosphate, and the pH was adjusted to 9.4 with ammonium hydroxide. Sample injection volume was 100 μL. PerkinElmer ELAN® DRCe ICP-MS was used for As and Se measurement. The sample introduction system included a cyclonic spray chamber (Glass Expansion, Inc., West Melbourne, Australia) and a Meinhard® type A nebulizer. The effluent from the HPLC column was directly connected to the nebulizer with PEEK tubing (1.59 mm o.d.) and a low dead volume PEEK connector. The ICP-MS was operated in DRC mode with methane gas flow of 0.25 mL/min and dwell time of 250 ms. Methane was selected as the reaction gas to remove possible interference from the carrier gas argon or other matrix in the sample. For the quality assurance purpose, graphite furnace atomic absorption (GFAA) spectroscopy was also employed to reanalyze 50% of all samples.

Results and Discussion

As and Se Speciation Analysis. The HPLC–ICP-MS system was able to monitor multiple ions with different m/z numbers, so that As and Se species can be analyzed simultaneously. The four inorganic species, namely As(III), As(V), Se(IV) and Se(VI), were the focus of this study. With 10 mM of mobile phase and a flow rate of 1.5 mL/min, all four species can be well separated within 9 minutes, as shown in the chromatogram of

a 50 μg/L mixed standard solution in Figure 1. The detection limits of the fours species were determined to be 1-3 μg/L, 1-3 μg/L, 3-5 μg/L and 3-5 μg/L, respectively. The sensitivity of the HPLC-ICP-MS system was found to decrease up to 25% after running about 8 hours of operation, probably due to sample coating on the sampler cone and skimmer cone. This error was corrected by recalibration with new prepared standards for every eight samples (every 1-1.5 hour). Spiking recovery was within 85-110%. After speciation analysis, all leachates were acidified with 1% nitric acid, and reanalyzed with ICP-MS for total As and Se concentration.

Impact of pH on As and Se Leaching. Figure 2a shows the Type I leaching results of total As for all three ashes. Arsenic leaching from Ash #1005 was negligible at lower pH of 3-6, but gradually increased as pH was elevated from 6 to 12. This leaching behavior is normally observed for oxyanionic elements during their interaction with solid adsorbent in aqueous solution, including arsenic, selenium and vanadium etc. (10, 16, 30-31), because the adsorption sites for these oxyanions are more and more occupied by hydroxide ions when pH increases. The sharp increase of soluble As concentration at pH less than 2 was probably due to dissolution of ash particles under such a acidic condition, and the increase of less adsorbable neutral oxyanion species. Ashes #110 displayed a leaching peak at pH 8, with maximum concentrations of 1000 μg/L. The decrease of As release at higher pH may be due to the relatively high Ca content in this sample, which can form precipitation with As species under alkaline conditions. The extremely high Ca composition (16.5%) of Ash #7 has made it very difficult to lower the leachate pH of this ash. Therefore, the leaching test for Ash #7 was conducted only at pH from 8.5-12.5.

Arsenic leaching in such a pH range was negligible, most likely due to the trap of As in the calcium phase.

Figures 2b shows the leaching results of total Se. For Ash #1005, the leaching of Se was not significant in pH range between 2.5 and 5. Increasing amount of Se was released when pH was increased from 5 to 8, at which a leaching maxima of 1800 μg/L was observed, followed by a slight decrease as pH was further increased. At the low pH end, a similar climbing trend was observed as pH was further decreased to below 2.5. This behavior is likely controlled by the same mechanism as that for As. For Ash #110, the soluble Se concentration was less than 100 μg/L across the entire pH range, probably due to the low Se content in this ash. The leachability was also gradually increased as pH was raised, but not as significantly as Ash #1005. Ash #7 displayed a low leachability of Se (less than 100 μg/L) in pH range of 8.5-12.5 although it had a fairly high Se concentration in solid ash. The enlarged graph in Figure 2b indicated that the soluble Se concentration decreased significantly as pH was raised from 10 to 12.5. This reduction may be caused by selenium precipitation with calcium (32) or by formation of ettringite ($3CaO \cdot Al_2O_3 \cdot 3CaSO_4 \cdot 32H_2O$) which can trap selenite or selenate through substitution of sulfate in its structure under very high pH conditions (32-34).

As and Se Leaching under Natural pH Conditions. *Leachate pH.* Type II experiments were performed for the speciation study for all three ashes under natural pH conditions. The final pH values of leachates from Ash #110 under atmosphere and nitrogen conditions fell in the range of 9.3-9.8 and 9.8-10.2, respectively. Leachates obtained under the nitrogen condition displayed slightly greater pH than those under the atmosphere condition, probably due to the removal of CO_2 and O_2 in the reactors through

nitrogen purging. Ash #1005 exhibited lower natural pHs between 5.6 and 6.2 under all experimental conditions. Ash #7 exhibited the highest natural pH between 12.0 and 12.4. There was no significant pH change observed for samples leached after 30-day leaching compared to those after 1-day leaching. The various levels of natural pHs of the three ashes correlated with their Ca contents sorted in order of #7 > #110 > #1005 (Table 1). For ashes #110 and #1005, a slightly lower pH was observed for leachate with a higher S/L ratio. For example, the pH of leachate from Ash #110 decreased from 9.8 to 9.3 as S/L ratio was raised from 1:20 to 1:2. On the contrast, Ash #7 displayed an elevated natural pH with the increase of S/L ratio.

Impact of Nitrogen Gas Purging. The purpose of N_2 gas purging during the leaching process was to obtain the leaching data of different As and Se species originally present in fly ash, and to determine whether the presence of air, especially oxygen, can alter their speciation in leachate during the leaching process. Figure 3a shows the As leaching and speciation data for Ash #110 under natural pH conditions. For all experiments, only As(V) was detected in leachates, and the total As concentration measured using ICP-MS (and GFAA for 50% of the samples) agrees with As(V) concentration. The results in the presence of air also agree with that in the absence of air, with less than 10% of error. Therefore, the As is the only species in this fly ash, and the As speciation does not change affected by the S/L ratio or presence/absence of air. On the other hand, the As(V) concentration slightly decreased from 197 μg/L to 126 μg/L as the S/L ratio was raised from 1:20 to 1:5. The slightly decreased leachability of As(V) with the increase of S/L ratio suggested that, in addition to adsorption/desorption, As leaching

from this ash was probably influenced by some soluble constituents in fly ash, i.e. calcium, which may form more adsorbable species or precipitation with As.

Figure 3b shows the Se leaching and speciation results for Ash #110. For all experiments, only Se(IV) was detected, and total Se concentrations analyzed using ICP-MS reasonably agree Se(IV) concentrations determined using HPLC-ICP-MS for the same sample. Therefore, Se(IV) is the only species in this ash, and its speciation was not affected by S/L ratio or presence/absence of air in the experimental period. Unlike As, soluble Se concentrations in leachates increased with the increase of S/L ratios, i.e. when S/L ratio was changed from 1:20 to 1:5 under atmosphere condition, Se(IV) concentration significantly increased from 21.9 μg/L to 75.3 μg/L. Therefore, direct adsorption/desorption likely to be the predominant process controlling Se leaching from this fly ash as a result of the greater solubility of calcium selenite compared to calcium arsenate. However, for the same S/L ratio, leachates obtained under atmosphere conditions contained slightly more soluble Se than those obtained under nitrogen condition, which could be caused by a mineralization process in the presence of oxygen that slightly increased selenium leaching.

Impact of Mixing Time on As Leaching. Figure 4 shows the As speciation results for leachates from Ash #1005. Only As(V) was detected in the leachate, and greater concentrations were observed for higher S/L ratio conditions, indicating that the As leaching from this ash was controlled primarily by adsorption/desorption. The low leachability of As(V) from Ash #1005 under natural pH was consistent with that exhibited from the leachability study in the same pH range (Figure 2a). The concentrations of arsenic in leachates from Ash #7 for most S/L ratios were too low to be

quantified in speciation analysis, therefore no graph was plotted. The low leachabilty of As was probably caused by the precipitation of As with the calcium at pH greater than 12.

As(V) leaching from Ash #1005 after 30 days increased. The long term release might be resulted from a slow diffusion process of As from the inner pores of fly ash to the surface and bulk solution. For Ash #7, the long term leaching effect was not significant, and the As(V) concentrations in leachates were less than 5 μg/L for most samples except that for the S/L ratio of 1:2, which had 20 μg/L of As(V).

Impact of Mixing Time on Se Leaching. Figures 5a and 5b show Se speciation results for leachates from Ash #1005 and Ash #7. Both Se(IV) and Se(VI) were detected in most leachates from these two ashes, with Se(IV) being the major species. Concentrations of both Se(IV) and Se(VI) increased with the increase of S/L ratio. For 1-day experiment using Ash #1005, the Se(IV) concentration increased from 134 μg/L to 334 μg/L while the Se(VI) increased from 0 μg/L to 91 μg/L as S/L ratio was raised from 1:20 to 1:2. The Se(IV) leaching trend agrees with that for Ash #110 (Figure 3), suggesting that Se(IV) leaching was mainly controlled by adsorption/desorption process. Results also indicated that the fraction of Se(VI) increased with increase of S/L ratio. This is because Se(VI) is not adsorbable, while Se(IV) is adsorbable under the slight acidic pH conditions (35). Therefore, under the natural pH condition of this ash (5.6 – 6.2), all Se(VI) but part of Se(IV) species was released to the solution. With the increase of S/L ratio, total concentrations of Se(IV) and its adsorption sites were increased. Due to the adsorption process, a relatively larger portion of the Se(IV) stayed with the ash. Therefore, the ratio of released Se(VI) to Se(IV) increased with the increase of S/L ratio.

When the leaching time extended to 30 days, significant increase of Se(IV) concentration in the leachate ratio was observed for the same S/L ratio, while the Se(VI) concentrations remained almost unchanged. The different behavior of Se(IV) and Se(VI) indicated that Se(IV) leaching may be a slow process, whereas Se(VI) leaching only needs a short time (i.e. 24 hours) to reach equilibrium because it is weakly bonded to the ash.

For Ash #7, no detectable (<5 μg/L) Se was released after 1 day leaching for any S/L ratios. However, after 30-day leaching, both Se(IV) and Se(VI) were considerably released, and the concentrations were increased significantly with the increase of S/L ratio. To explore the cause of such variation after 30-day leaching, other components including calcium and sulfate in all leachate samples from both ashes were also monitored, since these two components have been reported as two important factors on Se leaching or adsorption. Figure 6 shows the results. For Ash #1005, the calcium concentration was not changed after 30 days for any S/L ratio. Therefore, the increase of Se leaching after 30 days does not related to the calcium. However, for Ash #7, the calcium concentration in leachates was significantly reduced after 30 days, and the reduction ranges from 50% at low S/L ratio to almost 100% at high S/L ratio. The calcium concentration for 1-day leaching was likely controlled by the solubility of $Ca(OH)_2$ (36), as shown in Table 2. The ion product of $[Ca][OH]^2$ was fairly consistent and close to the K_{sp} value of $Ca(OH)_2$. The decrease of calcium concentration after 30 days may be caused by several mineralization processes in the presence of CO_2, oxygen and silicate (36-39). Sulfate concentration was negligible after 1-day leaching, but greatly increased after 30 days, from 8.5 mg/L with S/L ratio of 1:20 to 151 mg/L with S/L ratio

of 1:2. The variation of sulfate may be attributed to the precipitation/dissolution of certain calcium sulfate hydrate which was formed after 1 day leaching, resulting in the low sulfate concentration in leachate. Later during the weathering process, calcium was precipitated into the less soluble form, triggering the dissolution of sulfate.

The variation of Se(IV) and Se(VI) followed the same trend with sulfate, but opposite to that of calcium, indicating that selenium was likely trapped into the same hydrate product as sulfate after 1-day leaching, then released to liquid phase together with the dissolution of sulfate after a long term leaching. It was also noticed that Se(IV) concentrations in leachate after 30-day leaching were probably controlled by the solubility of $CaSeO_3$. Table 2 lists the ion products of $[Ca][SeO_3]$ calculated based on the concentrations of Se(IV) and Ca(II). These values were slightly greater than, but reasonably close to the K_{sp} ($1.45x10^{-7}$ @ 25^oC, 0 ionic strength) (32) of $CaSeO_3$, and the difference may be resulted from the ionic strength effect in the leachate. Total As and Se concentrations analyzed with ICP-MS (not shown in Figure 6), again, agreed well with the sum of different species for all leachate samples.

Acknowledgements

This work was supported by Electric Power Research Institute (EPRI), US Department of Transportation through the National University Transportation Center (UTC), and the Environmental Research Center (ERC) for Emerging Contaminants at the University of Missouri-Rolla (UMR). Authors also wish to thank many colleagues at Perkin-Elmer, Inc., especially Mr. Jack Quade and Ms. Cynthia Bosnak for their great help for metal speciation analysis using HPLC-ICP-MS. Conclusions and statements

made in this paper are those of the authors, and in no way reflect the endorsement of the aforementioned funding agencies.

References

[1] Kim A.G.; Cardone C. Preliminary statistical analysis of fly ash disposal in mined areas. *Proc: 12th International Symposium on Coal Combustion By-Product Management and Use*. American Coal Ash Association. 1997, 1, 11-1 to 11-13.

[2] Kim A.G.; Kazonich G. Release of trace elements from ccb: maximum extractable fraction. *Proceedings 14th International Symposium on Management and Use of Coal Combustion Products (CCPs).* 2001, 1, 20-1 to 20-15.

[3] EPRI C*hemical Characterization of Fossil Fuel Combustion Wastes*. EPRI report, 1987, EA-5321.

[4] Kim, Ann G. Physical and chemical characteristics of CCB. *Proc: Coal Combustion By-Products and Western Coal Mines: a Technical Interactive Forum,* Golden, CO, 2002, 25-42.

[5] ACAA (2006) 2005 *Coal Combustion Product (CCP) Production and Use Survey*. American Coal Ash Association.

[6] Otero-Rey, J. R.; Mato-Fernandez, M. J.; Moreda-Pineiro, J.; Alonso-Rodriguez, E.; Muniategui-Lorenzo, S.; Lopez-Mahia, P.; Prada-Rodriguez, D. Influence of several experimental parameters on arsenic and selenium leaching from coal fly ash samples. Anal. Chim. Acta. 2005, 531(2), 299-305.

[7] Baba, A.; Kaya, A. Leaching characteristics of fly ash from thermal power plants of soma and tuncbilek, Turkey. Environ. Monit. Assess. 2004, 91(1-3), 171-181.

[8] Brunori, C.; Balzamo, S.; Morabito, R. Comparison between different leaching/extraction tests for the evaluation of metal release from fly ash. Int. J. Environ. Anal. Chem. 1999, 75(1-2), 19-31.

[9] Jankowski, J.; Ward, C.R.; French, D.; Groves, S. Mobility of trace elements from selected Australian fly ashes and its potential impact on aquatic ecosystems. Fuel 2005, 85(2), 243-256.

[10] Iwashita, A.; Sakaguchi, Y.; Nakajima, T.; Takanashi, H.; Ohki, A. Kambara, S. Leaching characteristics of boron and selenium for various coal fly ashes. Fuel 2005, 84(5), 479-485.

[11] EPRI, Characterization of field leachates at coal combustion product management sites: arsenic, selenium, chromium, and mercury speciation. EPRI, 2006a, Palo Alto, CA. 1012578.

[12] van der Hoek, E.E.; Bonouvrie, P.A.; Comans, R.N.J. Sorption of As and Se on mineral components of fly ash: relevance for leaching processes. Appl. Geochem. 1994, 9, 403-412.

[13] Guerin, T.; Astruc, M.; Batel, A. Borsier, M. Multielemental speciation of As, Se, Sb and Te by HPLC-ICP-MS. Talanta 1997, 44, 2201-2208

[14] Hirata, S.; Toshimitsu, H.; Aihara, M. Determination of arsenic species in marine samples by HPLC-ICP-MS. Anal. Sci. 2006, 22, 39-43.

[15] Merrill, D.T.; Manzione, M.; Parker, D.; Petersen, J.; Crow, W.; Hobbs, A. Field evaluation of arsenic and selenium removal by iron coprecipitation. Environ. Prog. 2006, 6(2), 82-90.

[16] Goldberg, S.; Glaubig, R.A. Anion sorption on a calcareous, montmorillonitic soil - selenium. 1988, Soil Sci. Soc. Am. j. 52(4), 954-8.

[17] EPRI Chemical attenuation coefficients for selenium species using soil samples collected from selected power plant sites. EPRI, Palo Alto, CA. 2006b, 1012585.

[18] EPRI. Chemical attenuation reactions of selenium. EPRI, Palo Alto, CA. TR-1994, 103535.

[19] Wadge, A.; Hutton, M. The leachability and chemical speciation of selected trace elements in fly ash from coal combustion and refuse incineration. Environ. Pollut. 1987, 48(2), 85-99.

[20] Jackson, B. P.; Miller, W. P. Soluble arsenic and selenium species in fly ash/organic waste-amended soils using ion chromatography-inductively coupled plasma mass spectrometry. Environ. Sci. Technol. 1999, 33, 270-275.

[21] Narukawa, T.; Takatsu, A.; Chiba, K.; Riley, K. W.; French, D. H. Investigation on chemical species of arsenic, selenium and antimony in fly ash from coal fuel thermal power stations. J. of Environ. Monit. 2005, 7(12), 1342-1348.

[22] Goodarzi, F.; Huggins, F.E. Monitoring the species of arsenic, chromium and nickel in milled coal, bottom ash and fly ash from a pulverized coal-fired power plant in western canada. J. of Environ. Monit. 2001, 3(1), 1-6.

[23] Huggins F.; Senior C.; Chu, P.; Ladwig, K.; Huffman, G. Speciation of arsenic and selenium in fly-ash samples from full-scale coal-burning utility plants. Environ. Sci. Technol. 2007, 41(9), 3284-3289.

[24] Schlegel, D., Matusch, J., Dittrich, K. Speciation of arsenic and selenium compounds by ion chromatography with inductively coupled plasma atominc emission spectrometry detection using the hydride technique. J. Chromatogr. A. 1994, 683, 261-267.

[25] Manning, B. A.; Martens, D. A. Speciation of arsenic (III) and arsenic (V) in sediment extracts by high-performance liquid chromatography-hydride generation atomic absorption spectrophotometry. Environ. Sci. Technol., 1997, 31(1), 171-177.

[26] Lindemann, T.; Prange, A.; Dannecker, W.; Neidhart, B. Simultaneous determination of arsenic, selenium and antimony species using HPLC/ICP-MS. J. Anal. Chem. 2004, 364, 462-466.

[27] Orero Iserte, L.; Roig-Navarro, A. F.; Hernandez, F. Simultaneous determination of arsenic and selenium species in phosphoric acid extracts of sediment samples by HPLC-ICP-MS. Anal. Chim. Acta. 2004, 527(1), 97-104.

[28] Martinez-Bravo, Y.; Roig-Navarro, A. F.; Lopez, F. J.; Hernandez, F. Multielemental determination of arsenic, selenium and chromium(VI) species in water by high-performance liquid chromatography-inductively coupled plasma mass spectrometry. J. Chromatogr. A. 2001, 926(2), 265-274.

[29] Lindemann, T.; Prange, A.; Dannecker, W.; Neidhart, B. Stability studies of arsenic, selenium, antimony and tellurium species in water, urine, fish and soil extracts using HPLC/ICP-MS. Fresenius' J. Anal. Chem. 2000, 368(2-3), 214-220.

[30] Goldberg, S.; Glaubig, R.A. Anion sorption on a calcareous, montmorillonitic soil - selenium. Soil Sci. Soc. Am. j. 1988, 52(5), 1297-1300.

[31] Peacock, C. L.; Sherman, D. M. Vanadium (V) adsorption onto goethite (-FeOOH) at pH 1.5 to 12: a surface complexation model based on ab initio molecular geometries and EXAFS spectroscopy. Geochim. Cosmochim. Acta. 2004, 68(8), 1723-1733.

[32] Baur, I.; Johnson, C. A. Sorption of selenite and selenate to cement minerals. Environ. Sci. Technol. 2003, 37(15), 3442-3447.

[33] Hassett, D. J.; Pflughoeft-Hassett, D. F.; McCarthy, G. J. Ettringite formation in coal ash as a mechanism for stabilization of hazardous trace elements. Proc: 9th Int. Ash Use Symp., 1991, 2, 31-1to 31-17

[34] Lecuyer, I.; Bicocchi, S.; Ausset, P.; Lefevre, R. Physico-chemical characterization and leaching of desulfurization coal fly ash. Waste Manage. Res. 1996, 14(1), 15-28.

[35] Wang, T.; Wang, J.; Burken, J. G.; Ban, H.; Ladwig, K. The leaching characteristics of selenium from coal fly ashes. J. Environ. Qual. 2007, accepted.

[36] Lide, D. R. CRC Handbook of Chemistry and Physics. 87th Ed. CRC press, Boca Raton, Fl.

[37] Piantone, P.; Bodenan, F.; Chatelet-Snidaro, L. Mineralogical study of secondary mineral phases from weathered MSWI bottom ash : implications for the modeling and trapping of heavy metals. Appl. Geochem. 2004, 19(12), 1891-1904.

[38] Warren, C. J.; Dudas, M. J. Formation of secondary minerals in artificially weathered fly ash. J. Environ. Qual. 1985, 14(3), 405-410.

[39] Johnson, C. A.; Schweizer, C. Weathering processes in municipal solid waste incinerator bottom ash deposits. Mineralogical Magazine 1998, 62A, 723-724.

Table 1. Physical and chemical characteristics of fly ash samples

Sample ID	Coal Type	Mercury Control	Total As (mg/kg)	Total Se (mg/kg)	Total Ca (%)	LOI (%)	BET Area (m^2/g)
Ash #110	Bit/Sub 3:1	None	40.9	1.5	1.9	13.8	13.5
Ash #1005	Bit	None	44.9	36.1	0.5	12.7	18.4
Ash #7	Sub	None	29.1	17.8	16.5	0.2	1.2

Table 2. K_{sp} and calculated ion products of selected compounds

	1-day Leaching	30-day Leaching	
S/L	$[Ca][OH]^2$	$[Ca][OH]^2$	$[Ca][SeO_3]$
1:20	6.31E-07	2.83E-07	4.96E-07
1:10	9.62E-07	3.38E-07	7.96E-07
1:5	9.63E-07	3.47E-07	7.23E-07
1:2	1.59E-06	3.24E-08	1.96E-07
K_{sp} (32, 36)	5.02E-06	5.02E-06	1.45E-07

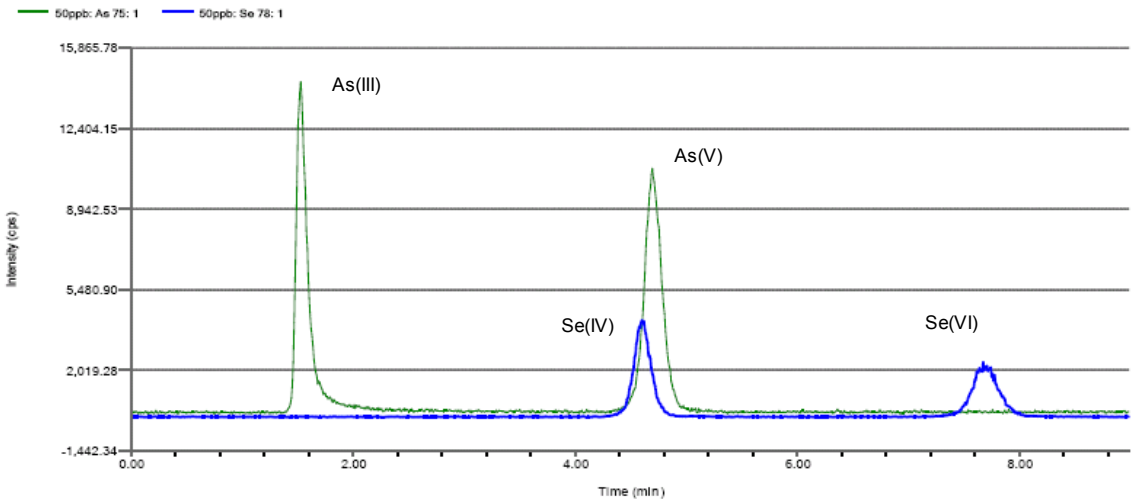

Figure 1. Liquid chromatogram of inorganic As and Se species (50 µg/L each).

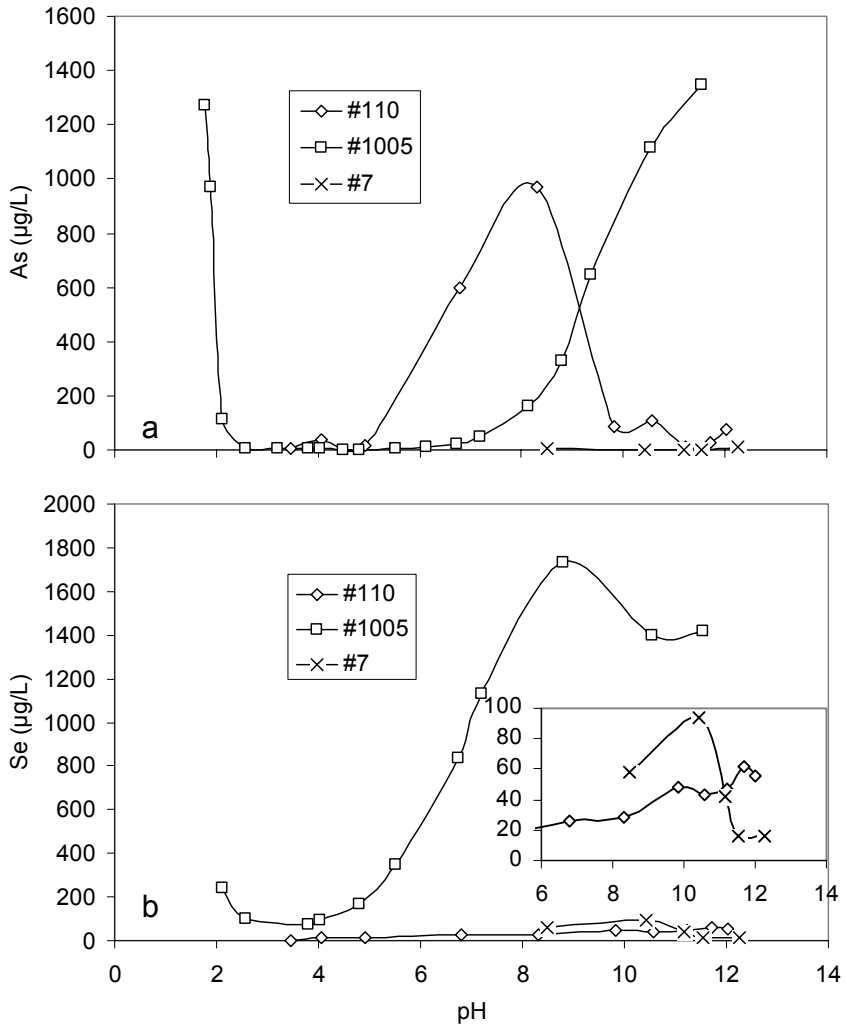

Figure 2. Background leaching of (a) As, (b) Se from Ash #110, Ash #1005 and Ash #7. Experimental conditions: S/L = 1:10; temperature = 20 – 25 ^{o}C; equilibration time = 24 hours.

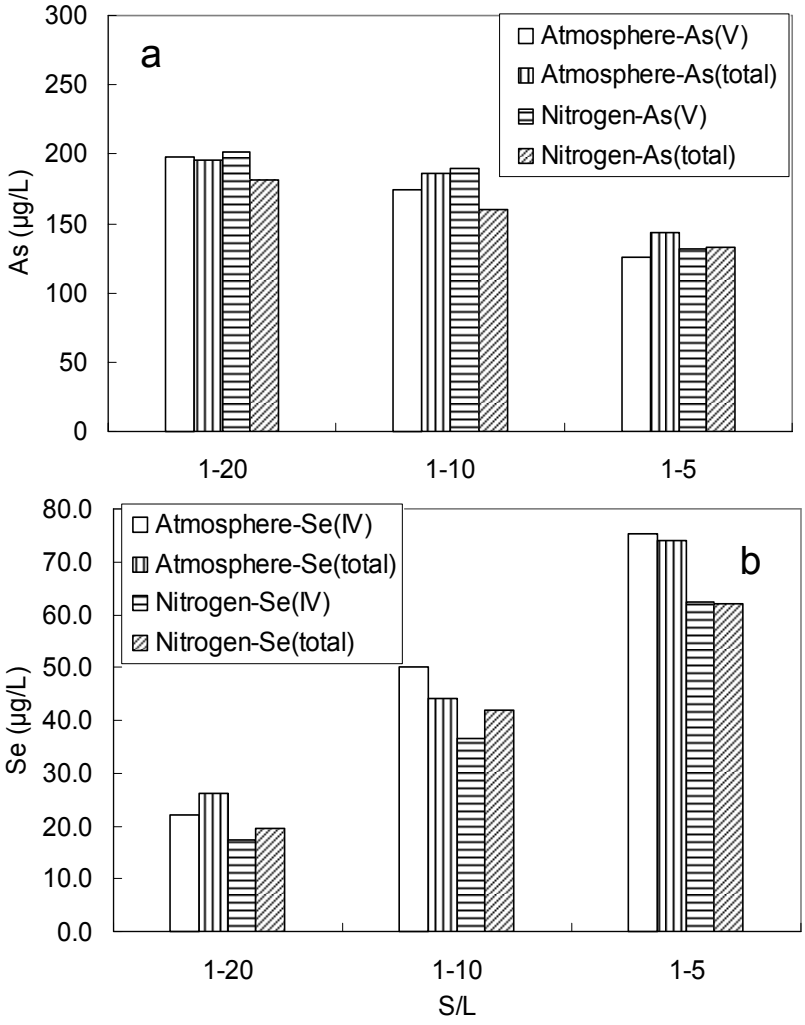

Figure 3. Speciation of (a) As and (b) Se in leachates from Ash #110 for different S/L ratios in the presence/absence of air. Experimental conditions: temperature = 20 – 25 ^{o}C; equilibration time = 24 hours.

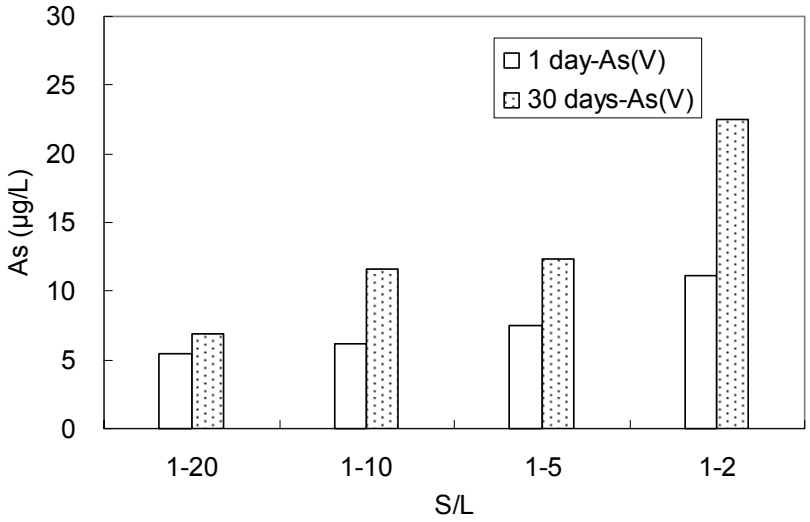

Figure 4. Speciation of As in leachates from Ash #1005 for different S/L ratios. Experimental conditions: temperature = 20 – 25 ^{o}C; equilibration time, 1 day and 30 days.

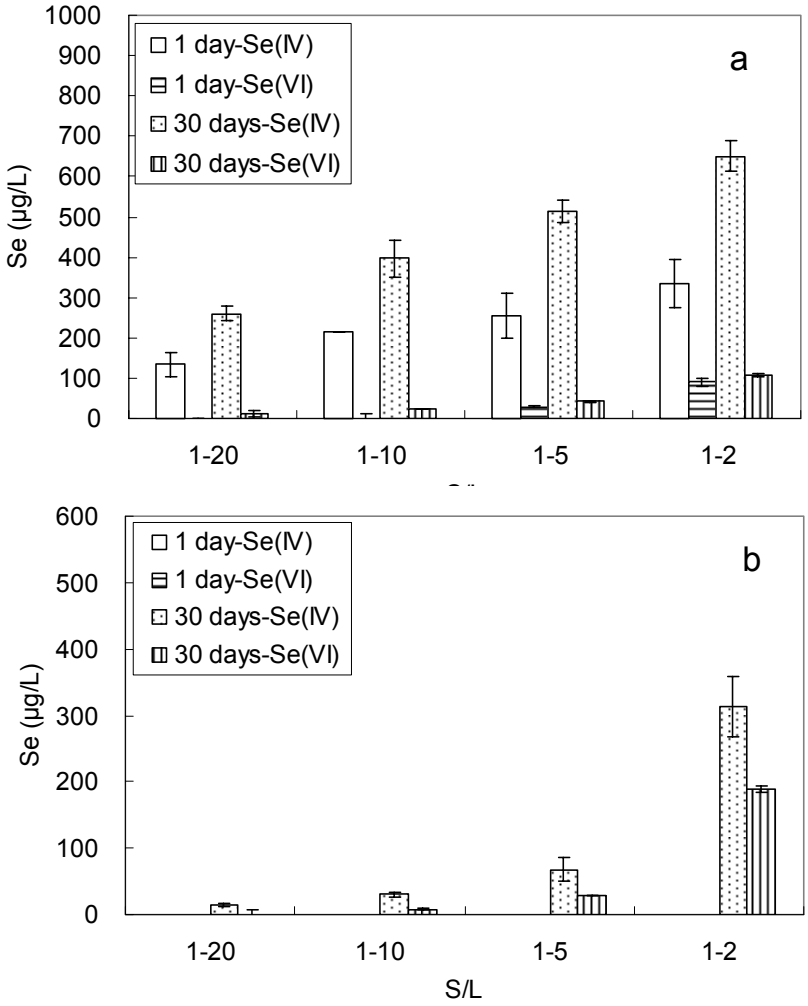

Figure 5. Speciation of Se in leachates from (a) Ash #1005, and (b) Ash #7 for different S/L ratios. Experimental conditions: temperature = 20 – 25 ^{o}C; equilibration time, 1 day and 30 days.

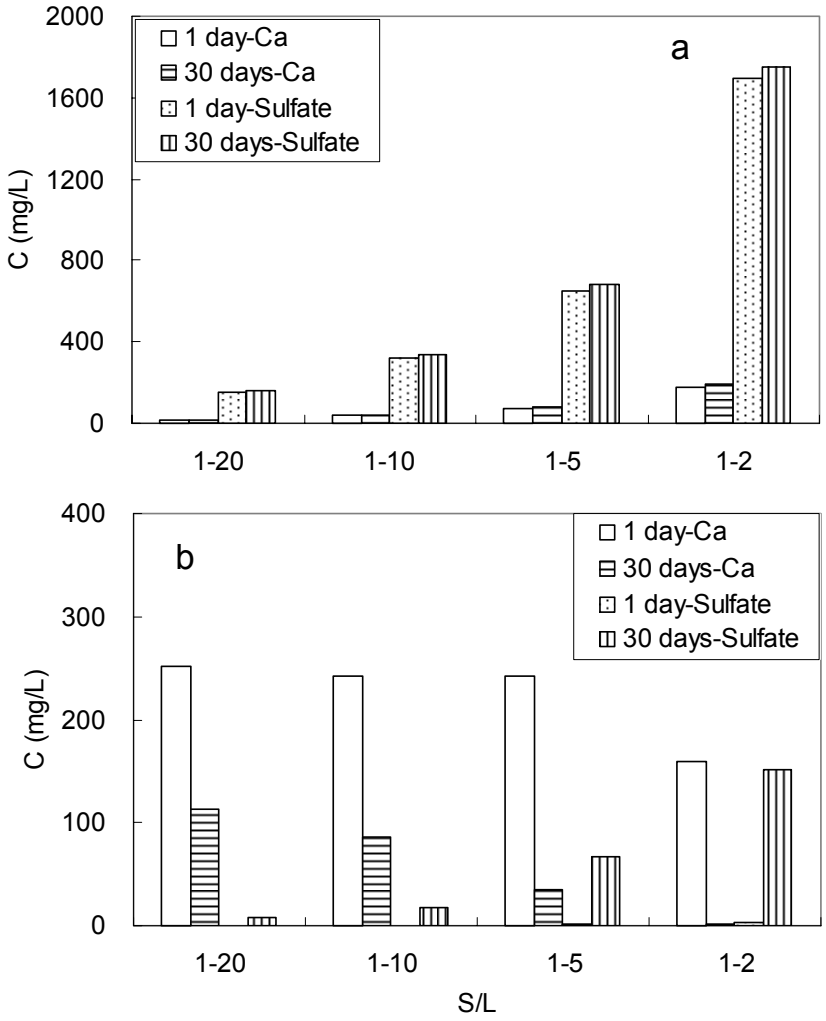

Figure 6. Calcium and sulfate concentrations in leachates from (a) Ash #1005 and (b) Ash #7 for different S/L ratios. Experimental conditions: temperature = 20 – 25 ^{o}C; equilibration time, 1 day and 30 days.

V. Calcium Effect on Arsenic (V) Adsorption onto Coal Fly Ash *(to be submitted to Environmental Science and Technology)*

TIAN WANG,[†] TINGZHI SU, [†] JIANMIN WANG,[*,†] KEN LADWIG[‡]

[†] Department of Civil, Architectural & Environmental Engineering, University of Missouri – Rolla, Rolla, MO 65409

[‡] Electric Power Research Institute (EPRI), 3420 Hillview Ave., Palo Alto, CA 94304

[*] Corresponding author phone: (573) 341-7503; email: wangjia@umr.edu

ABSTRACT

Batch tests indicated that arsenic (As) leaching is significantly affected by the calcium concentration in fly ash in the alkaline pH range. Arsenic leaching from low calcium fly ash from eastern bituminous coal increased with increase of pH in the alkaline pH range (pH 7 – 12). Fly ash from eastern bituminous coal with a slightly higher calcium content exhibited an arsenic leaching peak at pH 9, followed by decreased arsenic leaching up to pH 12. For alkaline ashes derived from subbituminous coal with much higher calcium content, significantly less arsenic was leached in the alkaline pH range. To improve understanding of arsenic leaching behavior, batch experiments with washed ash were performed to evaluate partitioning of As(V) spiked into the system, along with different amounts of calcium addition. Results suggested that the addition of calcium significantly reduced the soluble arsenic ratio in the alkaline pH range. This phenomenon was explained by postulating the formation of two highly adsorbable neutral arsenic species, $CaHAsO_4$ and $Ca_3(AsO_4)_2$, in this pH range. An adsorption model was developed to quantify the calcium impact on arsenic adsorption.

KEYWORDS Arsenic, Calcium, Adsorption, Fly ash

Introduction

High concentrations of arsenic (As) have long been recognized to be toxic to human and animals. Long term exposure to As can cause cancer of skin, liver, lung bladder and kidney (1). Effective January 2006, the Federal Maximum Contaminant Level (MCL) for arsenic in drinking water was revised by EPA from 50 μg/L to 10 μg/L (2). The stricter regulation may impact alternatives for the disposal and use of arsenic containing wastes and products, including coal fly ash. Although there have been extensive studies on the general leaching characteristics of arsenic from fly ash, (3-8) quantification of the calcium effect on arsenic leaching has been less well studied. van der Hoek et al. (9) conducted batch leaching tests for one acidic and one alkaline fly ash, and observed higher arsenic concentrations at higher pH for acidic ashes, but they observed the opposite behavior for alkaline ash, indicating different leaching mechanisms. By comparing arsenic leaching behavior from fly ash with its adsorption onto the major mineral compounds in fly ash, they concluded that arsenic leaching from acidic ash was likely to be controlled by surface complexation with iron oxide, while a calcium phase was shown to be responsible for alkaline ash. This conclusion agrees with that from Zielinski et al., who studied the mode of occurrence of arsenic in fly ash with XAFS spectroscopy (10). Results indicated that arsenic is associated with some combination of iron oxide, oxyhydroxide or sulfate in a highly acidic fly ash, but with a phase similar to calcium arsenate in a highly alkaline ash.

Several hypotheses have been proposed to explain the effect of calcium on arsenic leaching and adsorption on fly ash. One hypothesis is that arsenic is reacting with calcium and precipitates as calcium arsenate (11). However, Fruchter et al. (12) and van

der Hoek et al.(9) showed that As concentrations in leachate could not be modeled on the basis of solubility. Another hypothesis is that formation of secondary minerals such as ettringite may contribute to arsenic stabilization in fly ash (13-16). Since the formation of ettringite only occurs at pH greater than 11, this can only explain reduced leaching at very high pH levels (15). None of these hypotheses fully explain the arsenic leaching behavior across the full pH range.

Adsorption models that incorporate surface electrostatic effects have been applied to quantify arsenic adsorption on various media, including soil, iron hydroxide and ferric sludge (17, 18, 13). In most cases, this approach works well for fitting experimental data. However, it is very complicated in terms of the number of parameters to be predicted or calibrated, and results depend heavily on the initial assumptions (9). The model will be even more complicated if applied to a system with multiple constituents interacting with each other.

Overall, calcium is known to play an important role in the release of arsenic from fly ash. The objectives of this study are to compare the leaching behavior of arsenic from several acidic and alkaline fly ashes, to explore the mechanism of calcium effect on arsenic leaching and sorption/precipitation processes on coal fly ash, and to develop a robust adsorption model to quantify arsenic partitioning with fly ash with presence of calcium.

Materials and Methods

Fly Ash Samples. A total of seven ash samples were used in this study, collected from three different power plants. Ashes #1004, #1005, #1008 and #1009 were all collected from one pulverized coal power plant (Plant ID 33106) burning eastern

bituminous coal. The plant uses cold-side electrostatic precipitators (ESPs) to capture fly ash. Ashes #1004 and #1009 were collected from the same unit but at different times, when different eastern bituminous coals were being burned; the coal for Ash #1009 had higher calcium content. Ashes #1005 and #1008 were collected from the same plant and during the same coal burns as ashes #1004 and 1009, respectively, but from a separate unit with an ammonia-based selective non-catalytic reduction (SNCR) system for NOx control. Ashes #1015, #1018, and #7 were collected from power plants burning primarily subbituminous coal. Ashes #1015 and #1018 came from a cyclone boiler power plant (Plant ID 25410) with cold-side ESPs and burning a blend of 80% subbituminous and 20% bituminous coal. Ash #1018 was sampled from a unit with SNCR. Sample #7 came from a pulverized coal power plant (Plant ID 50213) with hot-side ESPs and burning 100% subbituminous coal.

In this paper, the four bituminous coal fly ashes with natural pH less than 7 are defined as acidic ashes, and the three subbituminous coal fly ash with natural pH greater than 7 were defined as alkaline ashes. The basic physical and chemical characteristics of these ashes, including natural pH, BET surface area (analyzed using Quantachrome Autosorb-1-C high performance surface area and pore size analyzer, Quantachrome Instruments, FL, USA), pH_{pzc} (analyzed using Zetasizer 3000, Malvern Instruments, Worcestershire, UK), loss-on-ignition (LOI) (determined using gravimetric methods), and total arsenic concentration are shown in Table 1. The total As in fly ash was determined using microwave-assisted acid digestion (0.4 g fly ash + 10 mL HNO_3 + 5 mL HF + 5 mL HCl) followed by graphite furnace atomic absorption (GFAA) measurement. The accuracy of the As determination was demonstrated by using a certified reference

material, NIST-1633a (National Institute of Standards and Technology, USA; certified As = 145±15 mg/kg, measured As = 156.3±1.3 mg/kg). Total Ca concentration was determined using X-Ray Fluorescence Spectroscopy (X-LAB 2000, SPECTRO Analytical Instruments GmbH & Co. KG).

Batch Leaching and Batch Titration Experiments. Batch leaching experiments were performed to determine the leaching behavior of arsenic from raw fly ash under different pH conditions; and batch titration experiments were employed to determine the surface site acidity and density. Detailed procedures for these two experiments are available in other papers (19, 20). Raw ash was dried and used for batch leaching experiments, while DI water washed ash was used for the titration experiments under the ionic strength of 0.01 M ($NaNO_3$). A solid/solution ratio (S/L) of 1:10 was used and pH was adjusted to the range of 2-12 for each group of samples. The mixture was shaken on an EBERBACH 6010 shaker for 24 hours, then allowed to settle overnight. The supernatant was collected and acidified using HNO_3 before arsenic and calcium analysis.

As(V) Partitioning with Different Calcium Additions. Batch partitioning experiments were performed to evaluate the effect of calcium on arsenic adsorption onto fly ash. In this experiment, fly ash samples were washed five times with DI water, and dried before use. The detailed washing procedure is described elsewhere (19). The solid/liquid ratio was 1:10. Ionic strength was adjusted with 0.01M $NaNO_3$ solution. For this study, samples were divided into several groups, 5 mg/L of As(V) was added to all samples as adsorbate, and a series of Ca concentrations were added to the different groups. After mixing on the shaker for 24 hours, all samples were allowed to settle

overnight. The supernatant was then collected for arsenic and calcium analysis. The final pH was measured using the remaining mixture in the bottle.

Analytical Method. A GFAA spectrometer (AAnalyst 600, Perkin-Elmer Corp., Norwalk, Connecticut, USA) and a Flame Atomic Absorption Spectroscopy (FLAA; Model 3110, Perkin-Elmer Corp., Norwalk, Connecticut, USA) were used to determine arsenic and calcium concentrations in solution, respectively. An Orion PerpHecT Triode pH electrode (model 9207BN) and a pH meter (perpHecT LoR model 370) were used for pH measurement.

Data Analysis. The non-linear regression program Kaleidagraph™ (Synergy Software, 2002) was used for titration modeling to determine the surface site density and acidity constants. SigmaPlot (SPSS Inc., 2001) was used as a multi-variable nonlinear regression program to determine the adsorption constants of each arsenic species on fly ash.

Results and Discussion

Arsenic and Cacium Leaching from the Raw Fly Ash. Batch leaching experiments were performed with six fly ash samples. Both arsenic and calcium concentrations in the leachate were analyzed and plotted in Figure 1a and 1b, respectively.

Arsenic leaching from all three acidic ashes was significantly affected by the pH as observed in Figure 1a. For ashes #1005 and #1004, arsenic release was minimal in their natural pH range, between 3 and 7. When pH is below 3, arsenic release increased significantly. On the other hand, when pH is above 7, soluble arsenic concentration was also increased. The major arsenic species in fly ash was reported to be As(V) in previous

research (21, 22). The As(V) speciation diagram (Figure 2) indicated that the neutral H_3AsO_4 species dominates when pH is less than 2. Therefore, the neutral arsenic molecule is considered not adsorbable by ash surface. The dissolution of ash particles under very acidic conditions might also contribute to the higher soluble arsenic concentration. When pH increases to above 2, the total concentrations of anionic arsenic species ($H_2AsO_4^-$ and $HAsO_4^{2-}$) also increase. These anions can be adsorbed by protonated ash surface site α. When pH is greater than 7, the protonated surface site α is no longer available, resulting in less arsenic adsorption on the ash surface.

Ash #1009 performed differently from the other two acidic ashes in Figure 1a. When pH was less than 9, it had a similar leaching pattern as the other two, with minimal release at pH 3-4. However, when pH was greater than 9, the soluble arsenic concentration decreased with the increase of pH, and when pH was greater than 11, the arsenic concentration began to increase again.

Unlike acidic ashes, alkaline ashes displayed very low leachability for arsenic under neutral and alkaline pH conditions (Figure 1a). One high arsenic concentration at pH 3 for Ash #1018 was most likely caused by ash dissolution. Comparing the leaching results from different ashes with their physical –chemical characteristics listed in Table 1 indicates that the general arsenic leaching behavior is correlated with the calcium content in fly ash matrix. The calcium contents in the three alkaline ashes are 20-30 times greater than those in Ash #1005 and #1004; acidic Ash #1009 has a calcium content about twice as high as the other two acidic ashes. Correspondingly, the soluble calcium concentrations in leachates from the alkaline ashes were significantly greater than for the acidic ashes below pH 11 (Figure 1b), but were more sensitive to pH change and

decreased faster with increase of pH. These results indicate that calcium leaching from alkaline ashes was a dissolution/precipitation controlled process, and the fairly low leachability of arsenic from the alkaline ashes across a broad pH range was likely associated with the precipitation or coprecipitation of arsenic with calcium phases. The situation is quite different for acidic ashes, where the soluble calcium concentration decreased smoothly with increase of pH, and arsenic leachability is more dependant on pH change. The observed correlation between arsenic leachability and calcium content in fly ashes is further evidence of the finding by van der Hoek et al. (9) that a calcium phase in fly ash is likely to control the release and adsorption of arsenic in the alkaline pH range. The leaching mechanism of arsenic from acidic ashes will be discussed more fully in the following section.

Arsenic Partitioning in Washed Fly Ash under Different Calcium Additions. To test the effect of calcium on arsenic adsorption on fly ash, and to further investigate the leaching mechanism of arsenic from acidic fly ashes, Ash #1008 and Ash #1005 were selected for partitioning experiments with different calcium additions. For all partitioning experiments, the ash was washed prior to testing and 5 mg/L of As were added to the system. For Ash #1008, sample bottles were divided into four groups, with calcium additions of 0 mg/L, 50 mg/L, 100 mg/l and 150 mg/L. Results are shown Figure 3. The As(V) partitioning curve without calcium addition has a similar trend as the raw ash leaching curve. Although only 5 mg/L of As(V) was added to the system, the maximum release reached 12 mg/L at pH 12, indicating that a significant amount of arsenic was released from washed fly ash. Addition of calcium significantly enhanced arsenic adsorption in pH range of 7-12, and a larger adsorption difference was observed at higher

pH. For example, at pH 8 with 50 mg/L of calcium addition, 25% more arsenic was adsorbed, while at pH 11, arsenic adsorption was increased by 75%. This effect became less significant with calcium addition above 50 mg/L. The arsenic partitioning curve in the presence of calcium is analogous to the leaching curve of raw Ash #1009 (Figure 1a), suggesting a similar mechanism applies in both circumstances.

Three Ca loadings were applied to As(V) partitioning experiment with Ash #1005: 0 mg/L, 100 mg/L and 500 mg/L. Results shown in Figure 4 were similar with those of Ash #1008, except that soluble Ca concentration decreased sharply at pH greater than 11 with 500 mg/L Ca addition, which may be caused by precipitation of $Ca(OH)_2$ at high Ca loading and high pH conditions.

To determine whether the precipitation of $Ca_3(AsO_4)_2$ occurred at high pH in this study, the products of $[Ca]^3 \times [AsO_4]^2$ were calculated based on the group of data with 50 mg/L of calcium addition for Ash #1008. Results are listed in Table 2. Instead of one consistent solubility product (K_{sp}), the large variation of the product, up to four orders of magnitude, indicated that the arsenic release was not a calcium arsenate precipitation controlled process. Ettringite formation contributes to the stabilization of arsenic in fly ash generally in alkaline ashes, and only above pH 11, while experimental data indicated that calcium effect in these acidic ashes became observable since pH 7-8,.

The current experimental data suggest that some other mechanism is at least partially responsible for controlling arsenic release in the acidic ashes. Calcium added into the system can form complexes with arsenic in forms of $CaH_2AsO_4^+$, $CaHAsO_4$, $CaAsO_4^-$, $Ca_3(AsO_4)_2$ (23). It has been reported that the neutral forms of metal complexes (24, 25), have higher affinity to the sorbent surface. Considering the occurrence of the

two neutral species $CaHAsO_4$ and $Ca_3(AsO_4)_2$ in the pH range where arsenic adsorption was enhanced, it is assumed that the adsorption of these two species contributed to the stabilization of arsenic in fly ash. This assumption is verified by the modeling process described below.

Modeling As(V) Adsorption onto Washed Ash. *Surface Site Characterization.* The surface site density and acidity constant of fly ash are essential parameters for metal adsorption modeling. A previously developed titration model (19) was used to determine these parameters. The model is expressed as:

$$\Delta V_{SS} = \sum_i \frac{V_0 S_{Ti} K_{Hi}}{C} \left\{ \frac{1}{[H^+] + K_{Hi}} - \frac{1}{[H^+]_0 + K_{Hi}} \right\} \quad (1)$$

where ΔV_{SS} is the net volume of stock acid/base (negative value for acid) solution consumed by surface sites (mL); V_0 is total volume of the ash mixture (mL); S_{Ti} is the total acid site concentration of species i (M); K_{Hi} is the acidity constant of the species i (M); C is the concentration of the acid/base stock solution (M); and $[H^+]_0$ is the hydrogen ion concentration of the control unit (without acid or base addition) (M). Note that the total surface site concentration $S_{Ti} = \Gamma_i \times SS$, where Γ_i is the surface site density for species i (mol/g-SS) and SS is the solids concentration (g/L).

After correction using the titration data for blanks, the net titration data for washed Ash #1008 with S/L ratio of 1:10 were plotted as the equilibrium pH as a function of the volume of acid (negative value) or base consumed by fly ash (mL), shown in Figure 5a. KaleidaGraph™ was employed for the curve fitting. Results showed that using three surface sites can best fit the experimental data. Table 3 lists the surface site density (Γ) and acidity constant (pK_H) for each site, α, β, and γ. Since the pH_{pzc} of this

ash was 6.2 (Table 1), which is between the pK_Hs of the site α and site β (3.2 and 7.3, respectively), the protonated surface sites α is positively charged, denoted as $\underline{S}_1OH_2^+$, while the protonated species of the other two surface sites are in neutral form. The titration curve fitting results and corresponding parameters for the other Ash #1005 were shown in Figure 5b and Table 3, respectively.

Modeling As(V) Adsorption. The concentrations of different As(V) species in the system can be calculated based on the following equations:

$H_3AsO_4 = H_2AsO_4^- + H^+$; $pK_{a1} = 2.26$; (26) (2)

$H_2AsO_4^- = HAsO_4^{2-} + H^+$; $pK_{a2} = 6.76$; (26) (3)

$HAsO_4^{2-} = AsO_4^{3-} + H^+$; $pK_{a3} = 11.29$; (26) (4)

$HAsO_4^{2-} + Ca^{2+} = CaHAsO_4$; $\log K_{a4} = 2.75$; (23) (5)

$AsO_4^{3-} + 1.5\ Ca^{2+} = Ca_{1.5}AsO_4$; K_{a5} (6)

The stoichiometry of $Ca_3(AsO_4)_2$ was converted to $Ca_{1.5}AsO_4$, to simplify the adsorption equations. K_{a4} and K_{a5} are the formation constants of $CaHAsO_4$ and $Ca_3(AsO_4)_2$, respectively. K_{a5} needs to be determined by modeling, because there is no published value available from literature.

Assuming that only the protonated surface site α (denoted as $\underline{S}_1$) is responsible for the adsorption of three negatively charged arsenic species, denoted as $[\underline{S}_1OH_2^+]=\alpha_+ S_T$, where S_{1T} is the total concentration an site α, and α_+ is the fraction of the protonated surface site, then: $\alpha_+ = \dfrac{[H^+]}{[H^+] + K_H}$; The two neutral calcium-arsenic species have no

specific selectivity on the three surface sites. Therefore, all surface sites were normalized as one with a total site density of $[S_T]$ when considering the two neutral species. Adsorption of different arsenic species by surface sites can be expressed as:

$$\underline{S_1}OH_2^+ + H_2AsO_4^- = \underline{S_1}\text{-}H_2AsO_4 + H_2O;\ K_{S1}; \quad (7)$$

$$\underline{S_1}OH_2^+ + HAsO_4^{2-} = \underline{S_1}\text{-}HAsO_4^- + H_2O;\ K_{S2}; \quad (8)$$

$$\underline{S_1}OH_2^+ + AsO_4^{3-} = \underline{S_1}\text{-}AsO_4^{2-} + H_2O;\ K_{S3}; \quad (9)$$

$$\underline{S} + CaHAsO_4 = \underline{S}\text{-}CaHAsO_4;\ K_{S4}; \quad (10)$$

$$\underline{S} + Ca_{1.5}AsO_4 = \underline{S}\text{-}Ca_{1.5}AsO_4;\ K_{S5}; \quad (11)$$

where K_{S1}, K_{S2}, K_{S3}, K_{S4} and K_{S5} are adsorption constants of the five arsenic species, respectively. These are the parameters to determine by modeling.

The total soluble adsorbed arsenic concentration $[As(V)]_D$ and total adsorbed arsenic concentration $[As(V)]_{ads}$ can be expressed with the following equations:

$$[As(V)]_D=[H_3AsO4]+[H_2AsO_4^-]+[HAsO_4^{2-}]+[AsO_4^{3-}]+[CaHAsO_4]+[Ca_{1.5}AsO_4] \quad (12)$$

$$[As(V)]_{ads}=[\underline{S_1}\text{-}H_2AsO_4]+[\underline{S_1}\text{-}HAsO_4^-]+[\underline{S_1}\text{-}AsO_4^{2-}]+[\underline{S}\text{-}CaHAsO_4]+[\underline{S}\text{-}Ca_{1.5}AsO_4] \quad (13)$$

According to previous research, if the total adsorbate concentration (in M) is less than 10% of the surface site concentration, which is true in this study, then the adsorption is in the linear range of the Langmuir isotherm (19), and the concentration of adsorbed species can be expressed as:

$$[\underline{S_1}\text{-}H_2AsO_4]=K_{S1}[\underline{S_1}OH_2^+][H_2AsO_4^-] \quad (14)$$

$$[\underline{S_1}\text{-}HAsO_4^-]=K_{S2}[\underline{S_1}OH_2^+][HAsO_4^{2-}] \quad (15)$$

$$[\underline{S_1}\text{-}AsO_4^{2-}]=K_{S3}[\underline{S_1}OH_2^+][AsO_4^{3-}] \quad (16)$$

$$[\underline{S}\text{-}CaHAsO_4]=K_{S4}[\underline{S}][CaHAsO_4] \quad (17)$$

$$[\underline{S}\text{-}Ca_{1.5}AsO_4]=K_{S5}[\underline{S}][Ca_{1.5}AsO_4] \quad (18)$$

The total arsenic concentration $[As(V)]_T$ in the system is:

$$[As(V)]_T = [As(V)]_D + [As(V)]_{ads}$$

Based on equations 2-18, $[As(V)]_D$ can be solved and expressed as:

$$[As(V)]_D=\frac{[As(V)]_T \times B}{B+C} \quad (19)$$

where,

$$B = \frac{1}{\alpha_0}+\frac{K_1K_2K_4[Ca]}{[H]^2}+\frac{K_1K_2K_3K_5[Ca]^{1.5}}{[H]^3} \quad (20)$$

$$C = \alpha^+[S_{1T}](\frac{K_{S1}K_1}{[H]}+\frac{K_{S2}K_1K_2}{[H]^2})+[S_T](\frac{K_{S4}K_1K_2K_4[Ca]}{[H]^2}+\frac{K_{S5}K_1K_2K_3K_5[Ca]^{1.5}}{[H]^3}) \quad (21)$$

$$\alpha_0=\frac{[H]^3}{[H]^3+[H]^2K_1+[H]K_1K_2+K_1K_2K_3} \quad (22)$$

Equations 19-22 were denoted as the surface adsorption model for arsenic with presence of calcium. SigmaPlot (nonlinear regression function) was used to fit the experimental data $As(V)_D$ as a function of pH and [Ca], and to determine the values of constants K_5, Ks_1, Ks_2, Ks_4 and Ks_5. The predetermined surface site densities (S_{1T}, S_T) and acidity constants (pK_H) from titration experiment were substituted into above equations. Modeling results for both ashes are listed in Table 4 together with the standard error and R^2. Soluble arsenic concentrations predicted by the adsorption model are also

plotted in Figure 3a and Figure 4a as solid lines. Results indicated that the modeling and experimental data agreed well with each other, and the formation constants of $Ca_3(AsO_4)_2$ (expressed as $Ca_{1.5}AsO_4$) determined from two ashes, 4.7 ± 0.7 and 3.8 ± 0.9 were not significantly different, suggesting the validity of the developed model on describing the calcium effect on arsenic adsorption on fly ash.

Discussion. This research demonstrated that different arsenic leaching behaviors from acidic and alkaline fly ashes were correlated with the calcium content in bulk ash, and a calcium phase was likely to be responsible for the stabilization of arsenic in the alkaline pH range. As(V) adsorption on to acidic fly ash was significantly enhanced by added calcium under basic conditions. Solubility product calculation indicated that this process was not controlled by precipitation of $Ca_3(AsO_4)_2$. Instead, it is hypothesized that calcium complexes with arsenic and forms two neutral species $CaHAsO_4$ and $Ca_3(AsO_4)_2$ which have a relatively high affinity for fly ash surfaces at high pH, resulting in increased arsenic adsorption. The adsorption model developed in this study successfully predicted As(V) adsorption behavior on an acidic Ash #1008, and the formation and adsorption constants of different arsenic species were determined.

Acknowledgements

This work was supported by the Electric Power Research Institute (EPRI) and the Environmental Research Center (ERC) for Emerging Contaminants at the University of Missouri-Rolla (UMR). The authors also gratefully acknowledge Mr. Shi Shu at University of Missouri-Rolla for his contribution to the leaching experiment and chemical analysis; and Dr. C.P. Huang and Mr. Minghua Li at the University of Delaware for providing the zeta potential measurement. Conclusions and statements made in this

paper are those of the authors, and in no way reflect the endorsement of the aforementioned funding agencies.

References

[1] Smith, A. H., Hopenhayn-Rich, C., Bates, M. N. Goeden, H. M., Hertz-Picciotto, I., Duggan, H. M., Wood, R., Kosnett, M. J., Smith, M. T. Cancer risks from arsenic in drinking water. Environmental Health Perspectives, 1992, 97, 259-267.

[2] EPA National Primary Drinking Water Standards. EPA, 2002, 816-F-02-013.

[3] Xu Y., Nakajima T., Ohki A. Leaching of arsenic from coal fly ashes 1. leaching behavior of arsenic and mechanism study. Environmental Toxicology Chemistry. 2001, 81(1-2), 55-68.

[4] Daniels, John L.; Das, Gautham P. Leaching behavior of lime-fly ash mixtures. Environmental Engineering Science, 2006, 23(1), 42-52.

[5] Baba, A.; Kaya, A. Leaching Characteristics of Fly Ash from Thermal Power Plants of Soma and Tuncbilek, Turkey. Environmental Monitoring and Assessment 2004, 91(1-3), 171-181.

[6] Brunori, C.; Balzamo, S.; Morabito, R. Comparison between different leaching/extraction tests for the evaluation of metal release from fly ash. International Journal of Environmental Analytical Chemistry 1999, 75(1-2), 19-31.

[7] Khanra, S.; Mallick, D.; Dutta, S. N.; Chaudhuri, S. K. Studies on the phase mineralogy and leaching characteristics of coal fly ash. Water, Air, and Soil Pollution 1998, 107(1-4), 251-275.

[8] Reardon, E. J.; Czank, C. A.; Warren, C. J.; Dayal, R.; Johnston, H. M. Determining controls on element concentrations in fly ash leachate. Waste Management & Research 1995, 13(5), 435-450.

[9] van der Hoek E.E., Bonouvrie P.A., and Comans R.N.J. Sorption of As and Se on Mineral Components of Fly Ash: Relevance for Leaching Processes. Applied Geochemistry. 1994, 9, 403-412.

[10] Zielinski, Robert A.; Foster, Andrea L.; Meeker, Gregory P.; Brownfield, Isabelle K. Mode of occurrence of arsenic in feed coal and its derivative fly ash, Black Warrior Basin, Alabama. Fuel 2006, 86(4), 560-572.

[11] Bothe, Jr., James V., Brown, P. W. Arsenic Immobilization by Calcium Arsenate Formation. Environmental Science and Technology. 1999, 33, 3806.

[12] Fruchter, J. S., Rai, D., Zachara, John M. Identification of solubility - controlling solid phases in a large fly ash field lysimeter. Environmental Science and Technology. 1990, 24(8), 1173-9.

[13] Parks, J. L., Novak, J., MacPhee, M., Itle, C., Edwards, M. Effect of Ca on As release from ferric and alum residuals. Journal - American Water Works Association. 2003, 95(6), 108-118.

[14] Warren, C. J., Dudas, M. J. Leaching behavior of selected trace elements in chemically weathered alkaline fly ash. Science of Total Environment. 1988, 76, 229-246.

[15] De Groot G. J., Wijkstra J., Hoede D., van der Sloot H. A. Leaching characteristics of selected elements from coal fly ash as a function of the acidity of the contact solution and the liquid/solid ratio. ASTM STP 1989, 1033, 170-183.

[16] Simons, H. S., Jeffery, J. W. An X-ray study of pulverized fuel ash. Journal of Applied Chemistry. 1960, 16, 328-336.

[17] Goldberg, S.; Glaubig, R.A. Anion sorption on a calcareous, montmorillonitic soil - arsenic. Soil Science Society of America Journal. 1988, 52(5), 1297-300.

[18] van der Hoek, E.E., Comans, R.N.J. Modeling arsenic and selenium leaching from acidic fly ash by sorption on iron (hydr)oxide in the fly ash matrix. c1996, 30(2), 517-523.

[19] Wang, J., Teng, X., Wang, H., Ban, H. Characterizing the metal adsorption capability of a class F coal fly ash. Environmental Science and Technology. 2004, 38(24), 6710-6715.

[20] Wang, T., Wang, J., Ban, H., Ladwig, K. Quantifying the Availability and the Stability of Trace Cationic Elements in Fly Ash. Waste Management 2007, 27, 1345-1355.

[21] Silberman D. and Harris W.R. Determination of Arsenic(III) and Arsenic(V) in Coal and Oil Fly Ashes. International Journal of Environmental Analytical Chemistry. 1984, 17(1), 73-83.

[22] Goodarzi F. and Huggins F.E. Monitoring the Species of Arsenic, Chromium and Nickel in Milled Coal, Bottom Ash and Fly Ash from a Pulverized Coal-fired Power Plant in Western Canada. Journal of Environmental Monitoring. 2001, 3(1), 1-6.

[23] Mironov, V. E., Kiselev, V. P., Egizaryan, M. B., Golovnev, N. N., Pashkov, G. L. Russian Journal of Inorganic Chemistry, 1995, 40, 1752-1753.

[24] MacNaughton, M.G., James, R.O. Adsorption of aqueous mercury(II) complexes at the oxide/water interface. Journal of Colloid Interface Science. 1974, 47, 431–440.

[25] Kinniburgh, D.G.; Jackson, M.L. Adsorption of mercury (II) by iron hydrous oxide gel. Soil Science Society of America Journal. 1978, 42, 45–47.

[26] Stumm, W., Morgan, J.J., 1996. Aquatic Chemistry. 3rd Ed. John Wiley & Sons.

Table 1. Sample characterization.

Sample ID	Coal Type	Natural pH (S/L = 1:10)	As (mg/kg)	Ca (%)	BET Area (m^2/g)	pH_{pzc}	LOI (%)
Ash #1005	Bit	5.5	44.9	0.50	18.43	6.2	12.7
Ash #1004	Bit	4.5	49.0	0.59	7.57	6.4	6.7
Ash #1008	Bit	6.5	139.4	1.11	6.48	6.2	8.5
Ash #1009	Bit	6.0	100.9	1.0	8.71	7.4	9.8
Ash #1015	Sub	10.6	37.2	14.3	25.65	7.6	14.8
Ash #1018	Sub	10.6	52.1	12.98	15.68	6.8	9.7
Ash #7	Sub	12.3	29.1	16.15	1.24	6.6	0.2

Table 2. Ion product of $[Ca]^3 \times [AsO_4]^2$ (with 50 mg/L of Ca addition).

pH	$[Ca]^3 \times [AsO_4]^2$
8.00	3.22E-25
9.15	8.79E-23
10.25	9.51E-22
10.70	1.16E-21
11.88	1.17E-21

Table 3. Surface site densities and acidity constants for Ash #1008.

Sample ID	Surface Site Parameters	α	β	γ
Ash #1008	Γ (10^{-5} mol/g)	44 ± 1.4	3.6 ± 1.6	5.4 ± 2.0
	pK_H	3.2 ± 0.1	7.3 ± 0.5	11.3 ± 0.9
Ash #1005	Γ (10^{-5} mol/g)	32 ± 1.4	2.5 ± 0.8	8.6 ± 2.7
	pK_H	3.0 ± 0.1	8.4 ± 0.5	11.6 ± 0.4

Table 4. Modeling results for arsenic partitioning with Ash #1008 and Ash #1005

Sample ID	Arsenic Species	H_2AsO_4	$HAsO_4$	$CaHAsO_4$	$Ca_{1.5}(AsO_4)$	R^2
Ash #1008	Formation Constant (logK)	/	/	/	4.7 ± 0.7	0.89
	Adsorption Constant (logKs)	2.6 ± 0.1	7.0 ± 0.2	1.9 ± 0.2	2.6 ± 0.5	
Ash #1005	Formation Constant (logK)	/	/	/	3.8 ± 0.9	0.95
	Adsorption Constant (logKs)	3.9 ± 1.3	6.8 ± 0.2	2.1 ± 0.1	3.0 ± 0.8	

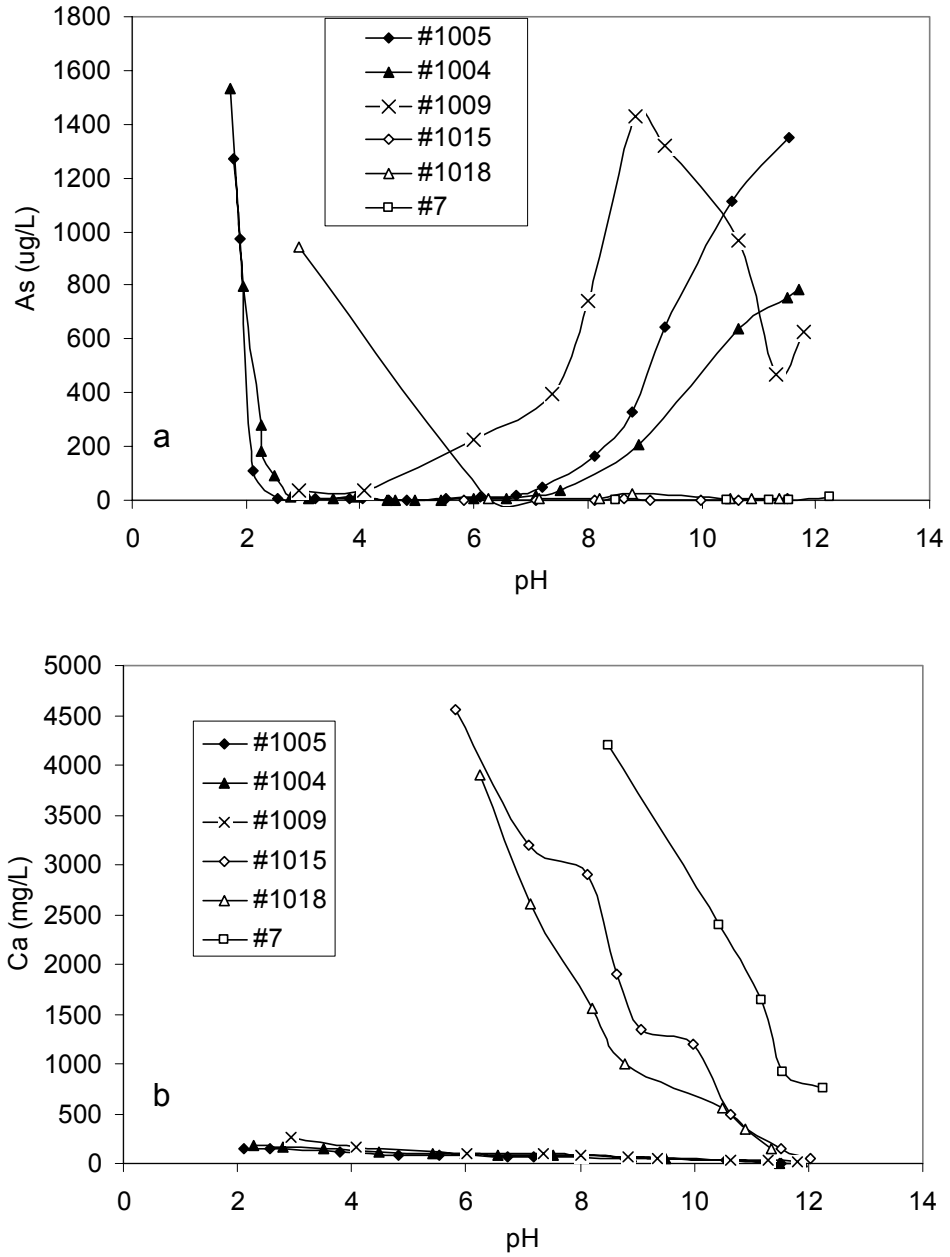

Figure 1. (a) As, (b) Ca leaching from acidic and alkaline coal fly ashes. Experimental conditions: S/L = 1:10; temperature = 20 – 25 ^{o}C; equilibration time = 24 hours.

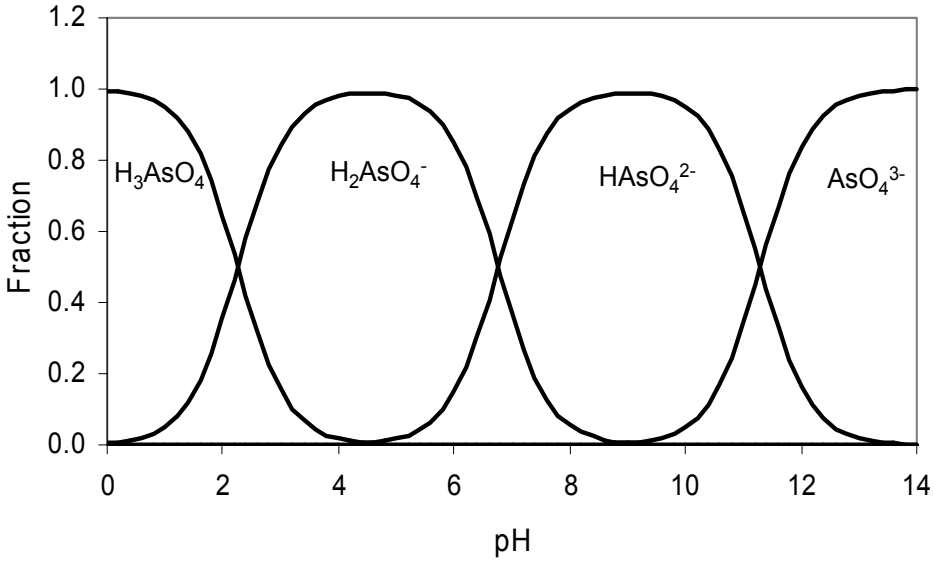

Figure 2. Speciation of arsenic acid.

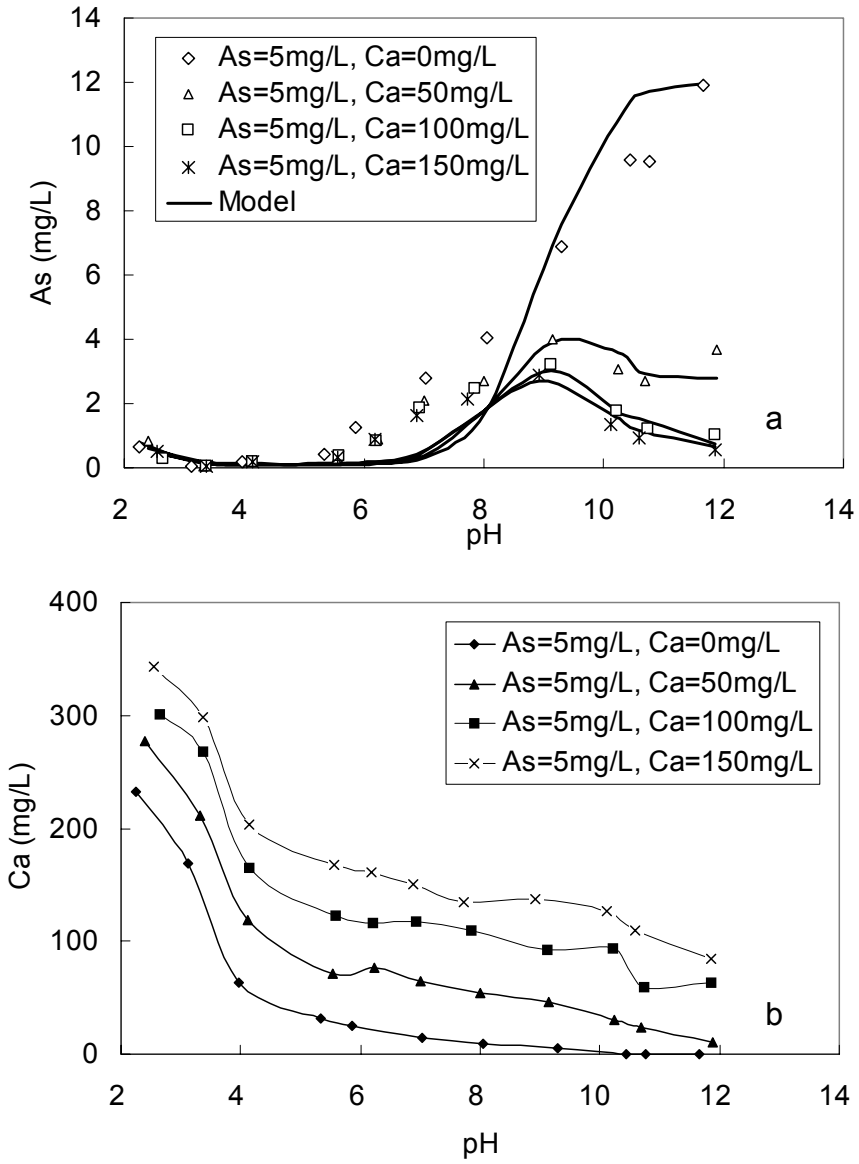

Figure 3. Arsenic partitioning for fly ash #1008 with and without addition of Ca. (a) Arsenic concentration as a function of pH; (b) Calcium concentration as a function of pH

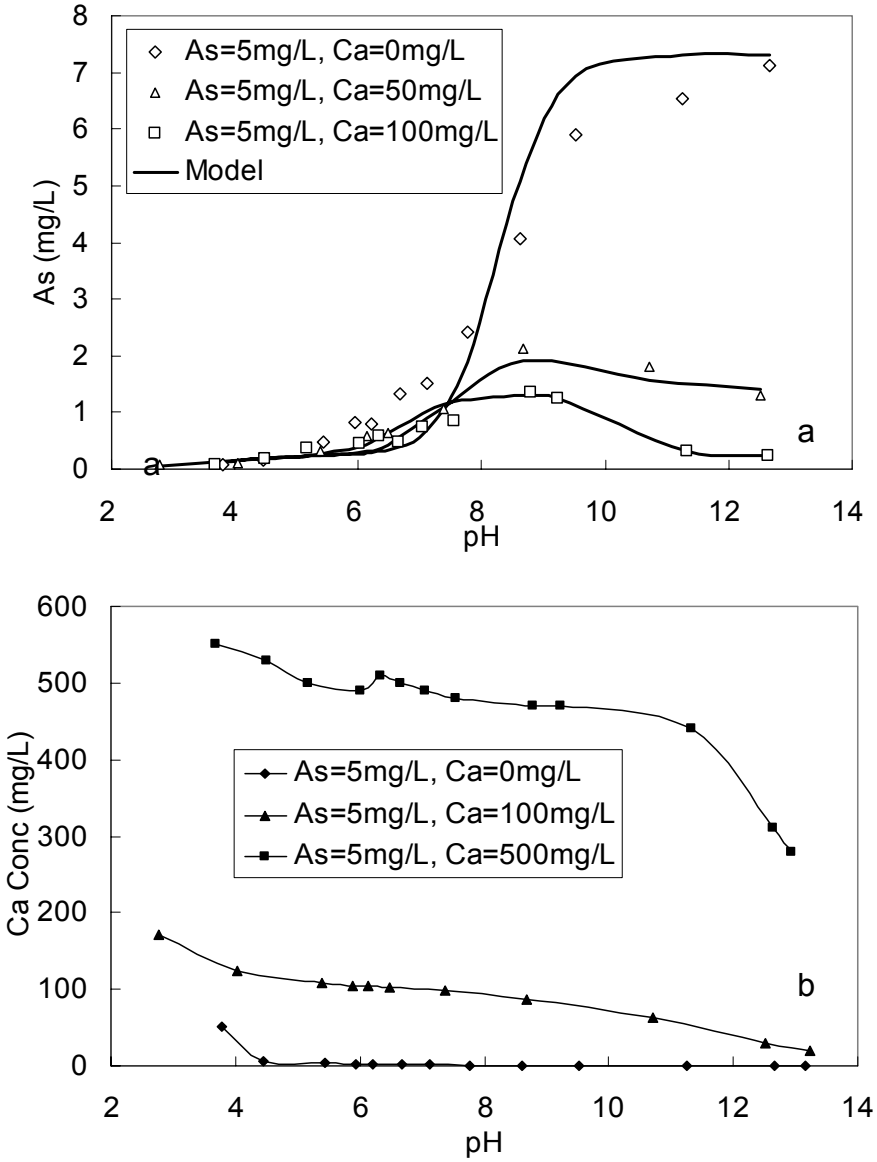

Figure 4. Arsenic partitioning for fly ash #1005 with and without addition of Ca. (a) Arsenic concentration as a function of pH; (b) Calcium concentration as a function of pH.

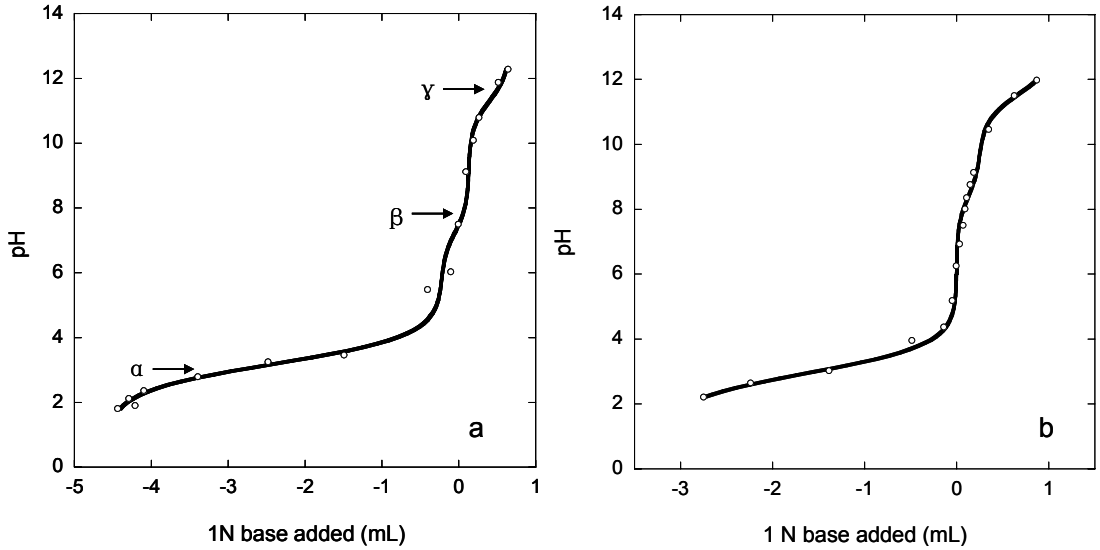

Figure 5. Titration and curve fitting results for (a) Ash #1008, (b) Ash #1005. Experimental conditions: S/L = 1:10; ionic strength = 0.01 M (NaNO3); temperature = 20 – 25°C; equilibration time = 24 hours (negative values were used for acid consumption on X axis).

SECTION

4. CONCLUSIONS

The primary results of this work are presented in five manuscripts for publication in peer-reviewed journals. Conclusions from this work have been reported in each paper, respectively, and have also been compiled and reported below.

Key conclusions on method development on quantifying the availability and stability of trace cationic trace elements from fly ash (Paper I) include the following:

1. The total leachable mass and the adsorption constant are parameters representing the availability and the stability of trace elements in fly ash, which play an important role on their leaching behavior from fly ash.
2. The batch leaching results with and without external element addition indicate that the trace elements originally present in fly ash have the similar adsorption-desorption behavior as those added externally.
3. The modeling approach described herein is appropriate to determine the intrinsic leaching characteristics of Cu(II), Cd(II), Ni(II) and other trace cationic elements with similar leaching mechanisms.

Key conclusions on the leaching characteristics of selenium from coal fly ashes (Paper II) include the following:

1. Selenium leaching from bituminous coal ashes is largely dependent on pH conditions, the least release occurred in pH range 3-4; whereas little selenium, if not none, was released from subbituminous coal ashes, probably due to the high calcium content in the latter type of ashes.

2. Se(VI) was hardly adsorbable on either type of ashes at studied pH conditions, while Se(IV) was considerably more adsorbable at neutral and slightly acidic pHs. The similarity between the leaching behavior of selenium from both ashes and the adsorption behavior of Se(IV) on fly ash indicated that Se(IV) was the predominant species in the released selenium from both types of ashes.
3. Sulfate added to the solution had no significant impact on selenium adsorption on both types of ashes.
4. The speciation-based adsorption model was capable of predicting Se(IV) adsorption by bituminous coal fly ash, and determining the adsorption constants ($\log K_S$) of $HSeO_3^-$ and SeO_3^{2-}.

Key conclusions on the leachability and speciation of arsenic and selenium in different types of fly ashes (Paper III) include the following:

1. For bituminous coal ash, the leaching of arsenic and selenium is mostly controlled by adsorption/desorption and slow diffusion processes. However, for subbituminous coal ash, the high calcium content may form precipitation with both arsenic and selenium and control their leaching.
2. As(V) and Se(IV) were major arsenic and selenium species in all three types of fly ashes from different coal source.
3. The presence/absence of air did not alter the speciation of arsenic and selenium in the leachate for the 1-day leaching experiment.
4. Substantially more arsenic and selenium were leached from both bituminous coal ash and subbituminous coal ash after 30-day leaching

compared to the normally used 1-day leaching experiment due to the slow diffusion process of arsenic and selenium for bituminous coal ash and the decrease of calcium concentration from the slow minimization process for subbituminous coal ash.

Key conclusions on the adsorption characteristics of arsenic (V) onto class F fly ash (Paper IV) include the following:

1. Arsenic leaching from the class F ash was largely dependent on pH conditions, with minimum release occurred in pH range 3-7. This behavior suggested that adsorption is one of the main mechanisms controlling the leaching of arsenic from the tested ash.
2. A speciation-based arsenic(V) adsorption model was developed and successfully applied to predicting arsenic(V) adsorption onto the class F ash under different S/L ratios. This research offers a substantial simplification of modeling arsenic(V) adsorption onto solid particles by eliminating insignificant surface electrostatic effect.

Key conclusions on the effect of calcium on arsenic(V) adsorption onto coal fly ashes (Paper V) include the following:

1. Arsenic leaching behaviors from acidic and alkaline fly ashes were correlated with the calcium content in bulk ash. The calcium phase in high-calcium samples was likely to be responsible for the stabilization of arsenic in the alkaline pH range.
2. Arsenic(V) adsorption on to acidic fly ash was significantly enhanced by added calcium under basic conditions. Solubility product calculation

indicated that this process was not controlled by precipitation of $Ca_3(AsO_4)_2$. Instead, it is hypothesized that calcium complexes with arsenic and forms two neutral species $CaHAsO_4$ and $Ca_3(AsO_4)_2$ which have a relatively high affinity for fly ash surfaces at high pH, resulting in increased arsenic adsorption.

3. The adsorption model developed in this study successfully predicted As(V) adsorption behavior on two acidic ashes with presence of calcium. The formation and adsorption constants of different arsenic species were determined.

5. SIGNIFICANCE AND IMPACT

The leaching behavior of cationic elements from coal fly ash has been investigated extensively in previous studies. However, the leaching behavior of oxyanions, which are normally more mobile in the environment, has been less studied. The proposed research described the leaching behavior of arsenic and selenium under various conditions including pH, S/L ratios, leaching time and types of fly ash. It also provided a better understanding of the leaching mechanism of arsenic and selenium for both bituminous and subbituminous coal ashes. Laboratory results provided useful information for EPRI and coal power plants to predict the leaching potential of trace elements from coal fly ash, their impact on groundwater quality, and to develop novel methods to control such potential contamination. The dependency of trace element leaching behavior on pH suggested that it is critical to regularly monitor the pH conditions in field leachate and try to avoid codiposal of very acidic or basic wastes into coal ash landfill. Nonetheless, it might be hard to find an optimal pH range for the leaching control of both cationic and anionic elements due to their different performances. The low leachability of subbituminous coal fly ashes indicated that blending bituminous coal ash with subbituminous coal ash at disposal site might be a practical protocol to reduce the leaching potential of arsenic and selenium. The proved calcium effect on arsenic leaching from and adsorption onto coal fly ash also suggested that adding lime might be another solution to stabilize arsenic in fly ash and minimize the potential environmental impact of fly ash disposal.

This research is the first study to develop a capability to quantify two intrinsic parameters determining the availability and stability i.e. total leachable mass and the

adsorption constant, of trace cationic elements in bituminous fly ash under various field conditions. The speciation-based adsorption model for arsenic and selenium also successfully described the adsorption behavior of arsenic and selenium onto bituminous coal ash, without considering the electrostatic effect and surface charge correction, which has significantly simplified the commonly used surface complexation model without sacrificing its effectiveness and accuracy.

This research also presented detailed information on the speciation of arsenic and selenium in fly ash leachate under natural pH conditions and its affecting factors including S/L ratio, presence of air and leaching time. This information provided insight into the field occurrence of arsenic and selenium at fly ash disposal sites and the weathering effect on the speciation-dependent toxicity and mobility of arsenic and selenium in natural environment. The speciation of arsenic and selenium varied from sample to sample, therefore, it is necessary to monitor not only the total concentration but also the speciation profile of these trace elements in field leachate for purposed of environmental risk assessment or waste management. The diffusion of trace elements in pore water and formation of secondary minerals need to be considered in long term leaching or weathering process, which likely increase the mobility of arsenic and selenium. The weathering process may also include oxidation/reduction and precipitation/dissolution processes, which were not thoroughly investigated in this research, but play important roles on the fate and transport of trace elements under field conditions.

6. FUTURE WORK

In this research, three monoprotic weak acid surface sites were assumed to be responsible for the adsorption of cationic and anionic trace elements on fly ash. However, to improve our understanding on the surface interaction between arsenic/selenium and fly ash, it would be beneficial to examine the exact physical-chemical form of these surface sites on different types of fly ash and their interaction with arsenic and selenium species. X-Ray Diffraction (XRD) may be used to determine the major mineral components in fly ash, which could contribute hydroxyl groups as surface sites. XAFS has been used to investigate the local bonding and chemical structures of specific elements in minerals and provide information on the identity, number of and distance to the next nearest neighbors around the element of concern. Therefore, XAFS can be used in future research to identify surface functional groups and the bonding structures of surface complexes between arsenic/selenium and surface sites.

The arsenic and selenium adsorption model developed in this research has been focused on the single adsorbate system with pH as a key factor. However, a more complicated scenario is expected in field conditions, with presence of dissolved organic matter or other competitive anions including carbonate, chromate, molybdate and vanadate. Cosorption test should be conducted by mixing for example 5 mg/L of As(V) or Se(IV) with 5, 10, 50 or 100 mg/L of molybdate in the solution and monitor the change of the adsorption ratio at different pH conditions. A more comprehensive model incorporating the above factors will assist on the evaluation of the fate and transport of these trace elements in natural environment with greater accuracy.

To date, few studies have been conducted on the preservation of fly ash leachate samples for speciation analysis of arsenic and selenium. Therefore, a robust, reliable preservation method is to be developed in future research, including determination of the suitable additive (e.g. EDTA, acetic acid, hydrochloric acid) for sample stabilization, the optimal dosage, storage temperature and storage time, etc.

Additional study is needed to investigate the influence of weathering process on the migration of arsenic, selenium and other trace elements at fly ash disposal sites. Possible influence factors include aerobic/anaerobic conditions, wetting and drying, and variation of temperature. Possible processes such as oxidation/reduction, precipitation, hydration, and mineralization might occur during the weathering process. For this study, a lab scale fly ash landfill composed of aerobic and anaerobic cells can be constructed, the aerobic conditions will be maintained with air injection. Synthesized rain water can be applied to generate leachate. The leachate will be collected and analyzed with HPLC-ICP-MS to determine the concentration and speciation of arsenic and selenium in leachate. The aerobic condition may accelerate the oxidation arsenic and selenium from low to high oxidation state, therefore changing their mobility and toxicity, Vise versa for the anaerobic cells. However, other processes such as the oxidation and precipitation of iron may be triggered at the same time and result in a more complicated situation. Biodegradation under aerobic and anaerobic conditions is another process needs to be concerned for real scenario. Wetting and drying is another naturally occurring process at landfill sites and may affect the partitioning and transport of trace elements among ash and groundwater. Change of temperature will increase or decrease the adsorption/desorption rate and the adsorption constants as well. Therefore, these factors

are also important to the migration of trace elements under field conditions and require further study to better predict the potential environmental impact from the disposal or management of coal fly ash.

APPENDIX A.

BATCH LEACHING RESULTS FOR OTHER ELEMENTS FROM FLY ASH

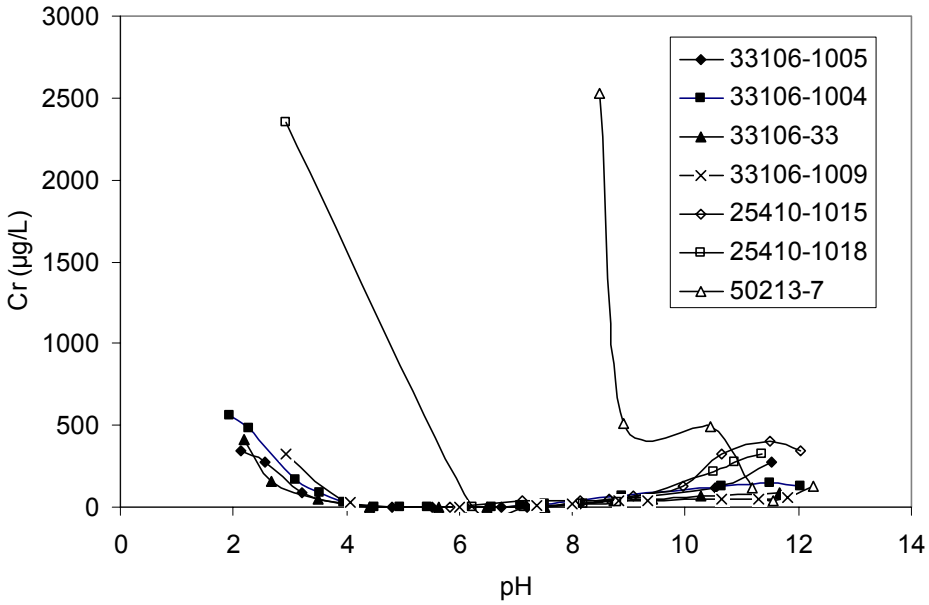

Figure Supplement 1. Chromium leaching from class F and class C ashes. Experimental conditions: S/L = 1:10; temperature = 20 – 25 ^{o}C; equilibration time = 24 hours.

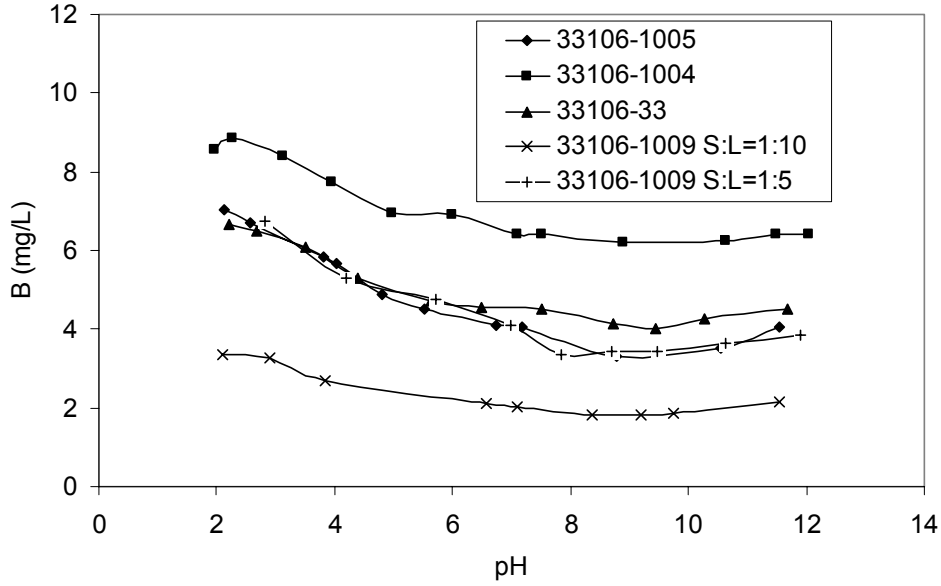

Figure Supplement 2. Boron leaching from class F ashes. Experimental conditions: S/L = 1:10; temperature = 20 – 25 ^{o}C; equilibration time = 24 hours.

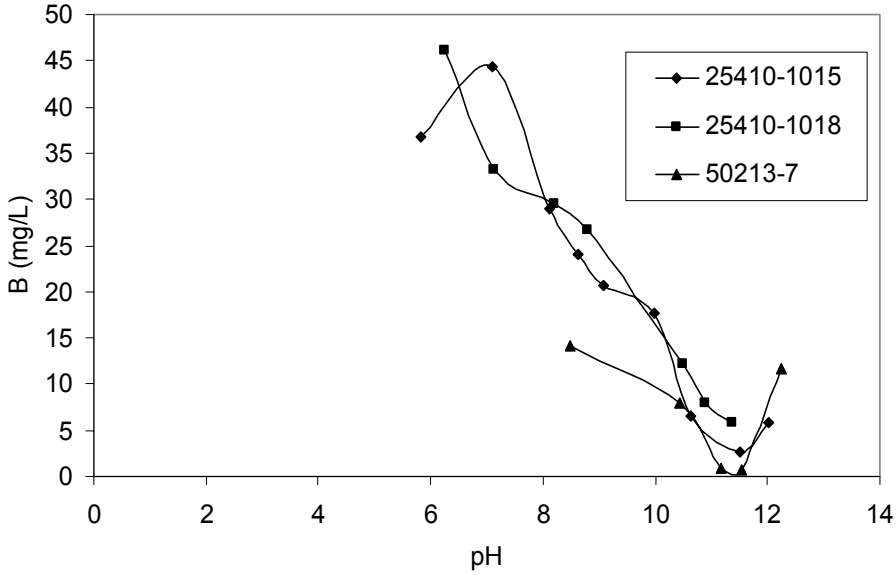

Figure Supplement 3. Boron leaching from class C ashes. Experimental conditions: S/L = 1:10; temperature = 20 – 25 °C; equilibration time = 24 hours.

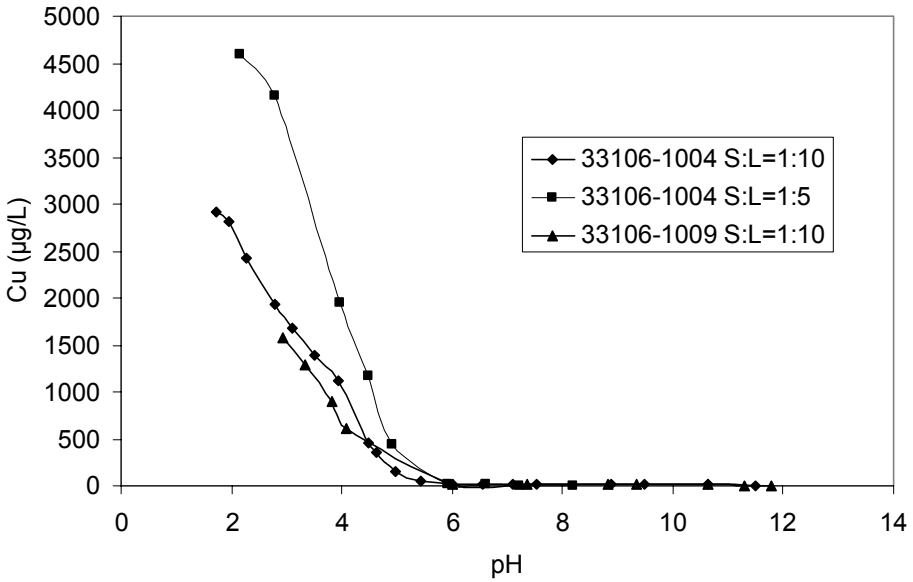

Figure Supplement 4. Copper leaching from ash 33106-1009 and 33106-1004. Experimental conditions: temperature = 20 – 25 °C; equilibration time = 24 hours.

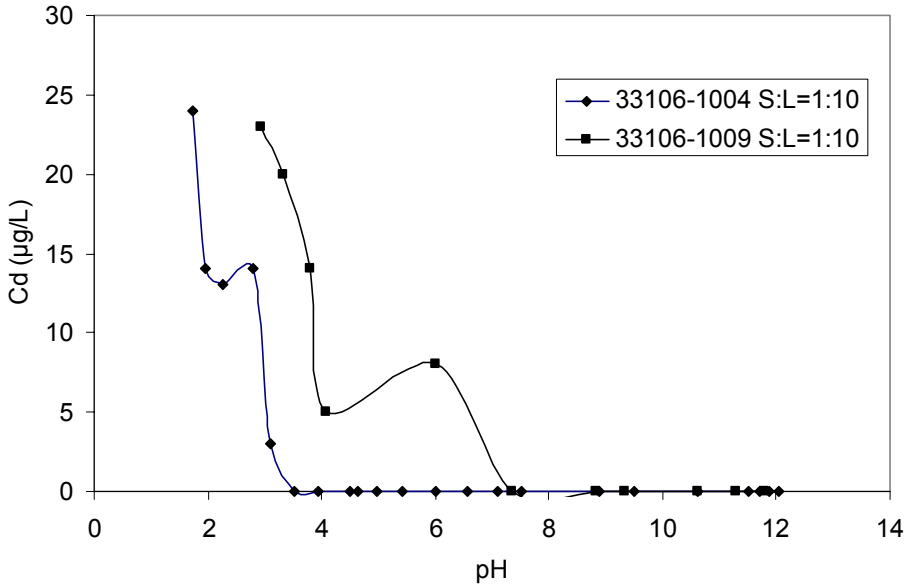

Figure Supplement 5. Cadmium leaching from ash 33106-1004 and 33106-1009. Experimental conditions: temperature = 20 – 25 °C; equilibration time = 24 hours.

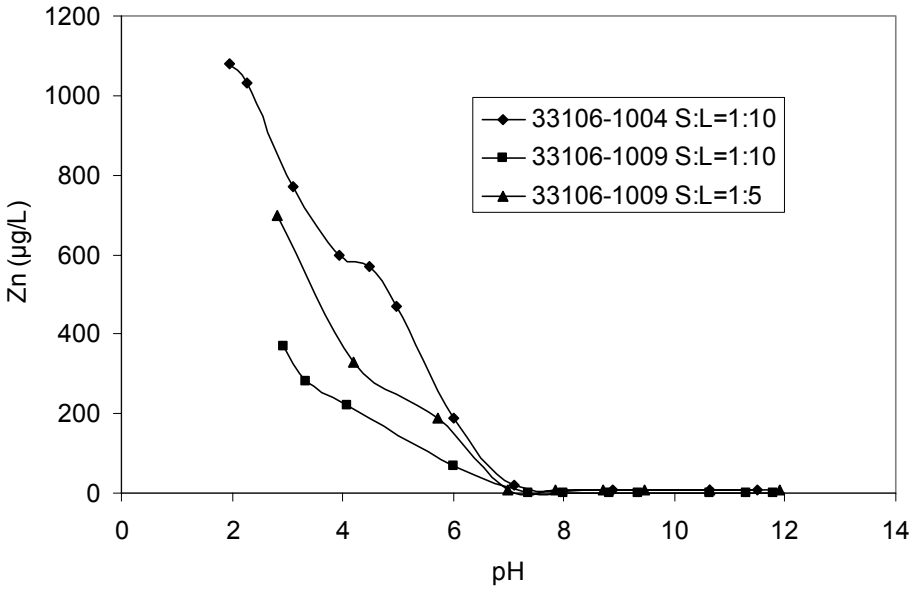

Figure Supplement 6. Zinc leaching from ash. 33106-1004 and 33106-1009. Experimental conditions: temperature = 20 – 25 °C; equilibration time = 24 hours.

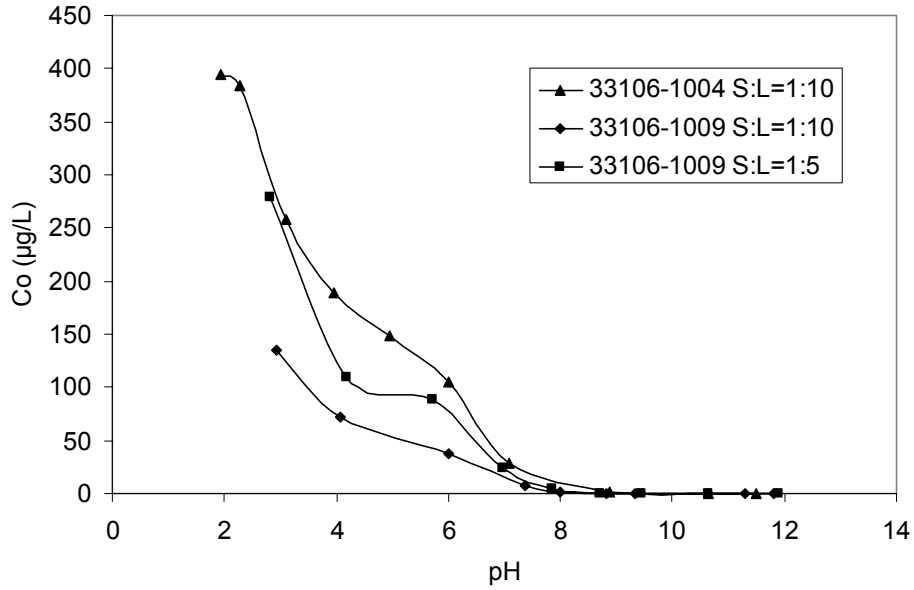

Figure Supplement 7. Cobalt leaching from ash 33106-1004 and 33106-1009. Experimental conditions: temperature = 20 – 25 oC; equilibration time = 24 hours.

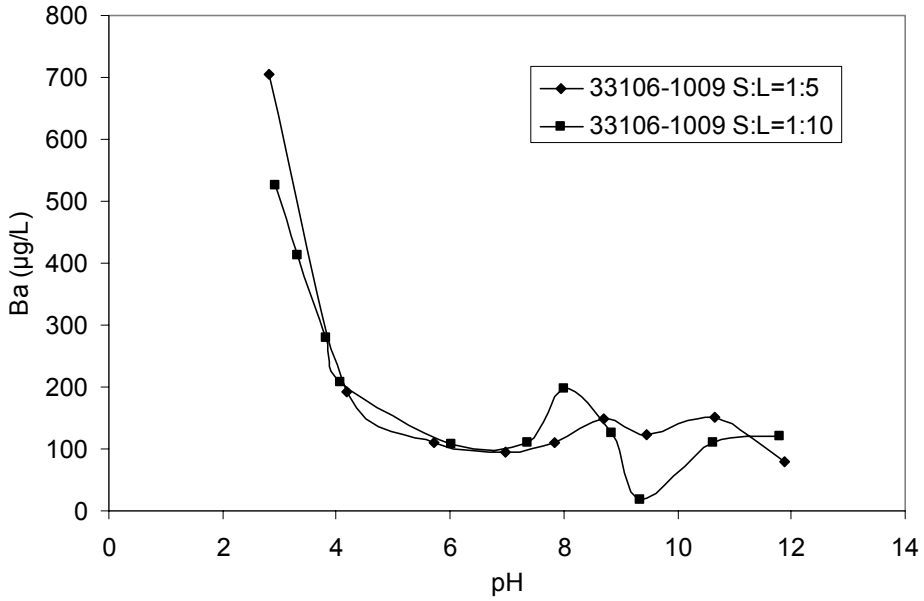

Figure Supplement 8. Barium leaching from ash 33106-1009. Experimental conditions: temperature = 20 – 25 ^{o}C; equilibration time = 24 hours.

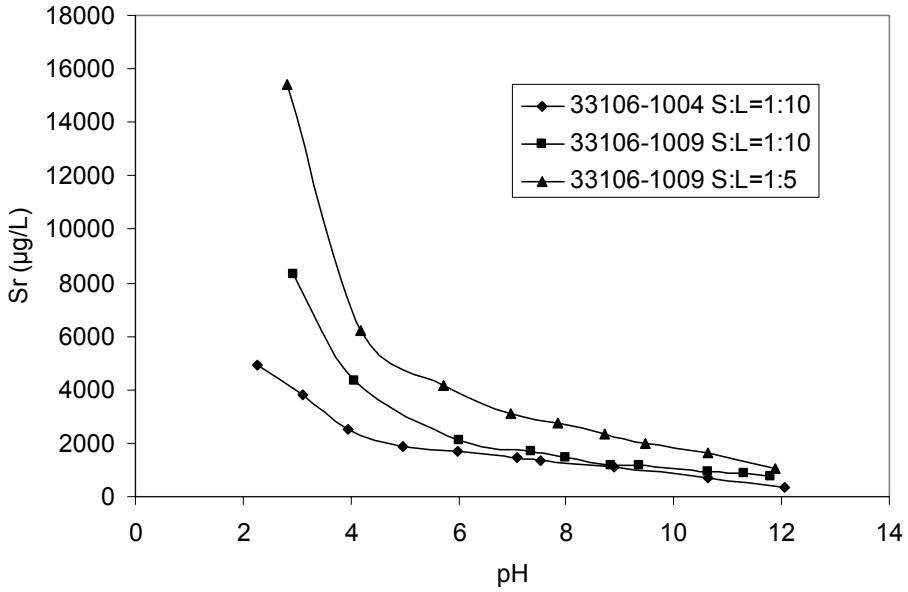

Figure Supplement 9. Strontium leaching from ashes 33106-1004 and 33106-1009. Experimental conditions: temperature = 20 – 25 °C; equilibration time = 24 hours.

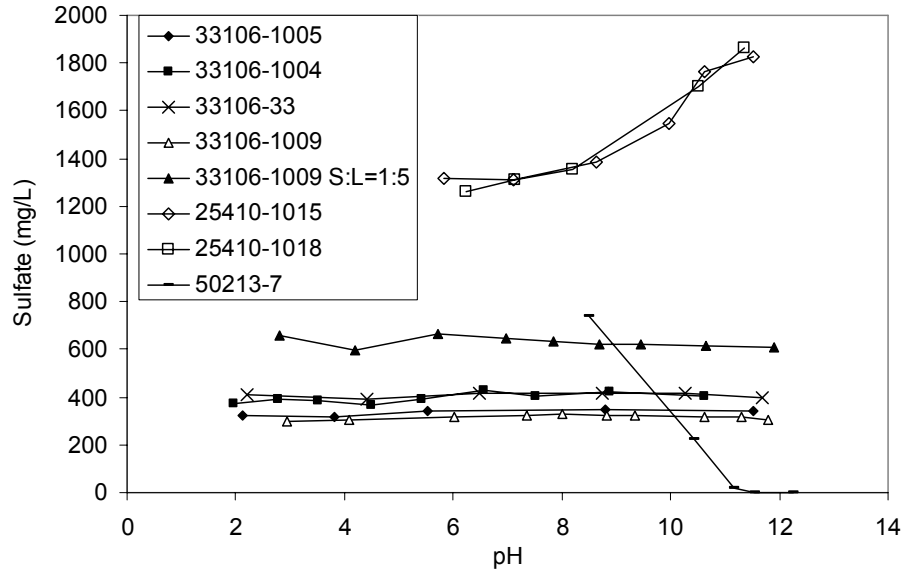

Figure Supplement 10. Sulfate leaching from class F and class C ashes. Experimental conditions: S:L = 1:10 (unless specified); temperature = 20 – 25 °C; equilibration time = 24 hours.

APPENDIX B.

AMMONIUM EFFECT ON LEACHING OF ARSENIC AND SELENIUM FROM FLY ASH

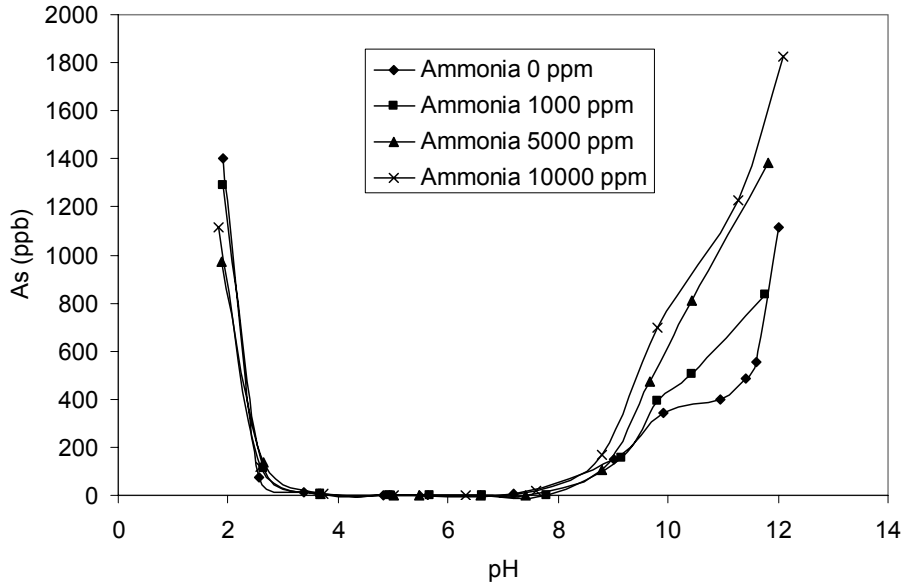

Figure Supplement 1. Arsenic leaching from ash 33106-1004 with different ammonia concentrations. Experimental conditions: S/L = 1:10; temperature = 20–25 ^{o}C; equilibration time = 24 hours.

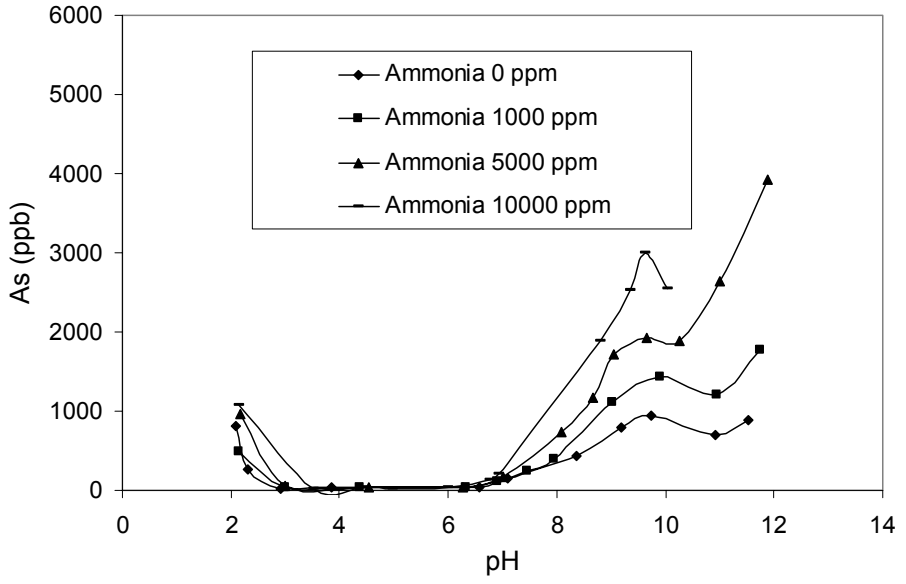

Figure Supplement 2. Arsenic leaching from ash 33106-1009 with different ammonia concentrations. Experimental conditions: S/L = 1:10; temperature = 20 – 25 ^{o}C; equilibration time = 24 hours.

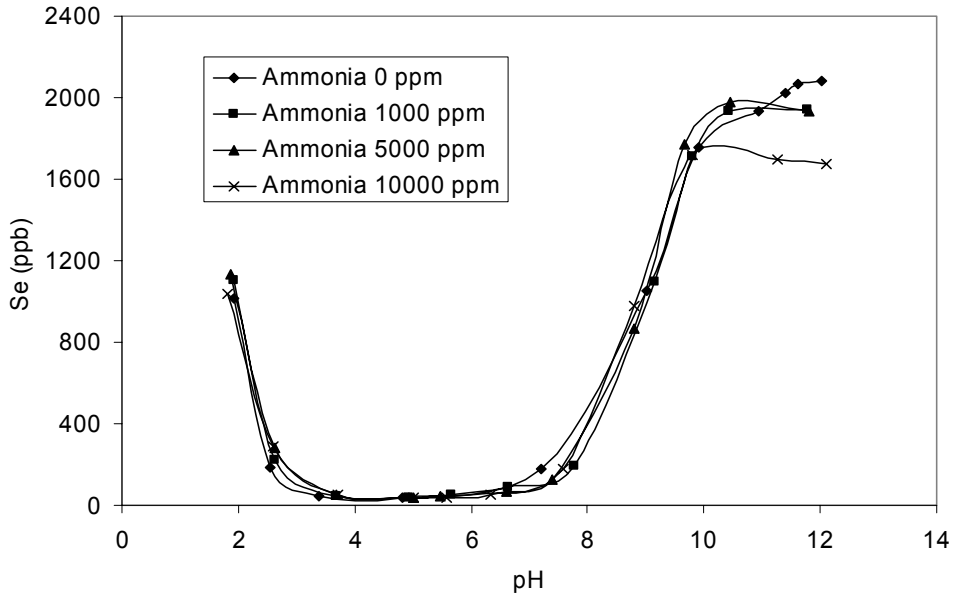

Figure Supplement 3. Ammonia impact on Se leaching from raw ash 33106-1004 with different ammonia concentrations. Experimental conditions: S/L = 1:10; temperature = 20–25 ^{o}C; equilibration time = 24 hours.

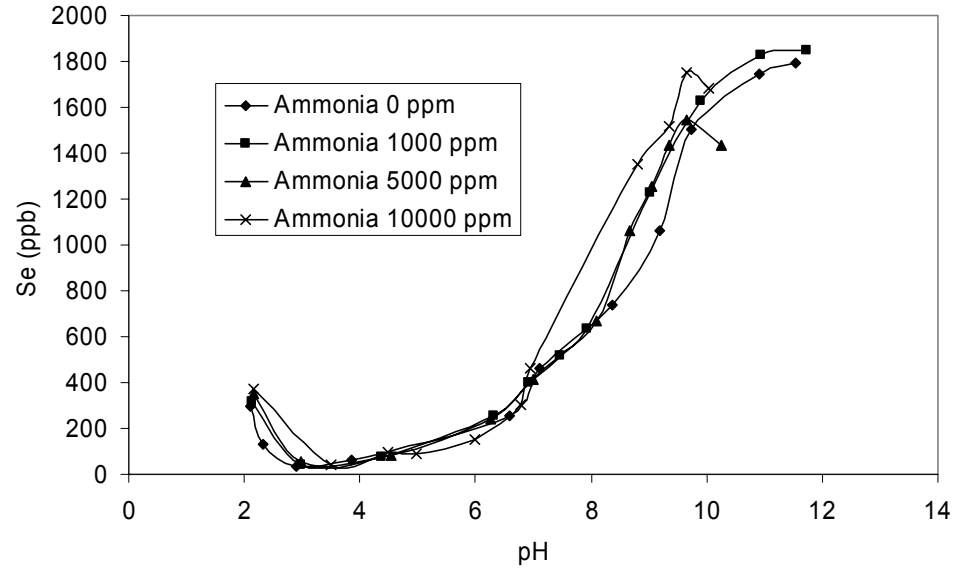

Figure Supplement 4. Ammonia impact on Se leaching from raw ash 33106-1009 with different ammonia concentrations. Experimental conditions: S/L = 1:10; temperature = 20–25 ^{o}C; equilibration time = 24 hours.

APPENDIX C.

METHOD DEVELOPMENT FOR FLY ASH TOTAL DIGESTION

Method Development for Fly Ash Total Digestion

Total compositions of trace elements in coal fly ash were determined using microwave aided digestion, followed by chemical analysis with ICP-MS (ELAN® DRC-e, PerkinElmer). To obtain complete digestion of coal fly ash with respect to the trace elements, A triple acid digestion method was developed using Multiwave 3000 (Anton Paar USA)

Experimental Design

The method development was performed based on a default digestion program for fly ash recommended by the manufacture, which hereby was named as triple acid method. A standard reference material, coal fly ash 1633b, was digested to verify the validity of this method. Three concentrated acid (3 mL HNO_3 + 2 mL HCl + 3 mL HF) and 0.1 gram of dry fly ash were added to each Teflon liner. The digestion process was power controlled and the details of the program was listed in Table 1. After digestion, the digestates were collected into 50mL polypropylene tubes, the liners were rinsed three times with DI water before dilution to final volume 25 mL. In case the digestion may not be complete, a parallel test was conducted, in which the program was run twice before the digestates were collected.

Considering the HF content in samples, A hydrofluoric acid-resistant introduction system was used for ICP-MS, including a Scott Spray Chamber and an Alumina Injector. However, it will always be beneficial if using HF could be avoided. Therefore a double acid digestion method was also tested, with a different acid matrix of 6 mL HNO_3 and 2 mL of HCl, and all other conditions the same with triple acid method.

For each digestion condition, three replicates and two reagent blanks were tested, the average values were reported as final results. The concentrations of 20 trace elements in digestates were analyzed with ICP-MS, and their total compositions in fly ash were calculated based on the sample weight, element concentration and digestate volume.

Results and Discussion

Digestates from triple acid digestion still had a certain amount of white particles undissolved, no matter whether the digestion process was repeated once or twice. Digestates from double acid digestion contained both black and white particles in solution, indicating the digestion is less complete. The calculated elemental compositions of the standard reference material 1633b were compared with the certified value reported by NIST. Results indicated that triple acid method is effective for complete digestion of most trace elements, except for Sr and Ba, which showed 35% and 50% of recovery, respectively. These two elements may be trapped in the white particles, and other technology such as XRF was recommended for the quantification. Cd had a relatively high recovery of 140% and Se displayed a lower recovery around 80%, all other elements showed very good agreement between the experimental data and certified values, with recovery of 90-113%.

Results for triple acid method also suggested that running the program twice did not make significant difference on the digestion, therefore one cycle is enough for complete digestion of most trace elements.

Results for double acid method suggested that digestion without HF was not complete for many trace elements, including Mo, V, Cr, Co, Cu, etc., which showed a low recovery around 60% or less. Therefore, HF is necessary for the complete digestion of coal fly ash.

As a summary, the triple acid digestion method and the default digestion program are appropriate for the complete digestion of most trace elements in coal fly ash, and will be used for digestion of real fly ash samples. Major elements as well as Sr and Ba will be analyzed with XRF.

Digestion of Coal Fly Ash #169 and #170

Two fly ash samples #169 and #170 were digested following the above developed method, two replicates were tested for each sample, and the average values were reported in Table 3.

Table Supplement 1. Fly ash digestion program conditions (for 8 vessels)

Power (w)	Ramp Time (min)	Hold Time (min)	Fan Speed
1200	10	50	1
1200	0	30	1
0	0	15	3

Table Supplement 2. Total composition of trace elements in SRM 1633b determined by different methods

Concentration (mg/kg)	Li	Be	V	Cr	Mn	Co	Ni	Cu	Zn	As	Se	Sr	Mo	Ag	Cd	Sb	Ba	Pb	Tl	Re
SRM 1633b			295.7	198.2	131.8	50.0	120.6	112.8	210.0	136.2	10.3	1041.0			0.8	6.0	709.0	68.2	5.9	
Triple acid-1 cycle	138.8	18.1	304.1	189.2	124.4	51.8	126.5	120.6	234.0	142.5	7.7	379.4	22.2	1.1	1.1	5.5	374.1	75.5	6.5	0.0
Recovery			**102.8**	**95.4**	**94.4**	**103.7**	**104.9**	**106.9**	**111.4**	**104.6**	**74.9**	**36.4**			**140.4**	**91.0**	**52.8**	**110.7**	**110.8**	
Triple acid-2 cycle	139.6	18.1	302.5	188.9	128.5	51.8	126.2	120.5	232.4	143.4	8.5	361.6	22.2	1.4	1.1	5.4	374.7	74.9	6.7	0.0
Recovery			**102.3**	**95.3**	**97.5**	**103.6**	**104.6**	**106.8**	**110.7**	**105.3**	**82.9**	**34.7**			**138.1**	**90.2**	**52.8**	**109.9**	**113.2**	
Double acid-1 cycle	98.0	8.8	178.5	183.6	79.7	32.1	76.1	72.6	142.2	139.7	9.6	606.1	7.6	0.0	0.7	UD	340.8	37.7	4.4	0.0
Recovery			**60.4**	**92.6**	**60.5**	**64.2**	**63.1**	**64.4**	**67.7**	**102.6**	**93.8**	**58.2**			**85.8**	**0.0**	**48.1**	**55.3**	**75.0**	

Table Supplement 3. Total composition of trace elements in fly ash #169 and #170

Concentration (mg/kg)	Li	Be	V	Cr	Mn	Co	Ni	Cu	Zn	As	Se	Mo	Ag	Cd	Sb	Pb	Tl	Re
#169	64.0	10.1	134.4	24.0	201.3	26.1	77.0	48.4	183.9	36.0	9.6	9.2	UD	1.0	5.2	52.4	2.1	UD
#170	97.3	17.8	239.7	152.3	284.2	42.8	123.2	82.2	190.4	56.2	3.8	10.8	UD	1.1	4.9	75.8	3.6	UD

UD = Undetectable

APPENDIX D.

MECHANISM STUDY OF ARSENATE ADSORPTION ON FLY ASH USING SURFACE ANALYSIS TECHNIQUES

Mechanism Study of Arsenate Adsorption on Fly Ash Using Surface Analysis Techniques

Abstract

Arsenate adsorption on one bituminous coal fly ash and one subbituminous coal fly ash, as well as their physical-chemical characteristic were studied with batch adsorption experiments and different analytical techniques XRF, FTIR and XPS. The major elements in these two ashes were determined to be Al, Si, C, O and Ca. As and C are two surface enriched elements, while Ca and Fe are bulk elements. For the subbituminous coal ash, FTIR spectra showed occurrence of new bands at 875 cm^{-1} and 885-905 cm^{-1} due to arsenate adsorption, the new bands were assigned to As-OCa, indicating reaction between arsenate and the calcium species on this ash. For the bituminous ash, no new band information was observed from the FTIR spectra of samples with various arsenate loading. The XPS quantitative analysis displayed that surface arsenic concentration (atomic percentage) on both ashes was increased by 7-8 times after reacted with arsenate solution.

Keywords: Arsenate; Fly ash; Adsorption; XPS; FTIR; Binding energy

Introduction

Arsenic (As) poses a remarkable water quality problem and challenge facing environmental engineering in the world. The tremendous mass of coal fly ash produced around the world combined with the concentration of As in that ash, pose a significant anthropogenic source of As, particularly arsenate. The leaching and adsorption of arsenate on fly ash surface is an important geochemical process in the transport of arsenate between fly ash and the surrounding environment. Therefore, comprehension of the arsenate adsorption mechanism on fly ash is important to predict potential impacts of fly ash on water quality and develop disposal and re-use methods with tolerable arsenic leaching.

Extensive studies have been conducted on the general leaching and adsorption characteristics of arsenic on coal fly ash using a variety of leaching and adsorption tests. Several mechanisms have been proposed to interpret arsenic leaching and adsorption behavior. By comparing arsenic leaching behavior from fly ash with its adsorption onto the major mineral compounds in fly ash, van der Hoek et al. (1994) concluded that arsenic leaching from acidic ash is likely to be controlled by surface complexation with iron oxide, while a calcium phase is shown to be responsible for alkaline ash. other researchers reported that formation of ettringite contributes to arsenic stabilization in fly ash at high pH conditions. However, few studies have been done to obtain direct evidence on the surface adsorption of arsenic on fly ash with surface analysis techniques.

Fourier Transform Infrared spectroscopy (FTIR) and X-ray photoelectron spectroscopy (XPS) are two commonly used surface analytical techniques. FTIR has been used to reveal the structure feature of components of fly ash (and surface composition of

fly ash (Mollah et al. 1994, Guerrero et al., 2004), or to investigate the adsorption mechanism of arsenic or selenium on metal oxides and hydroxides, including goethite, alumina and TiO_2 (Hsia, 1994; Goldburg, 2001; Myneni, 1998a, 1998b; Pena, 2006). X-ray photoelectron spectroscopy (XPS) provides qualitative, quantitative and chemical state information regarding the elements in the near surface region (~ 50 A) and detects the chemical shift of binding energy occurred in an adsorption process accompanied with charge transfer between adsorbate and adsorbent when strong covalent bond is formed (Takahiro et al. 2003; Ding and Dejong, 2000; Mollah et al. 1994). XPS in this study was used only for determinination of the surface elemental composition of fly ash.

In spite of the wide use of FTIR and XPS in adsorption research, their application on study of arsenic adsorption on fly ash or other field matrix sample is seldom reported. The objective of this work is to explore the adsorption mechanism of arsenic on different types of fly ash with batch adsorption experiments and surface techniques FTIR and XPS, and provide direct information on the interaction between arsenate and fly ash surface.

Experimental

Materials

The properties of fly ash largely depend on its coal source, for comparison, one bituminous coal fly ash 33106-1005 and one subbituminous coal fly ash 25410-1015 from two power plants were examined in this work. The latter was expected to have higher calcium content. The loss-on-ignition (LOI) and BET surface area of the two ashes are listed in Table 1. Both ashes were washed five times with deionized (DI) water at solid/liquid (S/L) ratio of 1:5. Air was used to agitate the mixture. Each washing cycle includes approximately 20 hour of mixing and 2 hour of settling. The supernatant was then removed and the washing process repeated. Washed ash was dried in a 105 °C oven for at least 24 hours to remove moisture, and stored in air tight containers before use. All the chemicals used were of ACS certified grade. Stock solution of arsenic was prepared by dissolving sodium arsenate heptahydrate ($Na_2HAsO_4.7H_2O$, Alfa Aesar) in DI water.

Bulk Elemental Composition

The bulk compositions of major elements and arsenic in two ashes were analyzed with XRF (X-LAB 2000, SPECTRO Analytical Instruments GmbH & Co. KG). The detection limit of XRF is approximately 10 ppm (mg/kg).

Batch Arsenic Adsorption Experiment

In the adsorption experiment, 2g of dried ash was mixed with 40 mL of arsenate solution for 24 hours. Three arsenate loading conditions, 0 mol/L, 0.013mol/L and 0.1mol/L, were employed for both ashes. The one without arsenate addition was used to obtain the background information of fly ash. pH was adjusted with HNO_3 or NaOH solution. According to batch leaching results available elsewhere (Wang et al., 2007), 33106-1005 displayed high arsenic adsorbability in acid and neutral range, and 25410-

1015 in neutral and basic range. Thus, One acid pH 3.7 and one neutral pH 6.5 were selected for ash 33106-1005; and pH 6.5 and 10.6 for ash 25410-1015. With S/L ratio of 1:20, the mixture was shaken for 24 hours to reach equilibrium. Then solids were separated from liquids by filtration through a 0.45 um membrane filter and vacuum dried. The liquid was analyzed with Graphite Furnace Atomic Absorbance Spectrometer (GFAA) for arsenic concentration, and arsenate adsorption density was calculated based on arsenate concentration difference before and after adsorption and the mass of fly ash. The dried solids were stored in vacuum desiccator before FTIR and XPS analysis.

FTIR and XPS analysis

FTIR spectra of samples were recorded on a Nexus 470 FT-IR (Thermo Electron Co.) using KBr pellet. 64 co-added scans were collected at 2 cm^{-1} resolution in the mid-IR region (4000-400 cm^{-1}). XPS analysis was carried out using a Kratos Axis 165 XP spectrometer using a Mg Kα anode (hν = 1253.6 eV) and a hemispherical analyzer. The binding energy scale was corrected by Si at 102.6 eV. This is the literature value of various silicates which have been shown to be the dominant forms of silicon in coal ash by X-ray powder diffraction (Cabaniss and Linton, 1984; Matijevic et al., E.; 1964). The fly ash samples were mounted by pressing a small quantity of material onto the double side tape which was attached on a piece of tantalum foil.

Results and discussion

XRF results

XRF is only capable of analyzing elements that has higher mass than sodium, therefore the light elements like carbon and oxygen can not be determined by XRF. As an alternative, the loss-on-ignition (LOI) of each ash was measured to indicate the bulk content of carbon. The total compositions of major elements together with arsenic are listed in Table 1. Results indicate that ash 25410-1015 contains much higher Ca content, and lower contents of Al and Si than the other ash, reflecting the different coal source of these two fly ashes.

FTIR results

The FTIR spectra of washed fly ash 33106-1005 with different arsenate loading and different pH conditions are shown in Figure 1. For the sample without arsenate adsorption, the bands at 1161, 1078, 795, 779 and 460 are characteristic bands of quartz. (glass structure by spectroscopy, J. Wong) The strong band at 1078 cm^{-1} is due to ν3 (Si-O-Si) asymmetric stretching. Bands at 795 and 460 are attributed to ν4 (Si-O-Si) symmetric stretching and ν2 (O-Si-O) bending vibrations, respectively. Another band at 560 cm^{-1} is assigned to the symmetric stretching mode of Al-O-Al (Sykes, 1996). The band assignments are also in good agreement with those reported by others (M.Y.A. Mollah et al. cement and concrete, 1994; van Roode 1987) the small shoulder at 910 cm^{-1} is not associated with silicon or aluminum oxides, the identification is unknown. Comparing the three spectra obtained at pH 3.7, there is no significant difference

observed, except that two bands at 3438 and 1625 cm^{-1} displayed increased intensity with increase of arsenate loading. The former band is assigned to the symmetric stretching of water molecule, or the OH hydrogen bonded to the oxygen ions of the frame work (Fermo et al. 1999; Nakamoto, K. 1997), Hsia et al. (1994) reported that arsenate adsorption on iron oxides is presented at band 1615 and 832 cm^{-1}, accordingly, the band at 1625 cm^{-1} in the current study might be assigned to bonding between arsenate and iron oxide in fly ash, however, the bending mode of water occurs at 1640 cm^{-1}, which is close to 1625, indicating that the difference of the two bands may be only relevant to the hydration of fly ash surface. In addition, the peaks at 810- 840 cm^{-1} didn't show corresponding increase (Hsia, 1994; Goldberg, 2001). Therefore, the impact of arsenate adsorption on the FTIR spectra of ash 33106-1005 is not clear, and further study or other techniques is necessary to make a through exploration. The other three spectra obtained at pH 6.5 provided similar results and no new bands occurred with respect to either the pH change, or the variation of arsenate loading.

The FTIR spectra of washed fly ash 25410-1015 with different arsenate loading and different pH conditions are reported in Figure 2. An additional spectrum of the raw ash is also displayed in the same figure. In spectrum a, the bands at 1080 cm^{-1} and 455 cm^{-1} are assigned to the (Si-O-Si) asymmetric stretching and symmetric stretching, respectively, of Si-O-Si from SiO_2. Another broad band in the range of 950-1020 cm^{-1} is due to the presence of silicate (Fermo et al. 1999; Rayalu et al. 2005). An interesting observation is that the band at 1080 cm^{-1} disappeared on the spectrum of washed ash, which might be due to the transformation of silicon from SiO_2 to silicate during washing. The band occurred at 1482 cm^{-1} in spectra a-d with a pH of 10.4-10.6 is assigned to carbonate, mostly calcite (Fermo et al. 1999; Nakamoto, K. 1997). The absence of carbonate bands in the spectra e-g of the same ash at pH 6.5 indicated that, at lower pH after adding enough acid, most carbonate on fly ash surface is dissolved and removed from the solid phase. With increase of arsenate loading at both pH conditions, new bands at 875 cm^{-1} and 885-905 cm^{-1} occur and become stronger as arsenate loading was increased. Myneni et al. (1998b) have assigned these bands to the symmetric and asymmetric stretching of As-OCa in $CaHAsO_4.2H_2O$ (haidingerite or pharmacolite). This observation serves as an evidence for the possible coordination between adsorbed arsenate and Ca in fly ash during arsenate adsorption process.

XPS Results

Samples with arsenate loading of 0 mol/L and 0.1 mol/L were selected for XPS analysis. The pH conditions selected were 3.7 and 10.6 for ash 33106-1005 and ash 25410-1015, respectively.

The binding energy reference values given in the "Handbook of X-Ray Photoelectron Spectroscopy" (Perkin-Elmer Corporation, 1979) and NIST (National Institute of Standards and Technology) database were used to assist the identification of specific elements in samples.

Quantitative results

The surface composition (atomic percentage) of major elements and arsenic in all ash samples appears in Table 2. For convenient comparison with the bulk composition listed in Table 1, the atomic percentages are converted to weight percentages and shown in Table 3. Comparing the surface composition and bulk composition of each element presented in Table 1 and Table 3, it is concluded that the As and C are surface enrich elements for both samples, whereas Ca and Fe are bulk elements. Si shows similar concentrations on surface and in bulk for both ashes. Al displays similar surface and bulk compositions in ash 33106-1005, but appears to be surface enriched in ash 25410-1015.

Results in Table 2 and Table 3 indicate that for both ashes, the surface concentration of arsenic has significantly increased after reacted with arsenate, which is 7-8 times as high as before. The substantial increase of As 3d signal shown in Figure 3 is another evidence on the surface adsorption of arsenate. Nevertheless, considering the surface As compositions are lower than the total adsorption densities, which are 27.5 mg/g and 50.4 mg/g for ash 33106-1005 and 25410-1015, respectively, there must be more arsenic adsorbed under the top surface detected by XPS, maybe due to multilayer adsorption.

The surface composition of Al and Si show slight decrease after arsenic adsorption, and Ca content slightly increases. However, since such changes are not as significant as that of arsenic, and the fly ash surface may not be ideally homogeneous, the variation of other element compositions is not necessarily caused by arsenic adsorption process.

Conclusions

This research demonstrated that arsenate adsorption on two fly ashes is correlated to the surface reaction between arsenate and the iron species for the bituminous coal ash or between arsenate and calcium species for the subbituminous coal ash. Results from XRF, FTIR and XPS consistently revealed that the major elements in these two ashes are Al, Si, C and O. The subbituminous coal ash 25410-1015 contains a much higher Ca content than the other one, which has played an important role in the adsorption of arsenate. Mineral components including quartz, aluminosilicate and calcite were identified in the two ashes with FTIR. The occurrence of new bands at 875 cm^{-1} and 885-905 cm^{-1} in the FTIR spectra of ash 25410-1015 after reacted with arsenate indicated that the adsorption phenomenon may be a result of arsenic coordination with calcium in fly ash. However, such bonding information was not observed from the spectra of ash 33106-1005 with different arsenate loading and pHs. XPS results indicated that the surface atomic percentage of As on both ashes were significantly increased after arsenate adsorption. The differentiation between the surface and bulk elemental compositions of two ashes indicated that As and C are two surface enriched elements, whie Ca and Fe are bulk elements.

Acknowledgements

This work was supported by the Electric Power Research Institute (EPRI). The authors also gratefully acknowledge Ms. Le Kang for technical assistance on XRF analysis, Mr. Jeff Wight for XPS analysis, and Mr. Joseph Counsil for FTIR analysis Conclusions and statements made in this paper are those of the authors, and in no way reflect the endorsement of the aforementioned funding agencies.

References

Cabaniss G. E.; Linton R. Characterization of surface species on coal combustion particles by x-ray photoelectron spectroscopy in concert with ion sputtering and thermal desorption. Environ. Sci. Technol. 1984, 18, 271 – 275.

Ding, M.; Dejong, B. XPS studies on the electronic structure of bonding between solid and solutes: adsorption of arsenate, chromate, phosphate, Pb^{2+} and Zn^{2+} ions on amorphous black ferric oxyhydroxide. Geochimica et Cosmochimica Acta. 2000, 64, 1209-1219.

Ersez, T.; Liesegang, J. Analysis of brown coal fly-ash using X-ray photoelectron spectroscopy. Applied Surface Science 1991, 51, 35-46

Fermo, P.; Cariati, F.; Pozzi, A.; Demartin, F.; Tettamanti, M.; Collina, E.; Lasagni, M.; Pitea, D.; Puglisi, O.; Russo, U. The analytical characterization of municipal solid waste incinerator fly ash: methods and preliminary results. Fresenius' Journal of Analytical Chemistry. 1999, 365, 666-673.

Goldberg, S.; Jonhston, C.T. Mechanisms of arsenic adsorption on amorphous oxides evaluated using macroscopic measurements, vibrational spectroscopy, and surface complexation modeling. J. Colloid Interface Sci. 2001, 234, 204-216.

Goodarzi F.; Huggins F.E. Monitoring the Species of Arsenic, Chromium and Nickel in Milled Coal, Bottom Ash and Fly Ash from a Pulverized Coal-fired Power Plant in Western Canada. Journal of Environmental Monitoring. 2001, 3, 1-6.

Guerrero, A.; Goni, S.; Campillo, I.; Moragues, A. Belite cement clinker from coal fly ash of high ca content. Environ. Sci. Technol. 2004, 38, 3209-3213.

Hsia, T.H.; Lo, S.L.; Lin, C.F.; Lee, D.Y. Characterization of arsenate adsorption oon hydrous iron oxide using chemical and physical methods. Colloids and Surfaces A:Physicochemical and Engineering Aspects. 1994, 85, 1-7.

Huggins, F. E.; Shah, N.; Zhao, J. Lu, F.; Huffman G. P. Nondestructive determination of trace element speciation in coal and coal ash by XAFS spectroscopy
Energy & Fuels 1993, 7, 482-489.

Huggins, F. E.; Goodarzi, F.; Lafferty, C. J. Mode of occurrence of arsenic in subbituminous coals. Energy & Fuels 1996, 10, 1001-1004.

Matijevic, E.; Janauer, G. E.; Kerker, M. reversal of charge of lyophobic colloids by hydrolyzed metal ions. I. $Al(NO4)_3$. Journal of Colloid Science (1964), 19, 333-346.

Mollah, M.Y.A.; Hess, T.R.; Cocke, D.L. Surface and bulk studies of leached and unleached fly ash using XPS, SEM, EDS and FTIR techniques. Cement and Concrete Research. 1994, 24, 109-118.

Myneni, S. C. B.; Traina, S. V.; Waychunas, G. A.; Logan, T. J. Vibrational spectroscopy of functional group chemistry and arsenate coordination in ettringite. Geochim. Cosmochim. Acta. 1998a, 62, 3499-3514.

Myneni, S. C. B.; Traina, S. J.; Waychunas, G. A., Logan, T. J. Experimental and theoretical vibrational spectroscopic evaluation of arsenate coordination in aqueous solutions, solids, and at mineral-water interfaces. Geochimica et Cosmochimica Acta. 1988b, 62(19/20), 3285-3300.

Nakamoto K. Infrared and Raman spectra of inorganic and coordination compounds; John Wiley & Sons: New York, 1997

National Institute of Standards and Technology Databases (http://srdata.nist.gov/xps/)

Pena M.; Meng X.G.; Korfiatis G.P.; Jing C.Y. Adsorption mechanism of arsenic on nanocrystalline titanium dioxide. Environ. Sci. Technol. 2006, 40, 1257-1262.

Perkin-Elmer Corporation Handbook of X-Ray Photoelectron Spectroscopy Physical Electronics Division; Eden Prairie: Minn, 1979.

Shoji, T.; Huggins, F. E.; Huffman, G. P. XAFS spectroscopy analysis of selected elements in fine particulate matter derived from coal combustion. Energy & Fuels 2002, 16, 325-329.

Sykes, Dan; Kubicki, J. D. Four-membered rings in silica and aluminosilicate glasses. American Mineralogist 1996, 81, 265-272.

Takahiro, Y.; Tetsuji, Y.; IIDA Y.; Shinichi, N. XPS study of Pb(II) adsorption on γ-Al_2O_3 surface at high pH conditions. J. Nucl. Sci. Technol., 2003, 40, 672-678.

van der Hoek, E.E.; Bonouvrie, P.A.; Comans, R.N.J. Sorption of as and se on mineral components of fly ash: relevance for leaching processes. Applied Geochemistry. 1994, 9, 403-412.

Van Roode, M.; Douglas, E.; Hemmings, R. T. X-ray diffraction measurement of glass content in fly ashes and slags. Cement and Concrete Research 1987, 17, 183-197.

Vempati, R. K. Fractionation and characterization of Texas lignite class F fly ash Cement and concrete research, 1994, 24, 1153-1164.

Wang, T., Wang, J. Calcium Impact on Arsenic Adsorption onto Coal Fly Ash, accepted by 2007 World of Coal Ash (WOCA) Conference, KY

Wong, J.; Angell, C. A. Glass Structure by Spectroscopy; Dekker: New York, 1976.

Zielinski, R. A.; Foster, A. L.; Meeker, G. P.; Brownfield, I. K. Mode of occurrence of arsenic in feed coal and its derivative fly ash, Black Warrior Basin, Alabama. Fuel 2006, 86, 560-572.

Table Supplement 1. Bulk composition (%) of two ashes (reacted with DI)

Fly Ash	As	Ca	Fe	Al	Si	C (LOI)	BET area (m^2/g)
33106-1005	0.0056	0.5	3.1	13.4	24.8	12.7	18.4
25410-1015	0.0030	14.1	4.2	6.1	11.7	14.8	25.7

Table Supplement 2. XPS surface composition (atomic percentage %) of two fly ashes

Element	As	Ca	Fe	Al	C	O	Si
33106-1005 DI	0.026	0.011	0.029	7.98	37.19	42.53	12.23
33106-1005 As0.1M	0.184	0.030	0.029	6.36	37.65	44.43	11.31
25410-1015 DI	0.044	0.355	0.043	12.75	30.53	50.01	6.26
25410-1015 As0.1M	0.365	0.482	0.048	8.92	36.00	49.23	4.94

Table Supplement 3. XPS surface composition (weight percentage %) of two fly ashes

Element	As	Ca	Fe	Al	C	O	Si
33106-1005 DI	0.115	0.025	0.094	12.759	26.409	40.271	20.259
33106-1005 As0.1M	0.829	0.071	0.099	10.290	27.074	42.602	18.975
25410-1015 DI	0.194	0.833	0.143	20.164	21.464	46.878	10.268
25410-1015 As0.1M	1.660	1.169	0.162	14.608	26.190	47.756	8.378

Note: The weight percentage is calculated based on the atomic percentage and atomic weight of each element.

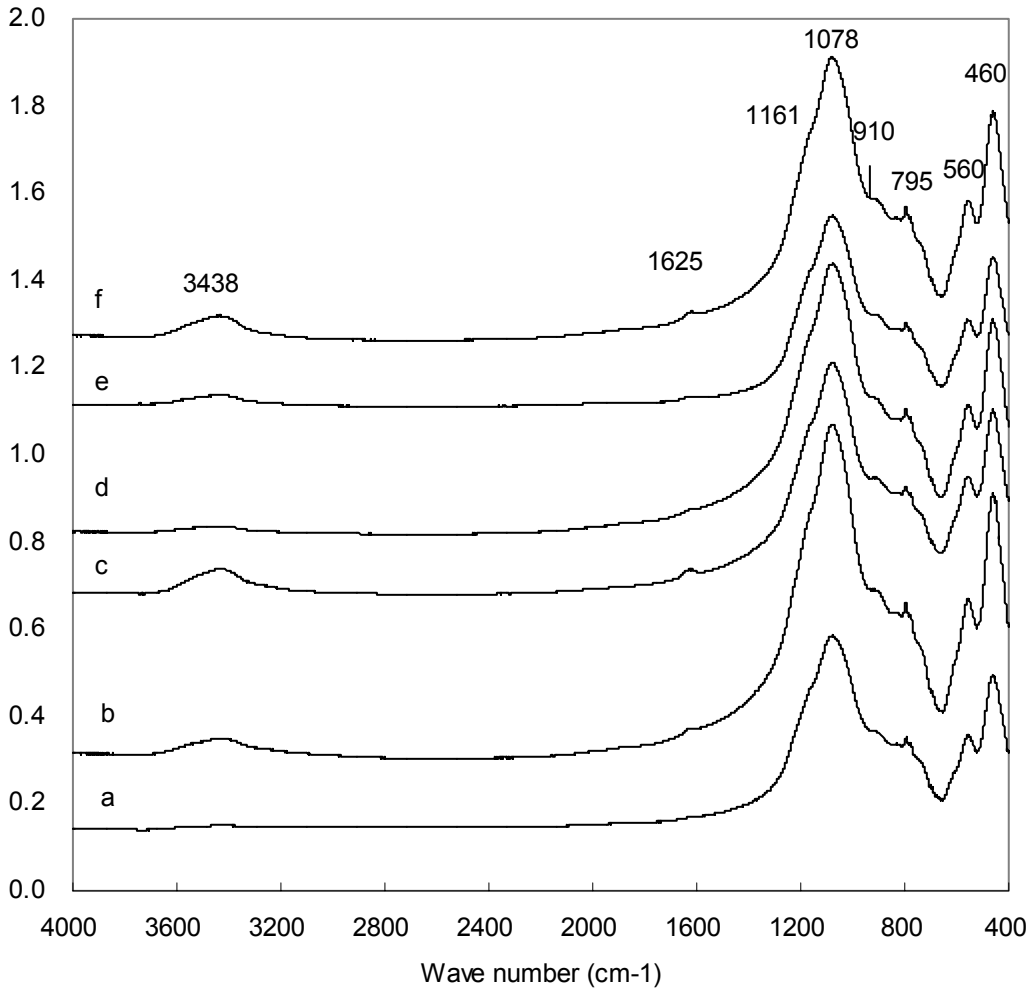

Figure Supplement 1. FTIR spectra of fly ash 33106-1005 at different pH and with different arsenate adsorption densities: (a) pH = 3.7, As 0 mg/g; (b) pH = 3.7, As 4.0 mg/g; (c) pH = 3.8, As 27.5 mg/g; (d) pH = 6.5, As 0 mg/g; (e) pH = 6.5, As 1.0 mg/g; (f) pH = 6.5, As 16.3 mg/g.

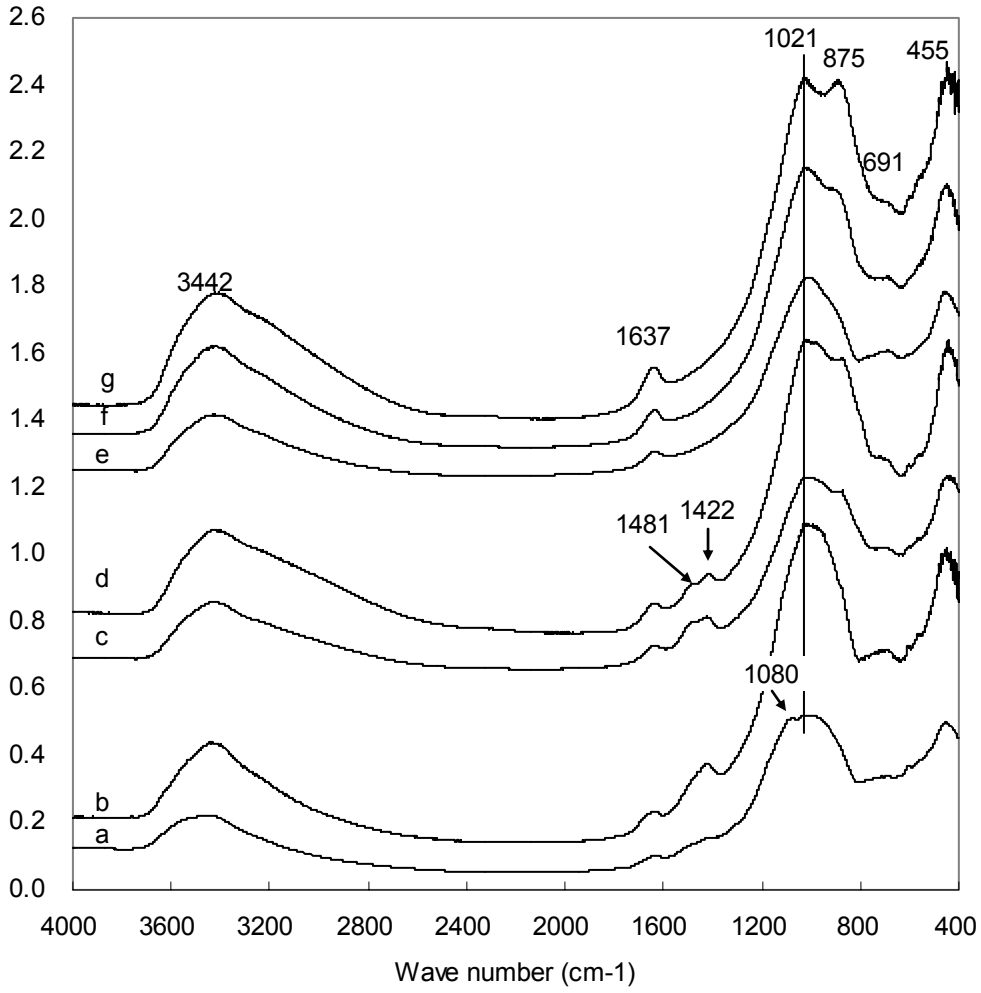

Figure Supplement 2. FTIR spectra of fly ash 25410-1015 at different pH and with different arsenate adsorption densities: (a) raw ash; (b) washed ash, pH = 10.4, As 0 mg/g; (c) washed ash, pH =10.6 , As 18.2 mg/g; (d) washed ash, pH = 10.6, As 50.4 mg/g; (e) washed ash, pH = 6.2, As 0 mg/g; (f) washed ash, pH = 6.4, As 15.2 mg/g; (g) washed ash, pH = 6.5, As 19.1 mg/g.

APPENDIX E.

QUALITY CONTROL/QUALITY ASSURANCE

Initial instrument calibration – For all the instruments used in this study, the instrument responses were calibrated with standard solution at different concentrations. XRF was calibrated with coal fly ash standard reference material (SRM) 1633b, purchased from National Institute of Standards and Technology (NIST). The linear ranges of the calibration were determined and used for the quantitative analysis of most analytes.

Instrument detection limit (IDL) – The quantitative IDL was determined by measuring 7-10 calibration blanks and multiply the standard deviation of the measurements by 3. IDL of XRF was provided by Mo-Sci Corp. who performed the analysis.

Method detection limit (MDL) – The quantitative MDL was determined by fortified reagent blank with 2-5 times concentration of the instrument detection limit. 7 replicates were performed and MDL was calculated by the equation of

$$MDL = SD \times t$$

SD = standard deviation of the replicated analysis
t = student's t value for a 99% confidence level and a standard deviation estimate with n-1 degrees of freedom (t = 3.14 for 7 replicate)

Quality control samples (QCS, also called as reference standards) –For the microwave acid digestion and ICP-MS analysis, coal fly ash SRM 1633b was used to check the method performance. Same amount of SRM was digested with the same reagent solution and the digestates were diluted and detected with ICP-MS at the conditions. The total elemental compositions were calculated and compared with the certified value, the mean concentration from three analysis of QCSs were within $\pm$15% of the stated value.

Laboratory reagent blank (LRB) – At least one LRB was prepared and detected for each batch of the samples (up to 20 samples). These blanks were prepared and detected with the same procedure of the samples except absence of the samples.

Laboratory fortified blank (LFB) – At least one LFB was prepared and detected for each batch of the samples (up to 20 samples). A known amount of the standard was added to the sample preparation reagent and proceeded with the same procedure of the analysis. The percent recovery was calculated by

$$\% \text{ Recovery} = 100 \times \text{Concentration detected/Concentration added}$$

The recovery should be within 80-120%. This quality control option was only performed for microwave digestion.

Laboratory fortified sample (LFS, also called as sample spike) – A LFS was performed with each batch of up to 15 samples. A known amount of the standard was added to the sample and mixed well; the extraction and analysis were proceeded with the same procedures of the samples process. The percent recovery of the LFS was calculated by the equation

$$\% \text{ Recovery} = 100 \times (C_{fs} - C_s)/C_{add}$$

C_{fs} = fortified sample concentration
C_s = sample concentration
C_{add} = concentration of standard added.

The recovery should be within 70-130%.

Calibration Check – To monitor the instrument performance/draft, standard solutions were detected during instrument analysis. At least one standard solution was detected for every 10-15 samples to make sure the instrument is calibrated and working preparedly. The recovery should be within 90-110%. For ICP-MS, recovery of 80-120% was ensured since a standard of lower concentration level (10 ppb) was used.

Precision of duplicated samples – At least one sample duplication was run for each batch of up to 20 samples. The precision of the duplication was expressed as the relative percent difference of duplicated samples (RPD) and was calculated with the following equition

$$RPD = 100 \times (C_h - C_l)/C_{av}$$

C_h = detected high concentration of duplicated sample
C_l = detected low concentration of duplicated sample
C_{av} = average of the C_h and C_l

BIBLIOGRAPHY

Banerjee, Kashi; Aguirre, Roman; Balczewski, Aaron; Gallagher, Paul M.; St. Germain, Darin; Amy, Gary L.A. Adsorption of arsenic (V) onto granular ferric hydroxide (GFH) in the presence of vanadium and silica. Proceedings - Water Quality Technology Conference and Exhibition (2004), wed11.4/1-wed11.4/15.

Natural Organic Matter Affects Arsenic Speciation and Sorption onto Hematite. Redman, Aaron D.; Macalady, Donald L.; Ahmann, Dianne. Division of Environmental Science and Engineering and Department of Chemistry and Geochemistry, Colorado School of Mines, Golden, CO, USA. Environmental Science and Technology (2002), 36(13), 2889-2896

Wu, C.H., Kuo, CY., Lin, C.F., Lo, S.L., 2002. Modeling competitive adsorption of molybdate, sulfate, selenate, and selenite using a Freundlich-type multi-component isotherm. Chemosphere, 47(3), 283-292.

Wijnja, H.; Schulthess, C. P. Effect of carbonate on the adsorption of selenate and sulfate on goethite. Soil Science Society of America Journal (2002), 66(4), 1190-1197.

Copper, chromium, and arsenic adsorption and equilibrium modeling in an Iron-Oxide-Coated sand, background electrolyte system. Khaodhiar, Sutha; Azizian, Mohammad F.; Osathaphan, Khemarath; Nelson, Peter O. Department of Civil, Construction, and Environmental Engineering, Oregon State University, Corvallis, OR, USA. Water, Air, and Soil Pollution (2000), 119(1-4), 105-120

ACAA, 2006. 2005 Coal Combustion Product (CCP) Production and Use Survey. American Coal Ash Association. http://www.acaa-usa.org/CCPSurveyShort.htm.

Agency for Toxic Substances and Disease Registry (ATSDR). Toxicological Profile for Selenium. http://www.atsdr.cdc.gov/toxprofiles/tp92.html., 2003.

ASTM C618-05. Standard Specification for Fly Ash and Raw or Calcined Natural Pozzolan for Use as Mineral Admixture in Portland Cement Concrete, American Society for Testing and Materials, *Annual Book of ASTM Standards*, 2005, Volume 80, West Conshohocken, Pennsylvania.

Baba, A., Kaya, A. Leaching characteristics of fly ash from thermal power plants of soma and tuncbilek, Turkey. Environ. Monit. Assess. 2004, 91(1-3), 171-181.

Belzile N., Tessier A. Interactions between arsenic and iron oxyhydroxides in lacustrine sediments. Geochimica et Cosmochimica Acta. 1990, 54, 103-109.

Brunori, C.; Balzamo, S.; Morabito, R. Comparison between different leaching/extraction tests for the evaluation of metal release from fly ash. Int. J. Environ. Anal. Chem. 1999, 75(1-2), 19-31.

Cockrell, C. F. and Leonard, J. W., Characterization and Utilization Studies of Limestone Modified Fly Ash." Coal Research Bureau, 1970, Vol. 60.

Dzombak, D. A., Morel, F. M. M. Surface Complexation modeling: Hydrous ferric oxide; John Wiley: New York, 1990.

EPA. Toxicity Characteristic Leaching Procedure. US Environmental Protection Agency, Method 1311, Test Methods for Evaluating Solid Waste: Physical/Chemical Methods (SW-846), 1992.

EPA. Synthetic Precipitation Leaching Procedure. US Environmental Protection Agency, Method 1312, Test Methods for Evaluating Solid Waste: Physical/Chemical Methods (SW-846), 1994.

EPA. Extraction Procedure Toxicity Test Method. US Environmental Protection Agency, Method 1310B, Test Methods for Evaluating Solid Waste: Physical/Chemical Methods (SW-846), 2004.

EPRI. Chemical Characterization of Fossil Fuel Combustion Wastes. EPRI Report, EA-5321. EPRI: Palo Alto, CA. 1987

EPRI. Leaching of inorganic constituents from coal combustion by-product under field and laboratory conditions. EPRI Report, TR-111773-V1. EPRI: Palo Alto, CA. 1991

EPRI. Chemical attenuation reactions of selenium. EPRI Report, TR-1994, 103535. EPRI: Palo Alto, CA. 1994

EPRI, Characterization of field leachates at coal combustion product management sites: arsenic, selenium, chromium, and mercury speciation. EPRI Report, 1012578. EPRI: Palo Alto, CA. 2006a

EPRI Chemical attenuation coefficients for selenium species using soil samples collected from selected power plant sites. EPRI Report, 1012585. EPRI: Palo Alto, CA. 2006b

Goldberg, S. Chemical modeling of anion competition on goethite using the constant capacitance model. Soil Sci. Soc. Am. j. 1985, 49(4), 851-856.

Goldberg, S., Glaubig, R.A. Anion sorption on a calcareous, montmorillonitic soil - selenium. Soil Sci. Soc. Am. j. 1988, 52(4), 954-8.

Goodarzi, F., Huggins, F.E. Monitoring the species of arsenic, chromium and nickel in milled coal, bottom ash and fly ash from a pulverized coal-fired power plant in western canada. J. of Environ. Monit. 2001, 3(1), 1-6.

Guerin, T.; Astruc, M.; Batel, A. Borsier, M. Multielemental speciation of As, Se, Sb and Te by HPLC-ICP-MS. Talanta 1997, 44, 2201-2208

Hansen, L.D. and Fisher, G.L. Elemental distribution in coal fly ash particles. Environ. Sci. Technol. 1980, 14(9) 1111-1117.

Hassett, D. J., Pflughoeft-Hassett, D. F., McCarthy, G. J. Ettringite formation in coal ash as a mechanism for stabilization of hazardous trace elements. Proc: 9th Int. Ash Use Symp. 1991, 2, 31-1to 31-17

Hering, J.G., Dixit, S. Contrasting sorption behavior of arsenic(III) and arsenic(V) in suspensions of iron and aluminum oxyhydroxides. In: O'Day, et al. (Eds), Advances in Arsenic Research. Oxford University Press 2005, pp 8 – 24.

Hirata, S.; Toshimitsu, H.; Aihara, M. Determination of arsenic species in marine samples by HPLC-ICP-MS. Anal. Sci. 2006, 22, 39-43.

Honeyman, B. D., Santschi, P. H. Metals in aquatic systems. Environ. Sci. Technol. 1988, 22(8), 862-71.

Huggins F.; Senior C., Chu, P., Ladwig, K., Huffman, G. Speciation of arsenic and selenium in fly-ash samples from full-scale coal-burning utility plants. Environ. Sci. Technol. 2007, 41(9), 3284-3289.

Isabel, B., Annette, J. C. Sorption of selenite and selenate to cement minerals. Environ. Sci. Technol. 2003, 37, 3442,-3447

Iwashita, A.; Sakaguchi, Y.; Nakajima, T.; Takanashi, H.; Ohki, A. Kambara, S. Leaching characteristics of boron and selenium for various coal fly ashes. Fuel 2005, 84(5), 479-485.

Jackson, B. P.; Miller, W. P. Soluble arsenic and selenium species in fly ash/organic waste-amended soils using ion chromatography-inductively coupled plasma mass spectrometry. Environ. Sci. Technol. 1999, 33, 270-275.

Jankowski, J.; Ward, C.R.; French, D.; Groves, S. Mobility of trace elements from selected Australian fly ashes and its potential impact on aquatic ecosystems. Fuel 2005, 85(2), 243-256.

Kim A.G., Cardone C. Preliminary Statistical Analysis of Fly Ash Disposal in Mined Areas. Proc: 12th International Symposium on Coal Combustion By-Product Management and Use. American Coal Ash Association. 1997, 1, 11-1 to 11-13.

Kim A.G., Kazonich G. Release of Trace Elements from CCB: Maximum Extractable Fraction. Proceedings 14th International Symposium on Management and Use of Coal Combustion Products (CCPs). 2001, 1, 20-1 to 20-15.

Kim, A.G. Physical and chemical characteristics of CCB. Proc: Coal Combustion By-Products and Western Coal Mines: a Technical Interactive Forum, Golden, CO, 2002, 25-42.

Kosson, D.S., van der Sloot, H.A., Sanchez, F., Garrabrants, A.C. An integrated framework for evaluating leaching in waste management and utilization of secondary materials. Environmental Engineering Science, 2002, 19, 159 – 204.

Lecuyer, I., Bicocchi, S., Ausset, P., Lefevre, R. Physico-chemical characterization and leaching of desulfurization coal fly ash. Waste Manage. Res. 1996, 14(1), 15-28.

Lindemann, T., Prange, A., Dannecker, W., Neidhart, B. Simultaneous determination of arsenic, selenium and antimony species using HPLC/ICP-MS. J. Anal. Chem. 2004, 364, 462-466.

Manning, B. A.; Martens, D. A. Speciation of arsenic (III) and arsenic (V) in sediment extracts by high-performance liquid chromatography-hydride generation atomic absorption spectrophotometry. Environ. Sci. Technol., 1997, 31(1), 171-177.

Martinez-Bravo, Y., Roig-Navarro, A. F., Lopez, F. J., Hernandez, F. Multielemental determination of arsenic, selenium and chromium(VI) species in water by high-performance liquid chromatography-inductively coupled plasma mass spectrometry. J. Chromatogr. A. 2001, 926(2), 265-274.

Mehnert, E., Hensel, B.R. Coal combustion by-products and contaminant transport in groundwater. Coal Combustion By-Products Associated with Coal Mining Interactive Forum: Southern Illinois University at Carbondale, Carbondale, IL. 1996

Merrill, D.T., Manzione, M., Parker, D., Petersen, J., Crow, W., Hobbs, A. Field evaluation of arsenic and selenium removal by iron coprecipitation. Environ. Prog. 2006, 6(2), 82-90.

Narukawa, T., Takatsu, A., Chiba, K., Riley, K. W., French, D. H. Investigation on chemical species of arsenic, selenium and antimony in fly ash from coal fuel thermal power stations. J. of Environ. Monit. 2005, 7(12), 1342-1348.

Orero Iserte, L., Roig-Navarro, A. F., Hernandez, F. Simultaneous determination of arsenic and selenium species in phosphoric acid extracts of sediment samples by HPLC-ICP-MS. Anal. Chim. Acta. 2004, 527(1), 97-104.

Otero-Rey, J. R., Mato-Fernandez, M. J., Moreda-Pineiro, J., Alonso-Rodriguez, E., Muniategui-Lorenzo, S., Lopez-Mahia, P., Prada-Rodriguez, D. Influence of several experimental parameters on arsenic and selenium leaching from coal fly ash samples. Anal. Chim. Acta. 2005, 531(2), 299-305.

Rajan, S.S.S. Adsorption and desorption of sulfate and charge relationships in allophanic clays. Soil Sci. Soc. Am. j. 1979, 43, 65–69.

Schlegel, D., Matusch, J., Dittrich, K. Speciation of arsenic and selenium compounds by ion chromatography with inductively coupled plasma atominc emission spectrometry detection using the hydride technique. J. Chromatogr. A. 1994, 683, 261-267.

Smith, A. H., Hopenhayn-Rich, C., Bates, M. N. Goeden, H. M., Hertz-Picciotto, I., Duggan, H. M., Wood, R., Kosnett, M. J., Smith, M. T. Cancer risks from arsenic in drinking water. Environ. Health Perspect. 1992, 97, 259-267.

U.S. EPA. Report to congress: Wastes from the combustion of coal by electric utility power plants. 1988, EPA/530-SW-88-002.

U.S. EPA SAB. "Leachability Phenomena-Recommendations and Rationale for Analysis of Contaminant Release by the Environmental Engineering Committee," Report EPA-SAB-EEC-92-003, U.S. EPA Science Advisory Board, Washington, D.C. 1991

U.S. EPA. Report to congress: Wastes from the combustion of fossil fuels: Volume 2, methods, findings and recommendations. 1999, EPA/530-R-99-010

U.S. EPA. Characterization of Mercury-Enriched Coal Combustion Residues from Electric Utilities Using Enhanced Sorbents for Mercury Control. 2006, EPA/600/R-06/008.

van der Hoek, E.E., Bonouvrie, P.A., Comans, R.N.J. Sorption of As and Se on mineral components of fly ash: relevance for leaching processes. Appl. Geochem. 1994, 9, 403-412.

van der Hoek, E.E., Comans, R.N.J. Modeling arsenic and selenium leaching from acidic fly ash by sorption on iron (hydr)oxide in the fly ash matrix. Environ. Sci. Technol. 1996, 30(2), 517-523.

van der Sloot, H.A., Kosson, D.S., Eighmy, T.T., Comans, R.N.J., Hjelmar, O. Approach towards international standardization: a concise scheme for testing of granular waste leachability. In Environmental aspects of construction waste materials; Goumans J.J.J.M., van der Sloot H.A., Aalbers Th.G., eds; Elsevier: Amsterdam, The Netherlands. 1994, 453-466.

Wang, J., Teng, X., Wang, H., Ban, H. Characterizing the metal adsorption capability of a class F coal fly ash. Environ. Sci. Technol. 2004, 38(24), 6710-6715.

Wadge, A., Hutton, M. The leachability and chemical speciation of selected trace elements in fly ash from coal combustion and refuse incineration. Environ. Pollut. 1987, 48(2), 85-99.

Zielinski, Robert A.; Foster, Andrea L.; Meeker, Gregory P.; Brownfield, Isabelle K. Mode of occurrence of arsenic in feed coal and its derivative fly ash, Black Warrior Basin, Alabama. Fuel 2006, 86(4), 560-572.

VITA

Tian Wang was born on July 5, 1976 in Tai'an, Shandong Province, China. In July 1997, she received her bachelor's degree in Water and Wastewater Engineering from Qingdao Institute of Architectural Engineering, Qingdao, Shandong, China. She worked for the Engineering Design Center in Weihai Sports Bureau as an assistant engineer for four years before continuing her education in Tongji University, and in May 2004, she received her master's degree in Environmental Engineering. In December 2007, she received her Ph.D. degree in Civil Engineering from the University of Missouri-Rolla, Rolla, MO, USA.

During her graduate programs, she published a number of journal and conference papers. Some of which are listed with the references of this research. She won the Nilishi Academic Scholarship at Tongji University in 2003 and was awarded as the 'Outstanding Employee' at the Engineering Design Center in 1999 and 2000.

Tian Wang has been a member of the American Chemical Society in 2006, she also served as a member of the Chinese Students and Scholars Association (CSSA) at University of Missouri-Rolla from 2004 to 2007.